To the Graduate Council:

I am submitting herewith a dissertation written by Christine Jo Kelly entitled "Bioprocess Design and Control using Bioluminescent Bacterial Reporters." I have examined the final copy of this dissertation for form and content and recommend that it be accepted in partial fulfillment of the requirements for the degree of Doctor of Philosophy, with a major in Chemical Engineering.

Paul Bienkowski, Co-Major Professor

Gary Sayler, Co-Major Professor

We have read this dissertation
and recommend its acceptance:

Accepted for the Council:

Associate Vice Chancellor and
Dean of The Graduate School

Bioprocess Design and Control using Bioluminescent Bacterial Reporters

A Dissertation
Presented for the
Doctor of Philosophy
Degree
The University of Tennessee, Knoxville

Christine Jo Kelly
May 1997

ACKNOWLEDGMENTS

I am grateful to my committee members for their support and contributions to my education and research at the University of Tennessee. I would like to thank Dr. Prados, Dr. White and Dr. Phelps for insightful discussion and perspective in reviewing my dissertation.

My advisor, Dr. Bienkowski, had the confidence in me to let me work independently and was always there to help when I needed him. Dr. Sayler generously provided the use of the Center for Environmental Biotechnology (CEB) facilities and financial support. I enjoyed and benefited from the CEB atmosphere of open collaboration and discussion among many disciplines of researchers that was due to his skillful management. Dr. Donaldson gave me consistent, clear, thorough and invaluable feedback on areas of scientific content, writing style, presentation and career choices.

In addition, I would like to thank all the students and staff at the CEB, who made my work entertaining, fun and challenging. Bruce Applegate and Debra Kuo especially helped me when I began my research by teaching me microbiological techniques and methods. I would like to especially thank Dr. Lajoie for his significant collaboration in this work, mentoring and insightful discussions.

Finally, and most sincerely I would like to thank my parents for providing me with a solid foundation to begin my work; my husband, Tim, for his unwavering support, cheerfulness and peacefulness; and Lorretta Hall for helping us raise Nolan while I worked on this research.

ABSTRACT

Bioreporters are bacteria that have been genetically engineered to emit light (bioluminescence). Bioluminescence is known to be biochemically related to induction of the *lux* operon and corresponding production of the *lux* system enzymes that catalyze the light producing reactions. Substrates for these reactions include oxygen, aldehyde and the electron transport system components $FMNH_2$, $NADH_2$ and ATP. The traditional use of bioluminescence has been as a signal of transcription under highly controlled experimental conditions. Bioluminescent reporters offer an opportunity to extend the traditional uses of bioluminescence to engineering scale process design, monitoring and control. However, to extend the application of bioreporters, a quantitative relationship between bioluminescence and relevant environmental conditions needs to be established.

Inducible and constitutive type bioluminescent reporters were examined in this research. The inducible reporters, *Pseudomonas putida* B2 and TVA8, contain the *lux* genes under toluene dioxygenase (*tod*) promoter control. Toluene induces both the *tod* and *lux* operon. The toluene dioxygenase enzymes catalyze the degradation of toluene as well as the co-metabolism of trichloroethylene (TCE). The constitutive reporter, Shk 1, is an activated sludge microorganism containing a plasmid with the *lux* genes under the control of constitutive promoter.

Experiments were conducted under batch, semi-continuous and continuous cultivation conditions; and utilized batch, chemostat and turbidostat reactors. The

primary conditions varied in these experiments were inducer, growth substrate and toxicant concentration. In limited experiments, pre-exposure to toluene, oxygen concentration, and growth source type were found to affect the bioluminescent response. Light was measured under steady-state and transient conditions with photomultiplier technology.

A simple mechanistic mathematical model was developed that described bioluminescence and the degradation of toluene and TCE by the *tod-lux* reporters under batch and continuous cultivation conditions. The model incorporated (1) degradation dependence on inducer and growth substrate, co-metabolic substrate, and biomass concentrations; and (2) bioluminescence dependence on inducer and growth substrate, luciferase and biomass concentrations.

In both batch and continuous cultivation, bioluminescence increased at a rate greater than cell growth upon exposure to increased toluene. An accumulation of active luciferase molecules as well as *in vivo* enzyme decay mechanisms were proposed to mechanistically explain this behavior.

In *tod-lux* bioreporter chemostat experiments, bioluminescence transiently increased in response to increasing feed concentrations, then declined as steady-state was approached. The transient maximum bioluminescence corresponded with the toluene feed concentration due to increased steady-state cell densities. The transient increase in bioluminescence corresponded to increased toluene (growth substrate and inducer) availability in the reactor. Limiting growth substrate and possibly lack of

induction of the *tod* operon was proposed to explain the decrease in light as the chemostat reached steady-state toluene concentration and cell density.

Bioluminescence from the Shk 1 reporter in a chemostat and a semi-continuous turbidostat reactor was compared. Steady-state bioluminescence for five different chemostat dilution rates was approximately the same (20 namp) and much lower than the steady-state bioluminescence from the turbidostat (160 namp). As the Shk 1 bioreporter does not require an inducer for light production, the difference in light was attributed to growth substrate availability.

The bioluminescent response of the Shk 1 reporter to pH and the toxicants cadmium, 2,4-dinitrophenol, hydroquinone and ethanol was examined (0 to 10,000 mg/L). In batch and continuous sampling systems with the Shk 1 bioreporter bioluminescence declined more severely with increasing cadmium, 2,4-dinitrophenol, and hydroquinone concentration, while bioluminescence remained constant upon exposure to 10,000 mg/L ethanol. The decrease in bioluminescence corresponded to the decrease in oxygen consumption rates of industrial activated sludge in response to hydroquinone exposure. Biosensors incorporating the Shk1 reporter were designed to contact the reporter with the process fluid to be sampled and were tested in bench scale activated sludge reactors. Additional growth substrate was required for the reporter to emit light. None of the designs tested provided a constant and significant level of bioluminescence.

TABLE OF CONTENTS

CHAPTER		PAGE
1.	Introduction and Background	1
	Introduction	1
	Background	5
	Bioremediation	5
	Activated Sludge Wastewater Treatment	6
	Genetics and Physiology of Bioluminescence	8
	Bioluminescent Reporters	13
	Biological Process Modeling	22
2.	Preliminary Studies	28
	Experimental Methods	28
	Bacterial Growth Media	28
	Bacterial Cell Quantification	31
	Light Measurement	32
	Toluene and TCE Measurement	36
	Preliminary Experiments	36
	Effect of Oxygen Concentration	38
	Effect of Kanamycin on Growth Rate	41
	Stability of the *tod-lux* Construct	42
	Comparison of Parent Strain F1 to Bioreporter B2	44
	Discussion	46
3.	Characterization of the *tod-lux* Bioreporter in Batch Culture	49
	Growth Curve and Bioluminescent Response	49
	tod-lux Bioreporter Cellular Yield	53
	Discussion	55
	Pre- and Multiple-Exposure to Toluene	56
	Methodology	56
	Results	57
	Discussion	61

Bioluminescent Response to a Range of Inducer Concentrations 61
Methodology 62
Mathematical Model Development 63
Results 69
Discussion 76

4. Characterization of the *tod-lux* Bioreporter in a Chemostat 81

Methodology 81
Reactor Analysis 83
Experimental Description 84

Chemostat Mathematical Modeling 84
Chemostat Cellular Yield 84
Reactor Mass Balance 85
Bioluminescence Modeling 86

Results 88
Chemostat Cellular Yield 88
Bioluminescence 89
Model Parameters 94
Transient Response to a Step Change 96

Discussion 98

5. Characterization of the Shk 1 Bioreporter in Batch Culture 101

Batch Bioluminescent Response 102
Batch Growth Curve 102
Effect of Various Carbon Sources on Shk 1 105
Discussion 108

Bioluminescent Response to Toxicants 109
Methodology 109
Results 110
Discussion 115

6. Characterization of the Shk 1 Bioreporter in a Chemostat and a Turbidostat 118

Methodology 118
Chemostat and Turbidostat Apparatus 118
Experimental Description 119

Results 122
Increasing Feed Carbon Concentration 122
Chemostat Compared to Turbidostat 124
Chemostat at Different Flow Rates 126

Discussion 126

7. Contacting Design 132

Continuous Sampling System 133
Methodology 133
Results 136
Discussion 137

Biosensor Design 139
Biosensor Configurations 140
Bioluminescent Response of Biosensors in Test Applications 142
Shk 1 Bioluminescent Response to Activated Sludge Components 148

Discussion 150

8. Discussion and Conclusions 154

Interpretations of Major Significant Experimental Results .. 156
Determination of Kinetic Parameters 156
Transcription Rate Dependence on Toluene Concentration 156
Accumulation of Luciferase to Explain Transient Bioluminescent Behavior 157
Bioluminescence Dependence on Oxygen Concentration 158
Bioluminescence Dependence on Growth Substrate .. 158
Bioluminescence Dependence on Toxicants 160
Bioluminescent Reporters as an Aid to Process

Design and Control 160

Co-metabolic Processes 161
A Proposed TCE Degradation System 162

Recommendations for Future Work 165
Carbon Starvation versus Induction Limitation 165
Estimation of in vivo Enzyme Degradation Rates ... 166
Biosensor Engineering 167

References 158

Appendices 180

FORTRAN Code for Model Solution 181

Vita 186

LIST OF TABLES

TABLE	TITLE	PAGE
Table 2-1	Growth media.	29
Table 2-2	Luria Broth.	29
Table 2-3	Minimal salts with succinate medium.	30
Table 2-4	Mineral salts medium.	30
Table 2-5.	Components of simulated wastewater.	31
Table 2-6.	Effect of kanamycin batch growth experimental conditions.	41
Table 3-1.	Experimental yield results.	55
Table 3-2.	Bioluminescent response rate (namp/hr) for multiple and single exposures of 10 mg/L toluene.	59
Table 3-3.	Comparison of model parameters with previous studies.	73
Table 3-4.	Remaining modeling parameters used in simulation.	75
Table 4-1.	TVA8 chemostat experimental conditions.	84
Table 4-2.	Biomass yield in TVA8 chemostat.	89
Table 4-3.	Chemostat model parameter values and method of determination...	96
Table 6-1.	Shk 1 chemostat feed concentration step changes	121
Table 6-2.	Turbidostat and chemostat operating conditions	122
Table 7-1.	Conditions for continuous sampling experiment	135
Table 7-2	Rate of bioluminescence decline upon exposure to hydroquinone in the continuous sampling system	137
Table 8-1.	Summary of major significant experimental results	155

LIST OF FIGURES

FIGURE #	TITLE	PAGE
Figure 1-1.	Bioluminescent system coupled to the electron transport system.	10
Figure 1-2.	Light producing reaction series	11
Figure 1-3.	*lux* genes, associated gene products, and the reactions involved in bioluminescence	12
Figure 1-4.	Depiction of a single cell of the bioreporter *Pseudomonas putida* B2	16
Figure 1-5.	First step in the degradation of toluene by the toluene dioxygenase pathway	20
Figure 1-6.	The degradation of toluene by the toluene dioxygenase pathway.	21
Figure 2-1.	*Pseudomonas putida* B2 cell optical density versus cell dry mass	33
Figure 2-2	Effect of cell density on bioluminescence measurement	35
Figure 2-3.	Sample gas chromatograph standard curve	37
Figure 2-4.	Experimental apparatus to examine the effect of oxygen concentration on bioluminescence	39
Figure 2-5.	Bioluminescent response of Shk 1 to decreasing oxygen concentration	40
Figure 2-6.	Growth rate of B2 at different kanamycin concentrations	43
Figure 2-7.	Colony forming units on selective and non-selective plates assessing the stability of the *tod-lux* construct in B2	45
Figure 2-8.	Comparison of toluene degradation between B2 and F1	47
Figure 3-1.	Determination of exponential growth rate for *Pseudomonas putida* TVA8	51
Figure 3-2.	TVA 8 batch growth curve: experimental cell density, logistic curve fit cell density, and bioluminescence with time	52

Figure 3-3.	Bulk growth rate from logistic curve, bioluminescence and specific bioluminescence for batch *Pseudomonas putida* TVA8..	54
Figure 3-4.	Bioluminescent response to multiple and single exposures of toluene	58
Figure 3-5.	Influence of pre-exposure to toluene on degradation (initial 10 mg/L toluene)	60
Figure 3-6.	Bioluminescence and toluene concentration for an initial toluene concentration of 25 mg/L	70
Figure 3-7.	Comparative toluene and TCE co-degradation as a function of time	71
Figure 3-8.	TCE degradation by B2 with a range of initial toluene concentrations	72
Figure 3-9.	Bioluminescent response by *Pseudomonas putida* B2 to different initial toluene concentrations	74
Figure 3-10.	Toluene and TCE degradation (experimental and model) for an initial toluene concentration of 37 mg/L	77
Figure 3-11.	Toluene and TCE degradation (experimental and model) for an initial toluene concentration of 54 mg/L	78
Figure 3-12.	Bioluminescence for initial toluene concentrations of 25 and 50 mg/L (experimental and model)	79
Figure 4-1.	TVA8 chemostat schematic	82
Figure 4-2.	Bioluminescence from a TVA8 chemostat with feed concentration step changes	90
Figure 4-3.	TVA8 chemostat cell density (model and experimental) and step feed toluene concentrations with time	91
Figure 4-4.	TVA8 chemostat specific bioluminescence and calculated reactor toluene concentration	93
Figure 4-5.	Bioluminescence (model and experimental) from a TVA8 chemostat with feed concentration step changes	95
Figure 4-6.	Bioluminescence, cell density and toluene concentration from a TVA8 chemostat with an increase in toluene feed concentration.	97
Figure 5-1.	Determination of Shk 1 exponential growth rate	103

Figure 5-2.	Shk 1 batch growth curve: experimental cell density, logistic curve fit cell density, and bioluminescence with time	104
Figure 5-3.	Bulk growth rate from logistic curve, bioluminescence and specific bioluminescence for batch Shk 1	106
Figure 5-4.	Bioluminescent response to various carbon sources	107
Figure 5-5.	Initial bioluminescent response of Shk 1 to cadmium, ethanol, and 2,4-dinitrophenol	111
Figure 5-6.	Initial bioluminescence and oxygen consumption rate of Shk 1 in response to hydroquinone	113
Figure 5-7.	Time-course bioluminescence of Shk 1 in response to a range of hydroquinone concentrations	114
Figure 6-1.	Turbidostat schematic	120
Figure 6-2.	Turbidostat circuit schematic	120
Figure 6-3.	Shk 1 chemostat with step changes in feed concentration	123
Figure 6-4.	Comparison bioluminescence in a chemostat and turbidostat loaded with the Shk 1 reporter	125
Figure 6-5.	Shk 1 chemostat at four dilution rates	127
Figure 6-6.	Theoretical chemostat operation	128
Figure 6-7.	Comparison of chemostat and turbidostat loaded with Shk 1	130
Figure 7-1.	Schematic of continuous sampling system to assess wastewater toxicity to activated sludge microorganisms	134
Figure 7-2.	Continuous sampling system response to hydroquinone	138
Figure 7-3.	Biosensor designs for contacting the Shk 1 reporter strain with a process fluid	141
Figure 7-4.	Bench scale activated sludge waste treatment reactor schematic utilized in testing biosensor designs	143
Figure 7-5.	Bioluminescent response of the air purged biosensors in beakers.	145
Figure 7-6.	Air purged sensor in reactors	147
Figure 7-7.	Dialysis type biosensor in a reactor in an effluent beaker	149
Figure 7-8.	Shk 1 bioluminescent response to components of sludge	151

Figure 7-9. Shk 1 bioluminescent response to dilutions of sludge 152

Figure 8-1 Proposed TCE remediation design using bioluminescence for monitoring and control of the bacterial process 163

Figure 8-2 Simple control algorithm for toluene, TCE and supplemental carbon source additions, as well as cell removal from the primary reactor 164

NOMENCLATURE

μ	instantaneous growth rate, day^{-1}
μ_{max}	maximum growth rate when $S>>K_S$, day^{-1}
A	air flow rate, L/min
C_{lucif}	effective cellular luciferase concentration, mass/cell
C_{TCE}	liquid TCE concentration, mg/L
C^{v}_{TCE}	reactor vapor TCE concentration, mg/L
C^{f}_{TCE}	feed TCE concentration, mg/L
C_{tol}	liquid toluene concentration, mg/L
C^{v}_{tol}	reactor vapor toluene concentration, mg/L
C^{f}_{tol}	feed toluene concentration, mg/L
$C_{tol,i}$	initial toluene concentration, mg/L
$C^{overall\ ss}_{tol}$	steady-state toluene concentration in the chemostat, mg/L
C_{eqb}	concentration of hydroquinone in the feed from the simulated equalization basin, mg/L
C_{shkl}	concentration of hydroquinone in the feed from the reporter cell supply vessel, mg/L
C_{samp}	concentration of hydroquinone in the sampling vessel, mg/L
D	dilution rate, day^{-1}
E	chemical symbol representing enzyme in Michaelis-Menten development
E_o	chemical symbol representing the total amount of enzyme
E'	energy availability term, dimensionless
F	feed flow rate, L/day
F_{sv}	fraction of volume sampled by the photomultiplier, L/L_R
H_{tol}	Henry's constant for toluene, dimensionless
H_{TCE}	Henry's constant for TCE, dimensionless
k_{tol}	maximum toluene degradation rate, mg toluene/L day
k_{TCE}	maximum TCE degradation rate, mg TCE/L day

k_{light}	overall light proportionality constant
k_{lucif}	maximum luciferase production rate, mg/cell day
k_d	in vivo luciferase decay constant, day^{-1}
$k_1^{'}$	Michaelis-Menten overall rate constant for reaction 1
$k_2^{'}$	Michaelis-Menten overall rate constant for reaction 2
k_1^1	Michaelis-Menten rate constant
k_2^1	Michaelis-Menten rate constant
k_{-1}^1	Michaelis-Menten rate constant
k_1^2	Michaelis-Menten rate constant
k_2^2	Michaelis-Menten rate constant
k_{-1}^2	Michaelis-Menten rate constant
K_1	dissociation constant for reaction 1 in Michaelis-Menten rate expression development
K_2	dissociation constant for reaction 2 in Michaelis-Menten rate expression development
K_{tol}	Michaelis-Menten constant for toluene degradation, mg/L
K_{TCE}	Michaelis-Menten constant for TCE degradation, mg/L
K_{light}	saturation constant for bioluminescence dependence on toluene, mg/L
K_{lucif}	saturation constant for luciferase dependence on toluene, mg/L
K_{luc}	mg active luciferase/mg total luciferase
K_d	luciferase *in vivo* decay rate, day^{-1}
K_s	Monod constant, mg/L
L_R	liters of reactor volume
L_{sv}	liters of volume sampled by the photomultiplier
L_R	liters of reactor volume
L_{sv}	liters of volume sampled by the photomultiplier
L_{luc}	the proportionality constant between active luciferase and the photon per second released, photon sec^{-1}/mg active luciferase
M	mass per cell, mg cell/cell
P_1	chemical symbol representing the product of reaction 1

P_2	chemical symbol representing the product of reaction 2
S	substrate concentration, mg/L
S_f	feed substrate concentration, mg/L
S_1	chemical symbol representing the reactant of reaction 1
S_2	chemical symbol representing the reactant of reaction 2
t	time, day
t_{lag}	batch lag time, day
V	reactor volume, L
V^L	liquid volume, mL
V^V	vapor volume, mL
V^L	reactor liquid volume, L
V^V	reactor vapor volume, L
v_{eqb}	volumetric flow rate from the simulated equalization basin, mL/min
v_{shk1}	volumetric flow rate from the reporter cell supply vessel, mL/min
V_{samp}	volume of the sampling vessel, mL
v_R	reaction rate $= -\frac{dS}{dt} = \frac{dP}{dt}$, mg/L day
v_R^{tol}	toluene reaction rate, mg/L day
v_R^{TCE}	TCE reaction rate, mg/L day
X_o	chemostat feed cell density, mg/L
X	cell mass density, mg/L
X_i	initial cell mass density, mg/L
X_f	cell mass density in the feed, mg/L
X^{ss}	chemostat steady-state cell mass density, mg/L
$Y_{X/S}$	cellular yield, mg cells/mg substrate

CHAPTER 1

INTRODUCTION AND BACKGROUND

Introduction

Bacteria are widely utilized in industry for the production of bulk chemicals, food products, pharmaceutical products, as well as in the treatment of wastes. The specific state of the bacteria in these processes can be difficult to assess. The inability to asses bacterial state can cause low rates of production, inefficient use of capital, or long process times. To address this problem, bacterial bioreporters have been genetically engineered that can indicate the state of bacteria in a specific process (King, 1990; DuBow, 1992; Van Dyk, 1995; Paton, 1995; Belkin, 1996; Applegate, 1996). Light producing (*lux*) bioreporters are engineered so that a change in the light response of the bioreporter is an indication of a specific cellular activity.

Historically, the primary use of engineered bioluminescent bacteria has been for detecting cellular energy substrates with luciferase extracts (Ulitzer, 1991; Danilov, 1989) and as a tool for signaling genetic transcriptional activity under highly controlled experimental conditions (Bronstein, 1994; Stewart, 1992). More recent environmental applications include specific chemical detection, toxicity and bioavailability assessment, and indication of microbial biomass (DeWeger, 1991; Steinberg, 1995). Bioluminescent reporters can have a wider application in process design, monitoring,

and control that takes advantage of both the genetic and the physiological properties affecting bioluminescence.

A bioreporter can be used as a tool for understanding and controlling bacterial processes, because the bioreporter is an engineered form of the bacterium employed in the process. Bioreporters can be contrasted to analytical sensors for environmental parameters. For example, an oxygen probe can measure dissolved oxygen in an activated sludge waste treatment basin, or a gas chromatograph can measure toluene concentration in an aquifer sample. Bacteria employed in a process will be exposed to oxygen and toluene, and these factors have important impacts on bacterial processes. However, a bioreporter can yield a measure of the bacterial response to oxygen and toluene.

There are two fundamental types of *lux* bioreporters differentiated at the genetic level. The constitutive type is engineered to produce light continuously, presumably under the control of a constitutive promoter. This bioreporter can signal toxicity by a significant decrease in bioluminescence, which is due to general disruption of metabolic activity. The inducible type is designed for specific promoter control of bioluminescence. This type of bioreporter changes its level of bioluminescence in response to a chemical inducer. An inducible reporter can also respond to toxicants with a reduction in bioluminescence. Both of these types of bioreporters enable evaluation of a particular response in bacteria not easily detectable by other methods.

Both constitutive and inducible bioreporters were examined in this study. Shk 1 is a presumably constitutive bioreporter constructed from an activated sludge bacterial isolate (Kelly, 1997), and it was designed to assess the toxicity of waste streams to activated sludge communities. *Pseudomonas putida* B2 (Applegate, 1996) and *Pseudomonas putida* TVA8 (Applegate, 1997) are inducible bioreporters with the *lux* operon under the control of the toluene dioxygenase (*tod*) promoter. These bacteria utilize toluene as a sole-carbon source and co-metabolize trichloroethylene (TCE). The *tod-lux* reporters were designed to indicate induction of the promoter for genes encoding enzymes specific for the degradation of common groundwater contaminants (toluene and TCE).

Fundamental characterization of the bioluminescent response by the bioreporter necessitates examining the response under a variety of experimental conditions to avoid bias in interpreting experimental results. For example, the bioreporter could respond differently to balanced growth conditions in batch reactors than with growth substrate limited continuous growth conditions in a chemostat. In this research, a variety of experimental configurations were utilized, including optimum condition batch growth, resting cell response, continuous culture growth (limiting and non-limiting growth substrate), and immobilized cell culture. The diversity of experimental conditions was a direct result of using the bioreporter to elucidate mechanisms important in bioluminescence as well as the degradative process. While adding complexity to the synthesis of this research, examining both an inducible

and a constitutive reporter provided an advantage in deducing the mechanisms important in the production of bioluminescence.

This research hypothesizes that (1) physiological as well as genetic properties of bioluminescent reporters influence bioluminescence, and these effects can be elucidated and described mechanistically; and (2) there is a quantitative relationship between the degradation of toluene, the degradation of TCE and the rate or extent of bioluminescence by the *tod-lux* reporter that can be measured by experiments and described mathematically.

Goals of this research were the following: (1) examine the bioluminescent response of both types of bioreporters to major environmental conditions appropriate to their application, including cultivation conditions, inducer concentrations and toxicant exposure; (2) develop a predictive model for bioluminescence and degradation kinetics of the *tod-lux* bioreporter; and (3) design a reporter/fluid contacting method to produce a consistent and reproducible bioluminescent signal for process control.

The results of this research can extend current applications of bioluminescent bacteria to include mechanistic understanding of the bacteria to aid in process design, monitoring, and control. In this study, factors important in process design and control were examined in two types of bioreporters. These factors were toluene pre-exposure, toluene concentration, exposure to multiple contaminants (toluene and TCE), and cultivation conditions (batch, semi-continuous and continuous).

Background

The following five topics are discussed in this section: (1) bioremediation of contaminated groundwater, (2) activated sludge wastewater treatment,(3) genetics and physiology of bioluminescence, (4) bioluminescent reporters, and (5) biological process modeling. Groundwater remediation and activated sludge waste treatment are bioprocesses that can benefit from the mechanistic monitoring that the *tod-lux* and Shk 1 bioreporters can provide.

Bioremediation

Groundwater contamination is an increasingly important concern in the United States. The widespread production and use of synthetic compounds have resulted in contamination of groundwater supplies. Bioremediation of these contaminated aquifers is an especially effectual mode of remediation due to its cost effectiveness, reduced risk of exposure, minimal environmental impact and liability, and destruction of the contaminants (Skinner, 1991).

In engineered bioremediation, whether *in situ* or bioreactor, on-line measurement of critical process variables is essential for process engineering decisions. Strategies for successful bioremediation must include control schemes that manipulate treatments to enhance effectiveness of degradation based on a measured process parameter. Creation of biosensors is one of the critical needs in all processes that utilize microorganisms, including bioremediation (Humphrey, 1984).

In situ remediation, particularly natural attenuation, requires a monitoring strategy for determining the success of bioremediation that involves demonstrating that biodegradation is occurring in the field (Rittmann, 1992). Direct evidence of biological performance toward the contaminant can validate treatment effects on-line in the remediation process (Brown, 1992).

Two common ground water contaminants are toluene and trichloroethylene. Toluene is a constituent of fuels, while TCE has been extensively used as a solvent, and is a contaminant of toxic and carcinogenic concern (Van Duren and Banerfee, 1976). Due to their toxicity, the EPA has issued maximum contaminant level guidelines for both of these compounds in drinking water supplies (Fetter, 1992). In a survey of contaminants on Department of Energy (DOE) lands, toluene was the most prevalent fuel hydrocarbon, and TCE was the most prevalent chlorinated hydrocarbon in ground water, soils, and sediments. The mixture of chlorinated and fuel hydrocarbons was given the highest priority for subsurface science research (Riley, 1992). At the Savannah River Site alone, the DOE estimates there is 4.4 million kg of TCE contaminated soil and groundwater (Hazen, 1991).

Activated Sludge Wastewater Treatment

Toxicity of wastewater to activated sludge communities can result in higher operating costs and reduced effluent water quality. Toxic shock causes death of microorganisms and loss of floc structure. The resulting small flocs (pin flocs) settle poorly in downstream clarifiers, and costly polymer addition is required to meet

effluent water quality standards. Effluent violations may result from release of toxicants to receiving waters from loss of specific degrading populations. These effects can be avoided if the incoming waste stream is screened for toxicity, and protective action taken. For example, the toxic stream can be diverted to a temporary holding basin and returned to the waste treatment system at a slower rate that does not impact sludge quality.

Toxicity Assessment Methods

An ideal assessment method for measurement of wastewater toxicity to activated sludge is inexpensive, on-line, easy to use, sensitive, and relevant to sludge microbial communities. Existing methods of assessing toxicity include the following: (1) analyzing for known chemical constituents that cause toxicity; (2) microscopic methods; (3) respirometric inhibition methods; and (4) bioluminescent methods. However, each of these methods has inherent limitations for on-line toxicity monitoring. Therefore, on-line monitoring of influent toxicity for the purpose of avoiding sludge damage is rarely employed.

Chemical analysis of influent wastewater for toxicants requires knowledge of the identity of potential toxicants, is expensive, and is not rapid enough for effective process control responses. The time available for diversion of toxic influents to holding basins is often on the order of seconds to minutes. Municipal treatment plants are especially susceptible to toxic shock because there are too many possible toxic compounds for chemical analysis. Drawbacks to microscopic methods are that they

are time consuming and difficult because cells must be quantified or examined under a microscope to determine toxic effects, and they are not effective as a preventative method.

Respirometric inhibition methods are the most commonly used methods to assess wastewater toxicity to activated sludge microorganisms (Kong, 1996; Strotmann, 1994). The oxygen consumption rate of the wastewater is compared to the consumption rate of a non-toxic control. The EC_{50} toxicity value is the concentration of toxicant for which there is a 50% reduction in oxygen consumption rate (Volskay, 1988). Decreases in respiration rate indicate toxicity. This method assesses the metabolic state of the entire community and is not specific to a certain population. Determination of toxicity with respirometry can be done on-line, but current technology tends to be expensive and time consuming. In batch grab samples there is a delay between a toxic compound in the incoming waste stream and the toxicity indication.

Genetics and Physiology of Bioluminescence

Bioluminescence refers to the emission of light from living organisms. While there are bacteria, fungi, fish, insects, shrimp and squid that emit light; bacteria are the most abundant (Meighen, 1991). Marine environments are the most common habitat where bioluminescent bacteria are found. The genera *Vibrio, Photobacterium* and *Xenorhabdus* contain most luminescent bacteria (Meighen, 1991). Bioluminescence reactions are catalyzed by enzymes called luciferases which require oxygen. The

bacterial bioreporters discussed here utilize *lux* system genes from *Vibrio* or *Photobacterium* species of bacteria.

The electron transport system consists of a series of membrane bound proteins that undergo oxidation and reduction reactions. The cycle begins with the diffusible hydrogen carrier $NADH_2$ donating two hydrogen atoms to a membrane bound flavoprotein. The flavoprotein expels two protons to the cell exterior and transports two electrons to an iron-sulfur protein. The iron-sulfur protein transfers the two electrons to a quinone which exports two more protons to the exterior of the cell and transports the electrons to cytochrome b. Cytochrome b transports the two electrons to cytochrome o which reduces oxygen to water. Hydrogen atoms are expelled to the exterior of the cell during this process which creates a potential across the cell membrane called the proton-motive force. The proton-motive force is the driving force for ATP generation from ADP by membrane bound ATPase (Brock, 1979; Neidhardt, 1990; Schlegel, 1990). Several of the components of the electron transport system participate in the production of bioluminescence: $NADH_2$, flavoprotein and ATP.

The pathway for the production of light branches off the electron transport system that transports electrons from the electron donor to the final electron acceptor (Figure 1-1) (Hastings and Nealson, 1977). The light producing reaction is the luciferase catalyzed co-oxidation of reduced flavin mononucleotide ($FMNH_2$) and a long chain (8-16 carbons) aliphatic aldehyde. The luciferase turnover time in this reaction is one of the slowest measured, on the order of 10 s (Nealson, 1979). $FMNH_2$ binds to the *lux* gene product luciferase to produce complex I (Figure 1-1);

this complex reacts with oxygen to produce complex II, which can decay, reducing the luciferase, without producing light. However, when complex II binds to an aldehyde, an excited intermediate termed complex III is formed. Complex III decays, oxidizing the aldehyde to fatty acid and emitting light at 490 nm.

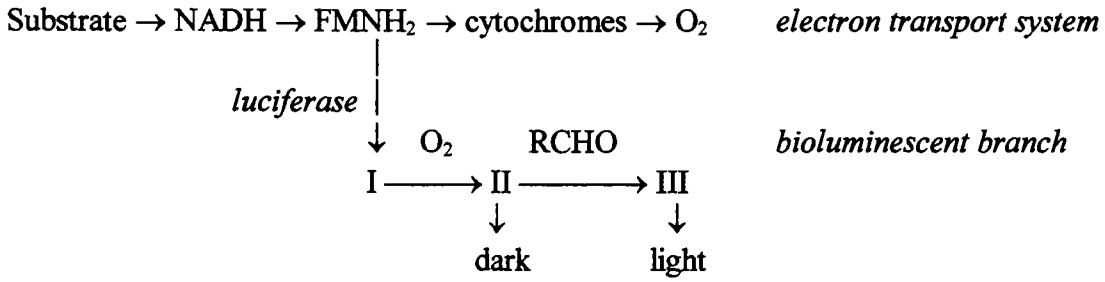

Figure 1-1. Bioluminescent system coupled to the electron transport system. Adapted from Hastings, J.W. and K.H. Nealson. 1977. Bacterial Bioluminescence. Annual Reviews in Microbiology. 31:549-95.

The primary substrates for the light reaction are $FMNH_2$, luciferase, oxygen and aldehyde (Figure 1-2). While the cellular oxygen concentrations are a result of environmental oxygen mass transfer into the cell; $FMNH_2$, luciferase and aldehyde concentrations are a result of complex cellular processes. $FMNH_2$ is a flavoprotein electron carrier that participates in the electron transport system. Luciferase is a *lux* gene product, and the concentration of luciferase is dependent on induction, transcription and translation of the *lux* genes. Intracellular aldehyde is produced in the cell by the reduction of fatty acid catalyzed by *lux* gene products.

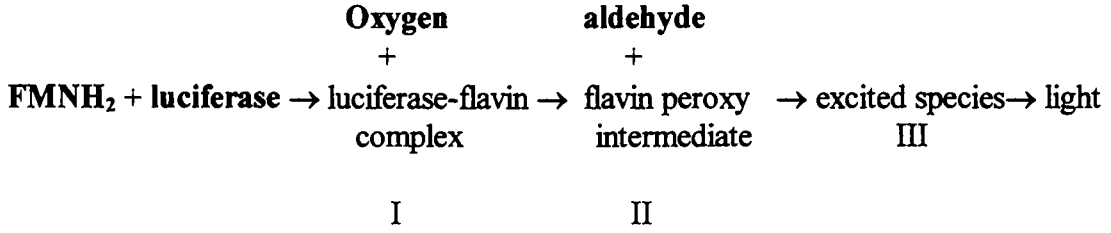

Figure 1-2. Light producing reaction series. Adapted from Hastings, J.W. and K.H. Nealson. 1977. Bacterial Bioluminescence. Annual Reviews in Microbiology. 31:549-95.

High dissolved oxygen levels are not required for maximum bioluminescence. Maximum luminescence can be maintained at 10% of normal oxygen uptake rates (Hastings, 1985). When oxygen is introduced to anaerobically grown bioluminescent bacteria (naturally bioluminescent facultative anaerobes) a flash of light is detected, and then bioluminescence declines to steady-state levels. This is due to oxygen limitation during anaerobic growth coupled with a build up of $NADH_2$ (Brock, 1984).

The *lux* operon consists of five genes (*luxCDABE*) that encode for the enzymes that catalyze the reactions responsible for the production of light (Figure 1-3). Reductase, the gene product of *luxC*, and synthetase (*luxE*) catalyze the reduction of fatty acid to aldehyde. Transferase, the gene product of *luxD*, transfers biosynthesis of fatty acids in the cell membrane for lipid synthesis to the light reaction. The *luxAB* genes encode for the luciferase enzyme which catalyzes the actual light producing oxidation of aldehyde back to fatty acid (Hastings, 1977; Hastings, 1985; Meighen, 1991).

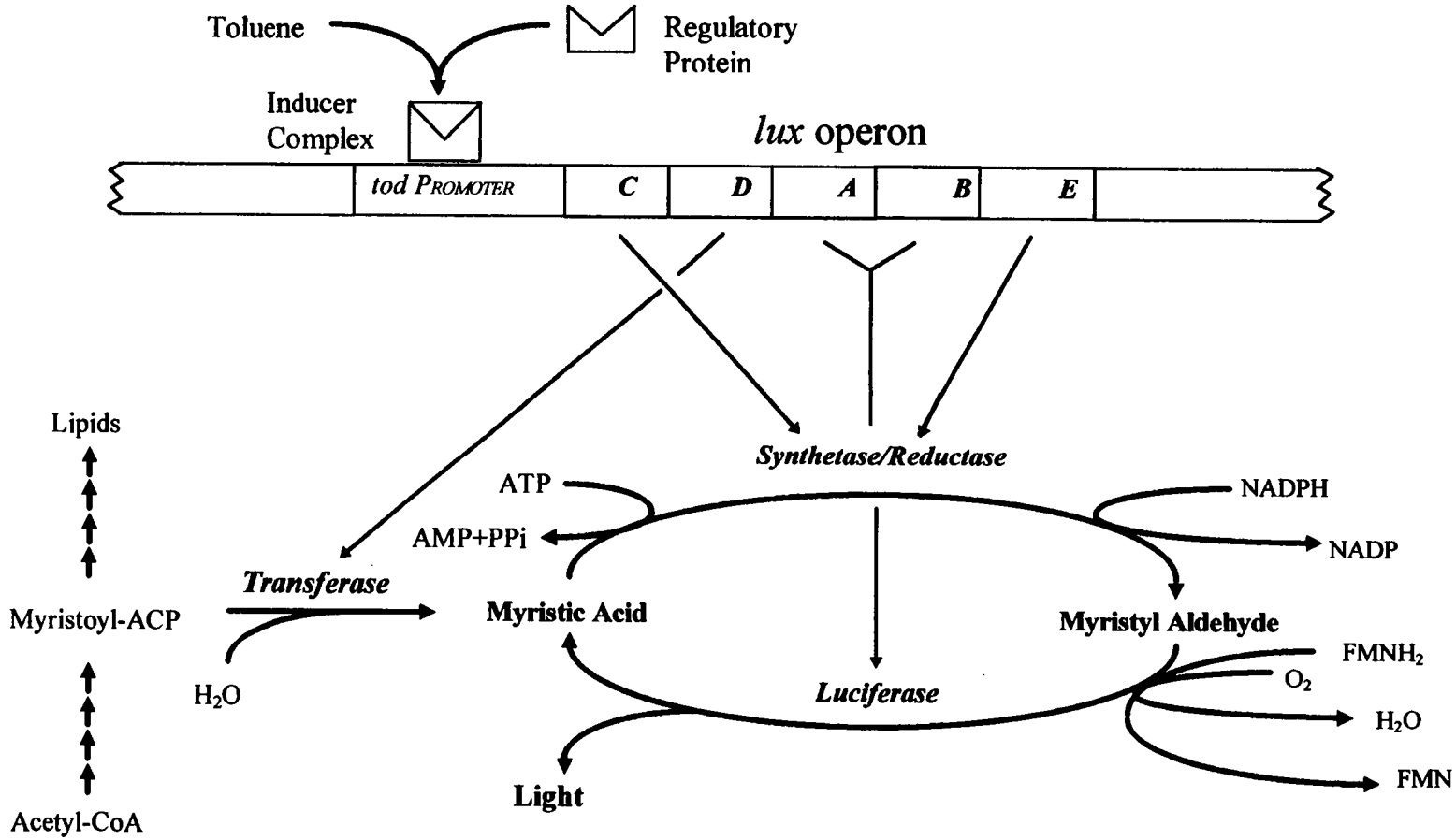

Figure 1-3. *lux* genes, associated gene products, and the reactions involved in bioluminescence. This figure was adapted from Sayler, G.S., U. Matrubutham, R. Palmer and C. Kelly. 1995. Application of Molecular Biology to Real Time Monitoring in Bioremediation. Proceedings for the OECD Workshop Amsterdam 1995 on Wider Applications and Diffusion of Bioremediation Technologies.

Bioluminescent Reporters

Previously developed bioluminescent reporters include bioluminescent bacteria used to assess toxicity or to assess the potential for degradation of groundwater contaminants.

Toxicity Bioreporters

The use of bioluminescent microorganisms for toxicity measurements is relatively simple, rapid, and does not require chemical identification of the toxic agents. Bioluminescent methods to assess toxicity include naturally luminescent marine bacteria and bacteria genetically engineered to produce bioluminescence. Bioluminescent methods are rapid and sensitive and have the capability to be used for on-line measurement.

Commercially available bioluminescent assays employ marine microorganisms, which tend to be sensitive to toxicants compared to activated sludge populations, and do not survive in typical activated sludge wastewater treatment systems. The Microtox system for assessing ecotoxicity is the benchmark of bioluminescent methods (Paton, 1995). This test consists of adding *Photobacterium phosphoreum* to a saline buffered, neutral pH solution and measuring the bioluminescent response to the addition of sample (Dutka, 1983). The inherent difficulties of Microtox are the requirements for pH and saline buffering, problems with reproducibility (Dutka, 1983), and that the organism is not representative of activated sludge communities.

Engineered bioluminescent toxicity assessment methods include *lux* marked bioreporters for copper toxicity and aluminum or nickel toxicity. Paton (1995) compared toxicity assessment with a constructed *lux* bioreporter and the marine bacterium *P. phosphoreum* on whisky distillery process and waste streams. The bioreporter was constructed by inserting the *lux* genes into the terrestrial bacterium *P. fluorescence*. The pH requirements of the marine bacterium interfered with toxicity assessment because of the low copper availability at neutral pH, while the *lux* marked bioreporter assessed copper toxicity at the process pH (Paton, 1995). DuBow (1992) constructed a biosensor by inserting the *lux*AB genes into *E. coli,* resulting in a reporter that responds with increasing bioluminescence in the presence of nickel or aluminum.

Inducible Bioreporters for Contaminated Groundwater Monitoring

The inducible reporters for groundwater contamination include *Pseudomonas fluorescens* HK44 for the degradation of naphthalene and the *tod-lux* reporters employed in this study.

nah-lux Bioreporter HK44

Reporter plasmid pUTK21, containing the *lux* genes (*lux*CDABE) from *Vibrio fischeri* inserted into the *nah*G of the salicylate degradation operon, was mated into a manufactured-gas plant soil isolate *P. fluorescens* HK9. The resulting strain was referred to as *Pseudomonas fluorescens* HK44. HK9 was able to degrade salicylate,

but not naphthalene (Nah-, Sal+ phenotype). However, HK44, due to the upper naphthalene degradation operon on reporter plasmid pUTK21, was able to degrade naphthalene (Nah^+ Sal^+ phenotype) (King, 1990).

HK44 was used to assess naphthalene bioavailability, which refers to what extent the compound is accessible to bacterial degradation. In a standardized assay bioluminescence from HK44 responded rapidly (15 min) to naphthalene, and a quantitative relationship between naphthalene concentration and bioluminescence was observed (Heitzer, 1992). The reporter was immobilized in a biosensor placed in a simulated contaminant stream. Bioluminescence was observed in response to both naphthalene and aqueous solutions of mixed contaminants containing naphthalene (jet fuel and manufactured-gas plant soil leachate) (Heitzer, 1994). Through the use of frequency analysis with sinusoidal perturbations in naphthalene feed concentration DiGrazia (1991) indicated bioluminescence was related to naphthalene biodegradation kinetics.

tod-lux Bioreporters B2 and TVA8

The inducible bioreporters examined in this study were *P. putida* B2 and TVA8. *P. putida* B2 was constructed by cloning the *tod* promoter fragment from plasmid pDTG514 in front of the promoterless *lux* gene cassette (*lux*CDABE) on plasmid pUCD615. The resulting plasmid (pUTK30) was mated into the wild type strain *P. putida* F1 (Applegate, 1997). The resulting bioreporter, *P. putida* B2, contained both the *tod* and *lux* operons under *tod* promoter control (Figure

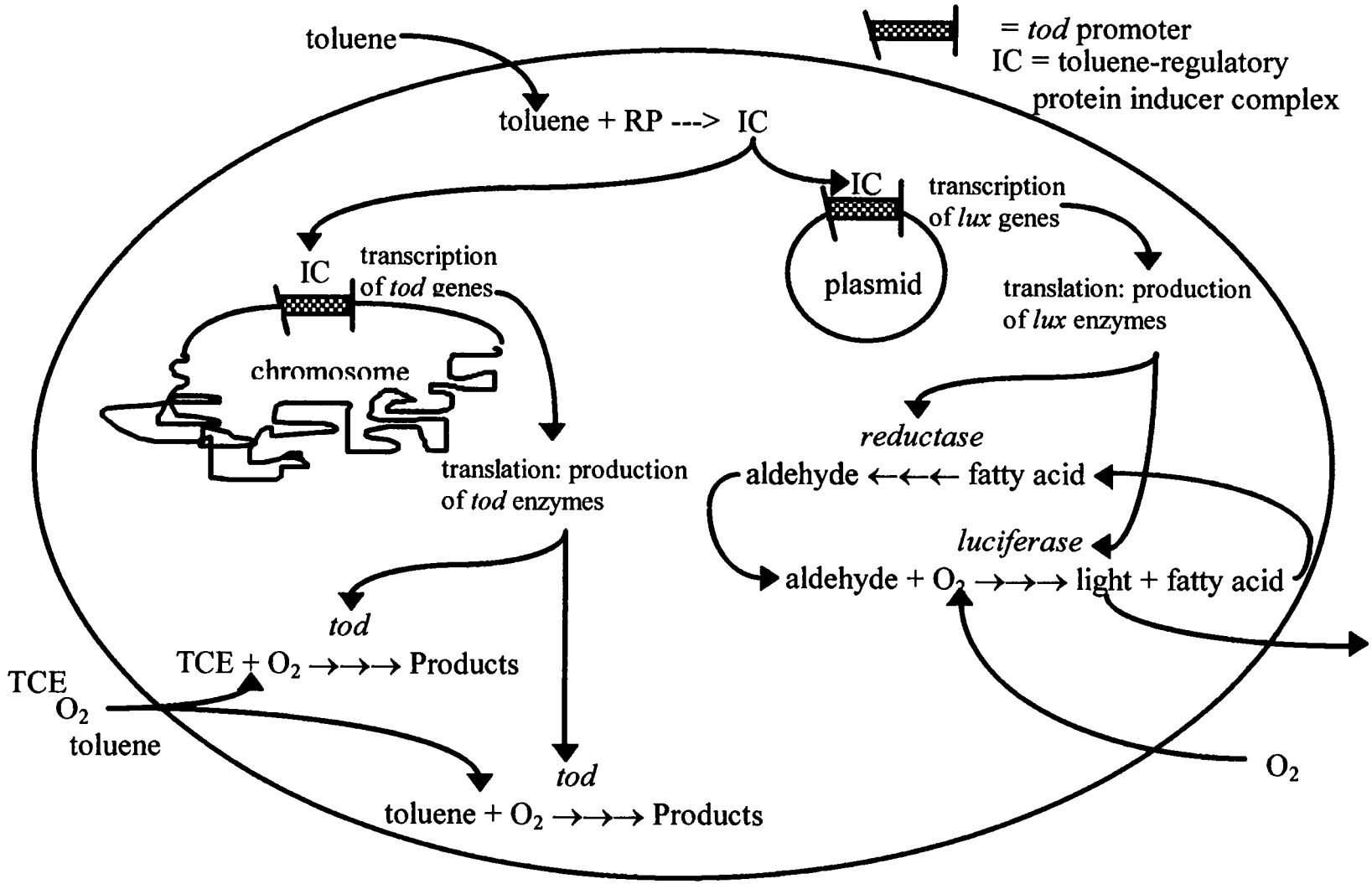

Figure 1-4. Depiction of a single cell of the bioreporter *Pseudomonas putida* B2.

1-4). *P. putida* TVA8 was constructed by introducing a *tod-lux* (*tod* promoter with *lux*CDABE) transcriptional fusion into the chromosome of *Pseudomonas putida* F1 (Applegate, 1997). The transposon insertion was shown to be stable under both selective (kanamycin) and non-selective conditions in both batch and continuous experiments by comparisons of colony counts, as well as *lux*A DNA colony hybridization. In addition, the reporter strain TVA8 was found to grow at similar rates to the parent strain F1. Toluene concentrations as low as 50 *u*g/L were found to increase background bioluminescence 80 fold (Applegate, 1997).

A *kan* marker was included in the genetic element inserted into *P. putida* F1 to create both bioreporters. The kanamycin resistance gene (*kan*) encodes for an enzyme that prevents the antibiotic kanamycin from binding to the ribosomes and inhibiting translation (Maniatis, 1982).

Toluene Dioxygenase

The *tod* promoter controls the expression of both the degradative and light producing enzymes in the *tod-lux* reporters; therefore, the *tod* promoter warrants a thorough discussion of its known regulatory properties. The general concept of signal transduction is discussed first for background. By the mid-1980s many two-component signal transduction regulatory systems were discovered. These systems consist of two families of homologous proteins; protein kinases (PK) and phosphorylated response regulators (PRR). The PK signals the PRR of environmental conditions, such as glutamine limitation, inorganic phosphate transfer rate limitation,

or osmotic pressure increase, through phosphorylation. The PK is the sensor of the environmental condition, and is often a transmembrane protein with the conserved C terminal region in the interior of the cell. This region contains the histadine residue that becomes phosphorylated upon the signal conditions. The PK in turn phosphorylates the aspartic acid residue in a conserved region of about 100 amino acids on the PRR near the amino terminal. PRR are often DNA binding proteins that regulate gene transcription (Neidhardt, 1990).

Regulation of aromatic hydrocarbon metabolism has been known to fall into the LysR, NtrC (σ^{54} dependent) or AraC regulatory families; however, recently the toluene dioxygenase system of *P. putida* F1 was found to possibly belong to the two-component signal transduction family (Lau, 1996). The *todS*-*todT* gene product proteins encoded by regions of DNA downstream of the *tod* operon are hypothesized to be the PK-PRR components of the regulatory system. The *todS* gene product structure is unique among protein kinases in that it consists of five known domains that include a leucine zipper (bZIP), a conserved histidine kinase at the amino terminus, a response regulator, a putative oxygen sensing element, and a duplicate histidine kinase at the C terminus. The bZIP domain in eukaryotes mediates protein dimeriztion and binds to DNA. Although the specific regulatory properties of the *todS*-*todT* system have not been elucidated, the system is involved in regulation of the *tod* operon as disruption of these DNA regions yields the strain unable to grow on toluene as a sole-carbon source.

Pseudomonas putida F1 was isolated from soil by enrichments with ethyl benzene. The organism grew equally well with toluene as the sole carbon source (Gibson, 1968). The first step in the oxidation of toluene utilizes a three component enzyme, a flavoprotein, and 2 non-heme iron proteins (Figure 1-5). This reaction was found to require 1 mol O_2 per mole of toluene, iron and NADH. The three enzyme components consist of (1) a flavoprotein, ferredoxin$_{TOL}$ reductase, (2) ferredoxin$_{TOL}$, and (3) an iron sulfur protein, ISP$_{TOL}$. Ferredoxin$_{TOL}$ transfers electrons from NADH, and reduces ferredoxin$_{TOL}$. Electrons are then transferred to ISP$_{TOL}$ which catalyzes the oxidation of toluene (Gibson, 1982).

Cis-toluene dihydrodiol undergoes several reaction steps to yield acetate and 2-hydroxypenta-2,4-dienoate (Figure 1-6) (Zylstra, 1988). In addition to the initial oxidation of toluene, each subsequent reaction step is catalyzed by a gene product of the toluene dioxygenase operon. *todA, todB, todC1* and *C2* encode for ferredoxin$_{TOL}$ reductase, ferredoxin$_{TOL}$ and ISP$_{TOL}$, respectively. *todD* encodes for a dehydrogenase, *todE* encodes a dioxygenase, while *todF* encodes for a hydrolase. The gene order for these enzymes is *todFC1C2BADE* (Zylstra, 1988). The nucleotide sequence of *todC1C2BAD* genes exhibits significant homology to the sequence for benzene dioxygenase, while the *todDE* resembles dehydrogenases from another *Pseudomonas* (Zylstra, 1989). The final three genes discovered in the *tod* operon are *todGIH*, which encode for enzymes that catalyze the final three reaction steps in the toluene degradation pathway (Figure 1-6) (Lau, 1994). The *tod* operon contains 10 genes

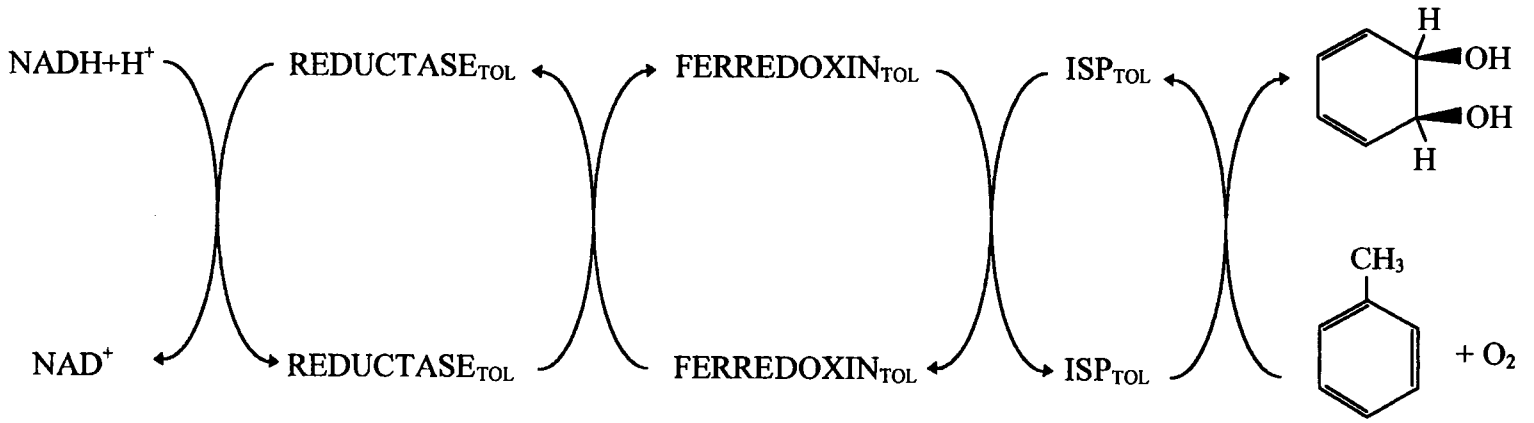

Figure 1-5. First step in the degradation of toluene by the toluene dioxygenase pathway. Adapted from Gibson, D.T., W. Yeh, T. Liu and V. Subramanian. 1982. Toluene dioxygenase: A multicomponent enzyme system from *Pseudomonas putida*. Oxygenases and Oxygen Metabolism. 51-61.

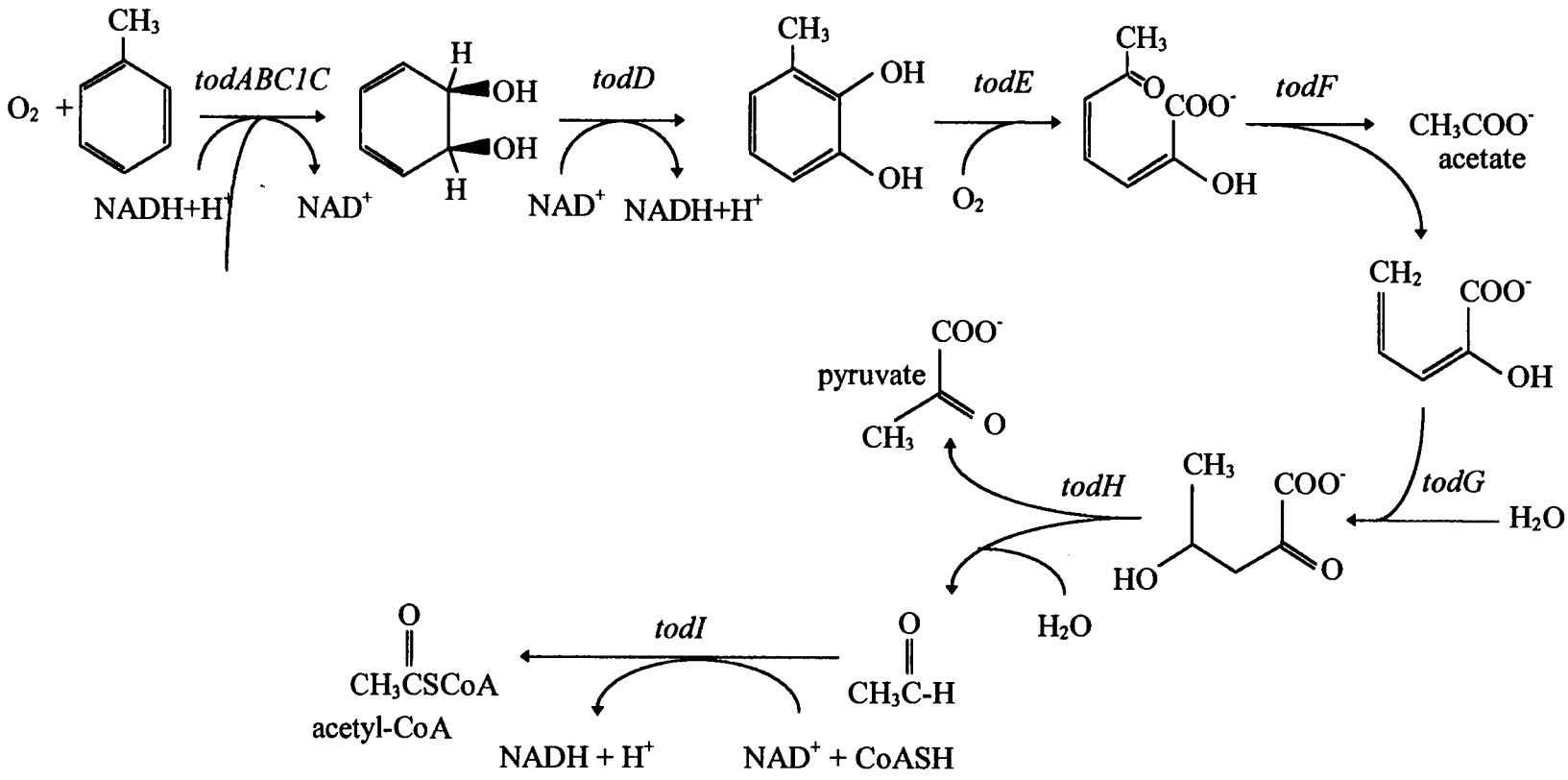

Figure 1-6. The degradation of toluene by the toluene dioxygenase pathway. Adapted from Lau, P.C.K., H. Bergeron, D. Labbe, Y. Wang, R. Brouseau and D.T. Gibson. 1994. Sequence and expression of the *todGIH* genes involved in the last three steps of toluene degradation by *Pseudomonas putida* F1. Gene. 146:7-13.

that encode for enzymes that catalyze 7 reaction steps in the degradation of toluene. The gene order is *todFC1C2BADEGIH* (Lau, 1994).

The *todR* and *todX* are genes located upstream of the *tod* structural genes that encode for proteins. A toluene inducible promoter was discovered upstream of these genes, and is assumed to control transcription of all *tod* genes. *todX* encodes for a membrane protein and is suggested to possibly be involved in transporting toluene into the cell, while *todR* was not found to have a significant affect on *tod* regulation, although it exhibits homology to other transcriptional activators (Wang, 1995).

In addition to degrading toluene, the toluene dioxygenase enzymes are responsible for the co-metabolic degradation of TCE. *Pseudomonas putida F1* cells were shown to degrade TCE after exposure to toluene, and lose the ability to degrade toluene when the *todC* gene was made defective by mutagenesis. (Wackett, 1988). TCE degradation was also observed by *E. coli* cells containing cloned *todC1C2BA* genes (Zylstra, 1989).

Biological Process Modeling

Biomass, substrate, and product concentrations are common variables for modeling of biological systems. Mathematical models are used to relate these variables to process parameters. Model development typically begins with a mass balance on the reactor volume. Expressions for the rate of consumption of substrate, product formation and production of biomass are proposed. A common rate expression for the consumption of substrate can be derived from the Michaelis-Menten method, while a

common biomass production expression is the Monod equation. Both of these equations have the same form.

Michaelis-Menten Kinetics

The following analysis is for derivation of Michaelis-Menten kinetics of two substrates competing for a single enzyme. It is an extension of the classical single substrate enzyme model for the rate of substrate utilization.

Consider the degradation of two substrates, S_1 and S_2, catalyzed by a single enzyme, E (Equations 1-1 and 1-2).

$$E + S_1 \underset{k^1_{-1}}{\overset{k^1_1}{\leftrightarrow}} ES_1 \xrightarrow{k^1_2} E + P_1 \qquad (1\text{-}1)$$

$$E + S_2 \underset{k^2_{-1}}{\overset{k^2_1}{\leftrightarrow}} ES_2 \xrightarrow{k^2_2} E + P_2 \qquad (1\text{-}2)$$

The dissociation constant, K, of these reactions can be expressed in terms of substrate and substrate-enzyme complex concentrations (reaction 1-1 is shown in Equation 1-3, a similar expression can be written for reaction 1-2).

$$\frac{[E][S_1]}{[ES_1]} = \frac{k^1_{-1}}{k^1_1} = K_1 \qquad (1\text{-}3)$$

The rate expression (change in substrate concentration with time) can also be expressed in terms of substrate and complex concentrations (Equation 1-4).

$$v_R = -\frac{dS_1}{dt} = k_1^1[E][S_1] - k_{-1}^1[ES_1] \qquad (1\text{-}4)$$

The quasi-steady-state approximation is applied (the rate of change of complex concentration is approximately zero). This assumption is valid when the substrate concentration is much greater than the enzyme concentration (Equation 1-5).

$$\frac{d[ES_1]}{dt} = \frac{d[ES_2]}{dt} = 0 \qquad (1\text{-}5)$$

The total amount of enzyme remains constant, resulting in the following expression.

$$[E] + [ES_1] + [ES_2] = [E_o] \qquad (1\text{-}6)$$

Simplifying these equations yields the Michaelis-Menten expression for two substrates competing for the same enzyme (Equation 1-7 and 1-8) (Baily and Ollis, 1986; Brock, 1984).

$$-\frac{d[S_1]}{dt} = \frac{k_1'[S_1]}{K_1\left(1+\frac{[S_2]}{K_2}\right)+[S_1]} \qquad (1\text{-}7)$$

$$-\frac{d[S_2]}{dt} = \frac{k_1'[S_2]}{K_2\left(1+\frac{[S_1]}{K_1}\right)+[S_2]} \qquad (1\text{-}8)$$

Monod Kinetics

The Monod equation expresses the cellular growth rate with a single limiting substrate for an enzyme catalyzed reaction (Equation 1-9).

$$\mu = \frac{\mu_{max} S}{K_s + S} \qquad (1\text{-}9)$$

K_s is the substrate concentration at which the growth rate is one-half of the maximum growth rate. At substrate concentrations below K_s there is a strong linear dependence of growth rate on substrate concentration, above K_s, there is a diminishing dependence of growth rate on substrate concentration (Baily and Ollis, 1986; Brock, 1984).

Steady-state Chemostat Model

A mass balance is performed on the substrate and cell mass (Equation 1-10) with the following assumptions:

- Monod cellular growth kinetics with a single substrate, $\mu = \frac{\mu_{max} S}{K_s + S}$
- steady-state, $\frac{dS}{dt} = \frac{dX}{dt} = 0$
- sterile feed , $X_f = 0$
- a yield coefficient defines the mass of cells obtained per mass of substrate, $Y_{X/S}$
- dilution rate is defined as $D = F/V$

accumulation = in - out + generation - consumption (1-10)

Cell mass balance. Applying the assumptions discussed above, the cell mass balance yields the following equation:

$$0 = 0 - FX + \mu XV \qquad (1\text{-}11)$$

Simplifying Equation 1-11 yields:

$$DX = \mu X \qquad (1\text{-}12)$$

As can be seen from Equation 1-12, only if the instantaneous growth rate is equal to dilution rate can a non-zero steady state cell density be maintained. Therefore, at

steady-state the instantaneous growth rate equals the dilution rate in a chemostat (Equation 1-13).

$$D = \mu \qquad (1\text{-}13)$$

If the Monod rate expression is substituted into Equation 1-13, the steady-state substrate concentration is a function of the dilution rate (Equation 1-14).

$$S = \frac{DK_s}{\mu_{max} - D} \qquad (1\text{-}14)$$

Substrate mass balance. A substrate mass balance on the reactor volume results in Equation 1-15.

$$\frac{dS}{dt} = FS_f - FS + 0 - \frac{\mu X}{Y_{X/S}} \qquad (1\text{-}15)$$

Applying the assumptions listed above, Equation (1-15) simplifies to Equation (1-16).

$$X = Y_{X/S}\left(S_f - \frac{DK_s}{\mu_{max} - D}\right) \qquad (1\text{-}16)$$

So the steady state-cell density in a chemostat is a function of the dilution rate and feed substrate concentration. The substrate concentration is near zero for low dilution rates, and only becomes significant as the dilution rate approaches the maximum specific growth rate. Therefore, the steady-state chemostat cell density depends primarily on the feed substrate concentration (Baily and Ollis, 1986; Brock, 1984).

Nomenclature:

μ	instantaneous growth rate, day^{-1}
μ_{max}	maximum growth rate when $S>>K_S$, day^{-1}
D	dilution rate, day^{-1}
E	chemical symbol representing enzyme in Michaelis-Menten development
E_o	chemical symbol representing the total amount of enzyme
F	feed flow rate, L/day
$k_1^{'}$	Michaelis-Menten overall rate constant for reaction 1
$k_2^{'}$	Michaelis-Menten overall rate constant for reaction 2
k_1^1	Michaelis-Menten rate constant
k_2^1	Michaelis-Menten rate constant
k_{-1}^1	Michaelis-Menten rate constant
k_1^2	Michaelis-Menten rate constant
k_2^2	Michaelis-Menten rate constant
k_{-1}^2	Michaelis-Menten rate constant
K_1	dissociation constant for reaction 1 in Michaelis-Menten rate expression development
K_2	dissociation constant for reaction 2 in Michaelis-Menten rate expression development
K_s	Monod constant, mg/L
P_1	chemical symbol representing the products of reaction 1
P_2	chemical symbol representing the products of reaction 2
S	substrate concentration, mg/L
S_1	chemical symbol representing the reactant of reaction 1
S_2	chemical symbol representing the reactant of reaction 2
S_f	feed substrate concentration, mg/L
t	time, day
V	reactor volume, L
v_R	reaction rate $= -\frac{dS}{dt} = \frac{dP}{dt}$, mg/L day
X	cell mass density, mg/L
X_f	cell mass density in the feed, mg/L
$Y_{X/S}$	cellular yield, mg cells/mg substrate

CHAPTER 2

PRELIMINARY STUDIES

This chapter discusses methodology and preliminary experiments. The methods described are (1) bacterial growth media, (2) biomass quantification, (3) light measurement, and (4) toluene and TCE quantification.

The preliminary experiments were performed to ensure appropriate conditions for subsequent experiments. They consisted of the following: (1) bioluminescent response of Shk 1 to oxygen concentration, (2) effect of antibiotic (kanamycin) on B2 growth rate, (3) the stability of the *tod-lux* construct in *Pseudomonas putida* B2, and (4) the comparison of toluene degradation rates between the bioreporter B2 and the parent strain F1.

Experimental Methods

Bacterial Growth Media

Several types of bacterial growth media were used for the experiments in this research. This section identifies which medium was used for each type of experiment (Table 2-1) and provides media recipes (Table 2-2 through 2-5).

The solid media used in dilution plating were complex media (chemically undefined), while each of the liquid media were synthetic, or completely chemically defined. Solid media R2A and PIA were prepared formulations (Difco Laboratories,

Detroit, MI). The succinate minimal medium was used for the batch experiments with succinate as the carbon source, while mineral salts medium was used as the growth medium when toluene was used as the sole carbon source.

Toluene was supplied in vapor form to batch cultures for the batch growth experiments and overnight culture preparation. A glass tube, equipped with a glass bulb at the bottom filled with 200 *u*L pure toluene, and a hole in the side of the tube, was inserted in the rubber stopper of the flask. Toluene vaporized from the bulb and exited the hole to the vapor space above the culture. The toluene vapor partitioned into the liquid phase provided substrate for growth.

Table 2-1. Growth media.

solid media for plates	**liquid growth media for *tod-lux* bioreporters**	**liquid growth medium for Shk 1 toxicity reporter**
Luria broth (LB)	minimal salts + succinate	simulated wastewater medium
R2A	mineral salts	
Pseudomonas isolation agar (PIA)		

Table 2-2. Luria Broth.

Compound	**amount**
tryptone	10 g
yeast extract	5 g
NaCl	10 g
agar	17 g
distilled H2O	1000 mL

Table 2-3. Minimal salts with succinate medium.

Minimal salts[a]	concentration	trace elements[b]	dissolved in 190 mL water and 10 mL concentrated HCl
sodium succinate	2.7	MgO	2.0 g
KH_2PO_4	0.68 g/L	$CaCO_3$	0.4 g
K_2HPO_4	1.73 g/L	$FeCl_3.6H_2O$	1.08 g
ammonium nitrate	0.2 g/L	$ZnSO_4.7H_2O$	0.288 g
$MgSO_4.7H_2O$	0.0.1 g/L	$CuSO_4.5H_2O$	0.05 g
NH_4NO_3	1.0 g/L	$CoSO_4.7H_2O$	0.0056 g
$CaSO_4.2\ H_2O$	0.054 g/L	H_3BO_3	0.0124 g
trace elements	0.1 mL/L	$Na_2MoO_4.2H_2O$	0.098 g

[a] Davis and Mingioli, 1950.
[b] Meynell and Meynell, 1965.

Table 2-4. Mineral salts medium[a].

solution A	concentration	solution B	concentration	metals 44*	concentration
Na_2HPO_4	141.2 g/L	nitrilo triacetic acid	10	EDTA	2.5 g/L
KH_2PO_4	136 g/L	$MgSO_4$	14.5 g/L	$ZnSO_4.7H_2O$	1.1 g/L
		$CaCl_2$	3.3 g/L	$MnSO_4.H_2O$	1.5 g/L
solution C	**concentration**	$(NH_4)_6Mo_7O_{24}.4H_2O$	9.3 g/L	$FeSO_4.7H_2O$	5 g/L
$(NH_4)_2SO_4$	200 g/L	$FeSO_4.7H_2O$	99 g/L	$CuSO_4.5H_2O$	0.39 g/L
		metals 44*	50 mL/L	$Co(NO_3)_2.6H_2O$	0.25 g/L
				$Na_2B_4O_7.10H_2O$	0.18 g/L

40 mL of solution A + 20 mL of solution B + 5 mL of solution C per L of media.

[a] Stanier, 1957.

Table 2-5. Components of simulated wastewater.

Component	Amount	Component	Amount
EASM		**Nitrogen Trace**	
Basal Inorganic	982 mL	distilled water	987 mL
Phosphorous	6 mL	Trace mix	8.3 mL
Nitrogen	6 mL	FeEDTA	2.1 g
Substrates	6 mL	$(NH_4)_2SO_4$	36.5 g
		$MnSO_4.H2O$	1.6 g
Basal Inorganic			
distilled water	8,882 mL	**Trace Mix**	
$CaSO_4.2H_2O$	7.4 g	distilled water	100 mL
salts	1000 mL	EDTA, Na_2	0.5 g
		$Na_2MoO_4.2H_2O$	0.1 g
Salts		$CoCl_2.6H_2O$	0.002 g
distilled water	1,000 mL	$ZnSO_4.7H_2O$	0.1 g
Na_2SO_4	3.2 g	$CuSO_4.5H_2O$	0.02 g
NaCl	0.8 g		
$MgSO_4.7H_2O$	1.0 g	**Substrates**	
adjust to pH 7.4		distilled water	750 mL
		$NaC_2H_3O_2.3H_2O$	169 g
Phosphorous		propionic acid	7 mL
distilled water	1,000 mL	butyric acid	5 mL
KH_2PO_4	0.65 g	methanol	22 mL
K_2HPO_4	2.3 g	isopropanol	20 mL
		ethylene glycol	15 mL
		acetone	11 mL
		ethanol	5 mL
		adjust to pH 7.4	

Bacterial Cell Quantification

Bacteria in suspended solutions were quantified turbidometrically, by optical density measurement correlated to cellular dry mass. Dilution plating was also performed, primarily to detect contamination and stability by comparing selective (kanamycin) to non-selective medium plates.

Optical density was measured with a spectrophotometer (Beckman model DU-70, Fullerton, CA) at 600 nm wavelength. The correlation between optical density (OD_{600}) and *Pseudomonas putida* B2 cell dry mass was determined by growing a large volume of cells, and measuring the cell density of dilutions of this culture. The culture was centrifuged for 10 min at 10,000 rpm to pellet the cells. The supernatant was poured off, and the pellet was resuspended in a small volume of water. This volume was vacuum filtered through a 0.2 *um* filter of known weight, then the filter was dried to a constant weight. The optical density of the dilutions versus the corresponding dry weight was plotted, and a linear least squares regression performed (Figure 2-1). This was done twice with the following cultures: 1L of 0.76 OD_{600}, and 0.87L of 0.59 OD_{600}. The linear regression resulted in the following correlation equation:

$$\text{cell dry mass (g/L)} = 0.5 \times OD_{600} \qquad (2\text{-}1)$$

Light Measurement

Bioluminescence was measured with photomultiplier technology. Two photomultiplier configurations were employed: (1) scintillation counter, and (2) a liquid light guide connected to a photomultiplier tube. The scintillation counter (Wallac, model MicroBeta 1450, Gaithersburg, MD) consisted of an automated photomultiplier that measured light from each well in a multi-well plate.

The second type of light measurement consisted of conducting light from the reaction vessel (a glass reactor or vial in a light tight chamber) through a liquid light guide to a photomultiplier tube (Oriel Corporation, model 7070, Stratford, CT). The

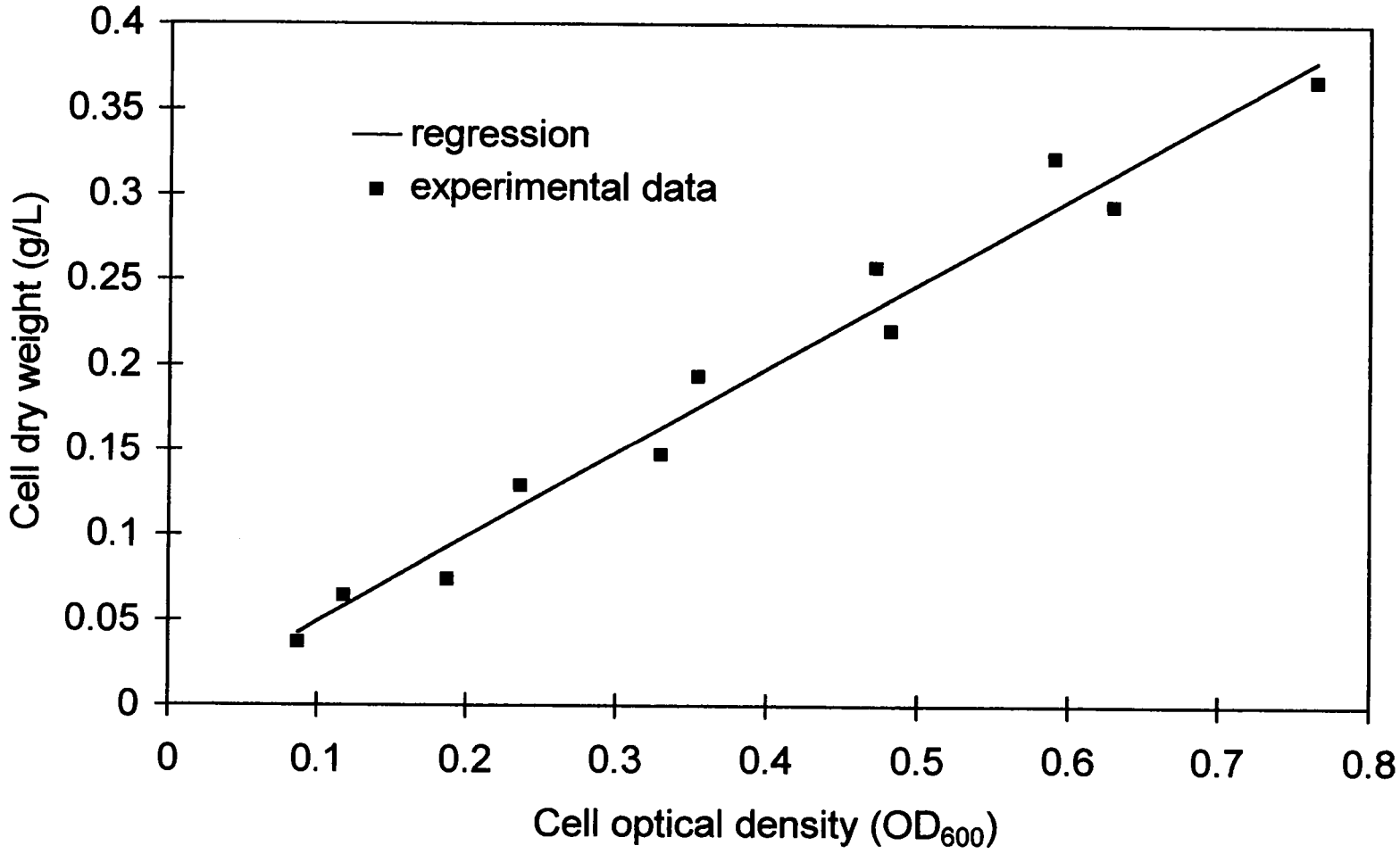

Figure 2-1. *Pseudomonas putida* B2 cell optical density versus cell dry mass.

liquid light guide was a plastic tube filled with clear fluid. The light entered the tube at one end and was transmitted via internal reflection to the other end of the tube. One end of the liquid light guide was placed against the clear glass of the reaction vessel, while the other was placed in the photomultiplier tube housing.

A photomultiplier measured the light in both types of configurations. The photomultiplier converted the light signal to an electrical current, and consisted of a photoemissive detector material that freed an electron when bombarded with a photon. The electrons created a current which was amplified and measured. Therefore, the number of photons per second that entered the photomultiplier housing was proportional to the electric current.

Bioluminescence and Culture Density

In the scintillation counter experiments, initial values of light were measured and compared with solutions of the same cell density. However, in vial or reactor experiments, a time course of light was often taken, where the cell density varied over time. The light measurement of interest was average bioluminescence per cell. The photomultiplier received light from the cells in a specific volume of liquid in front of the liquid light guide. To obtain specific bioluminescence, the electric current magnitude was divided by the cell culture density. To determine if bioluminescence increased proportionately with cell density, dilutions of a light producing culture of *P. putida* B2 were prepared and bioluminescence immediately measured. Bioluminescence was linear with cell density up to about 600 mg/L (Figure 2-2).

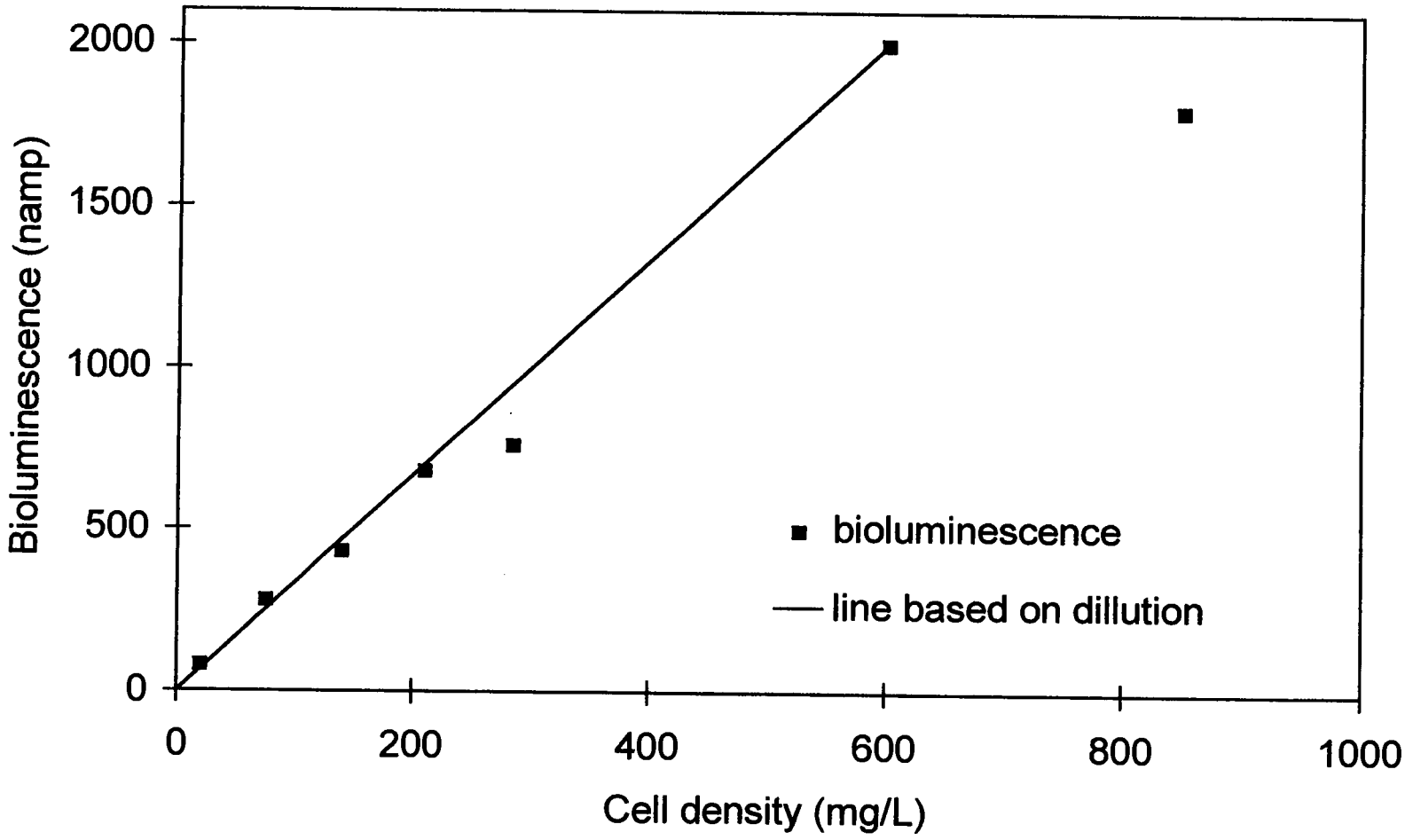

Figure 2-2. Effect of cell density on bioluminescence measurement.

Toluene and TCE Measurement

Toluene and TCE concentrations were monitored using head-space injections of 25 *u*L to a gas chromatograph (Shimadzu, model GC-14A, integrator chromatopak C-R4A) equipped with an electron capture detector and flame ionization detector in series and a 30 m Supelco Vocol column. A constant oven temperature of 150 °C, injector temperature of 250 °C and detector temperature of 250 °C were maintained. Calibration curves (Figure 2-3) were obtained using identical experimental sample vials. A known amount of distilled water and toluene or TCE were charged to the vial. The vial was shaken to equilibrate for 5-10 min, and then the head-space was sampled with a gas tight syringe. Concentrations are generally expressed as if all the solute were present in the liquid phase (except as noted).

Preliminary Experiments

The preliminary experiments performed were to determine the effect of oxygen concentration on bioluminescence by Shk 1, the effect of kanamycin concentration on growth rates of B2, the stability of the *tod-lux* construct in B2, and to compare B2 and F1 toluene degradation rates. These experiments were important in determining appropriate conditions for experiments that were central to the focus of this work.

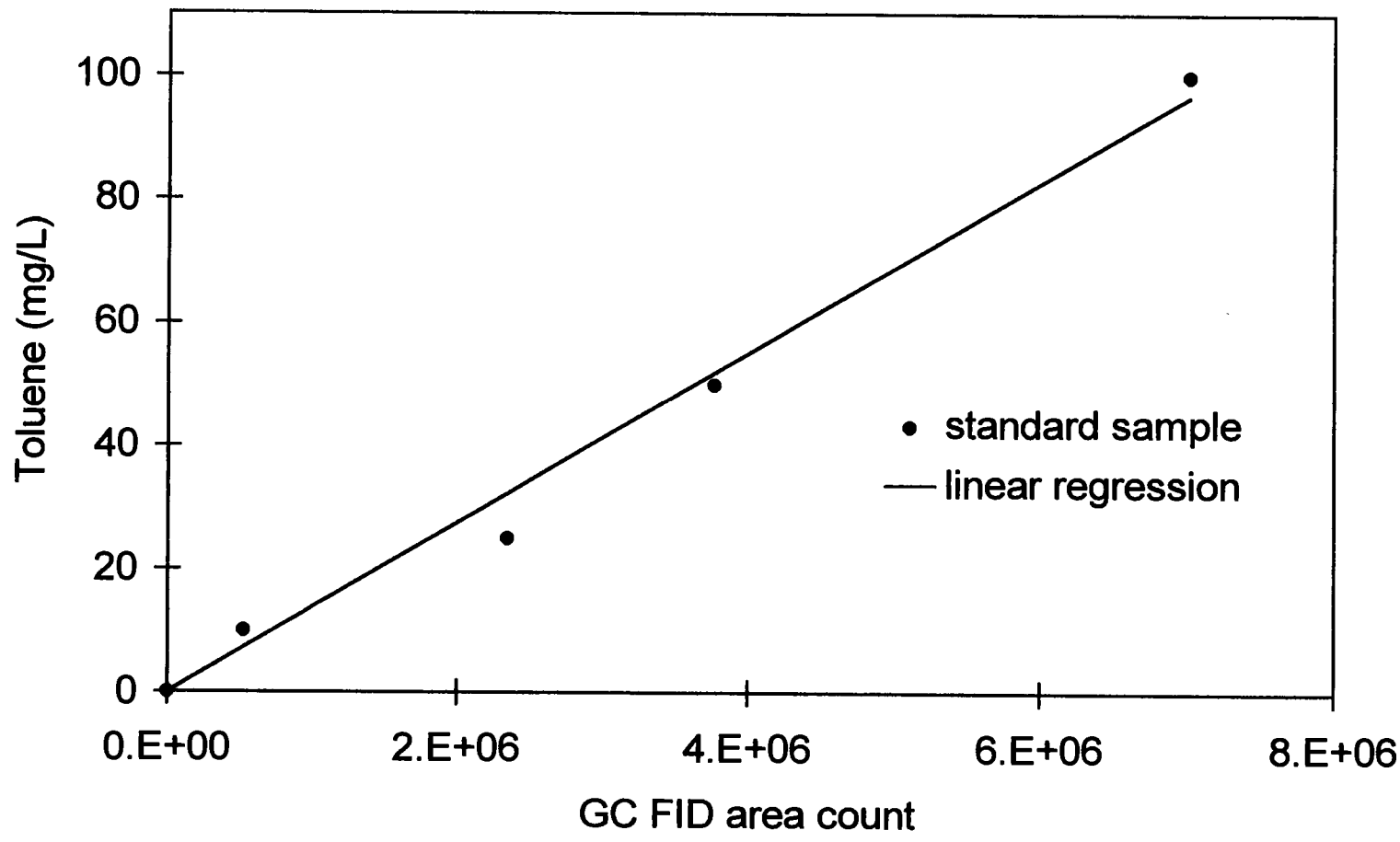

Figure 2-3. Sample gas chromatograph standard curve.

Effect of Oxygen Concentration

The effect of oxygen concentration on bioluminescence was examined because oxygen is a primary substrate in the bioluminescence reaction. Experimental and sensor design had to ensure oxygen was not a limiting substrate for bioluminescence. For example, dissolved oxygen concentrations in the activated sludge reactors were maintained at 2 mg/L, much lower than water saturation levels.

Methodology

A beaker equipped with air and nitrogen input streams, a dissolved oxygen meter, liquid light guide, and photomultiplier was loaded with mid-log phase Shk 1 reporter cells (Figure 2-4). The air feed was controlled by a solenoid valve connected to a dissolved oxygen meter/controller. Dissolved oxygen set-points were stepped down from 7, 5, 3, 2,1, 0.5 to 0 mg/L, with at least 5 minutes at each set-point. Bioluminescence was recorded automatically on a computer. The oxygen concentration was recorded every 1 min. After 20 minutes at 0 mg/L dissolved oxygen, the dissolved oxygen set-point was increased to 3 mg/L.

Results

Bioluminescence levels remained approximately constant at 137 namp until the oxygen concentration fell below 0.2 mg/L (Figure 2-5). At this low oxygen concentration, bioluminescence rapidly declined at a rate of 15 namp/min. When the oxygen set-point was increased, bioluminescence immediately increased at a rate of 14

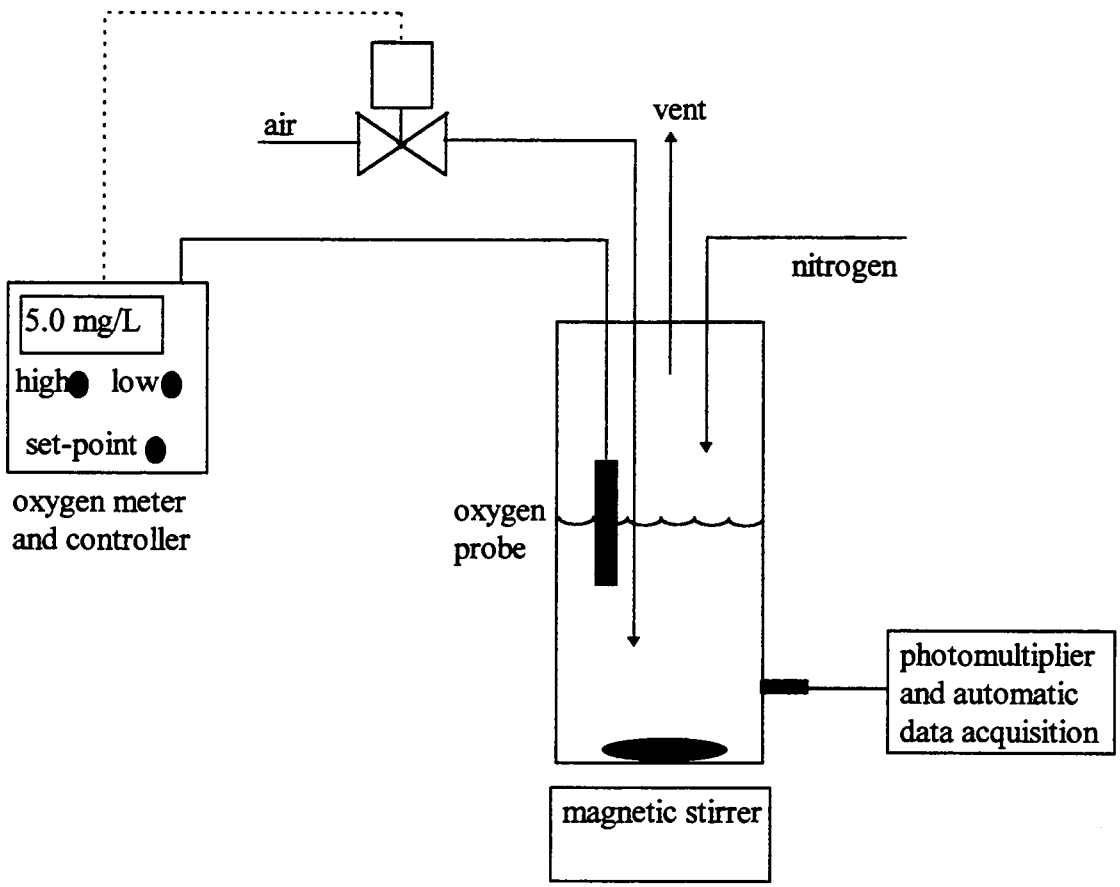

Figure 2-4. Experimental apparatus to examine the effect of oxygen concentration on bioluminescence.

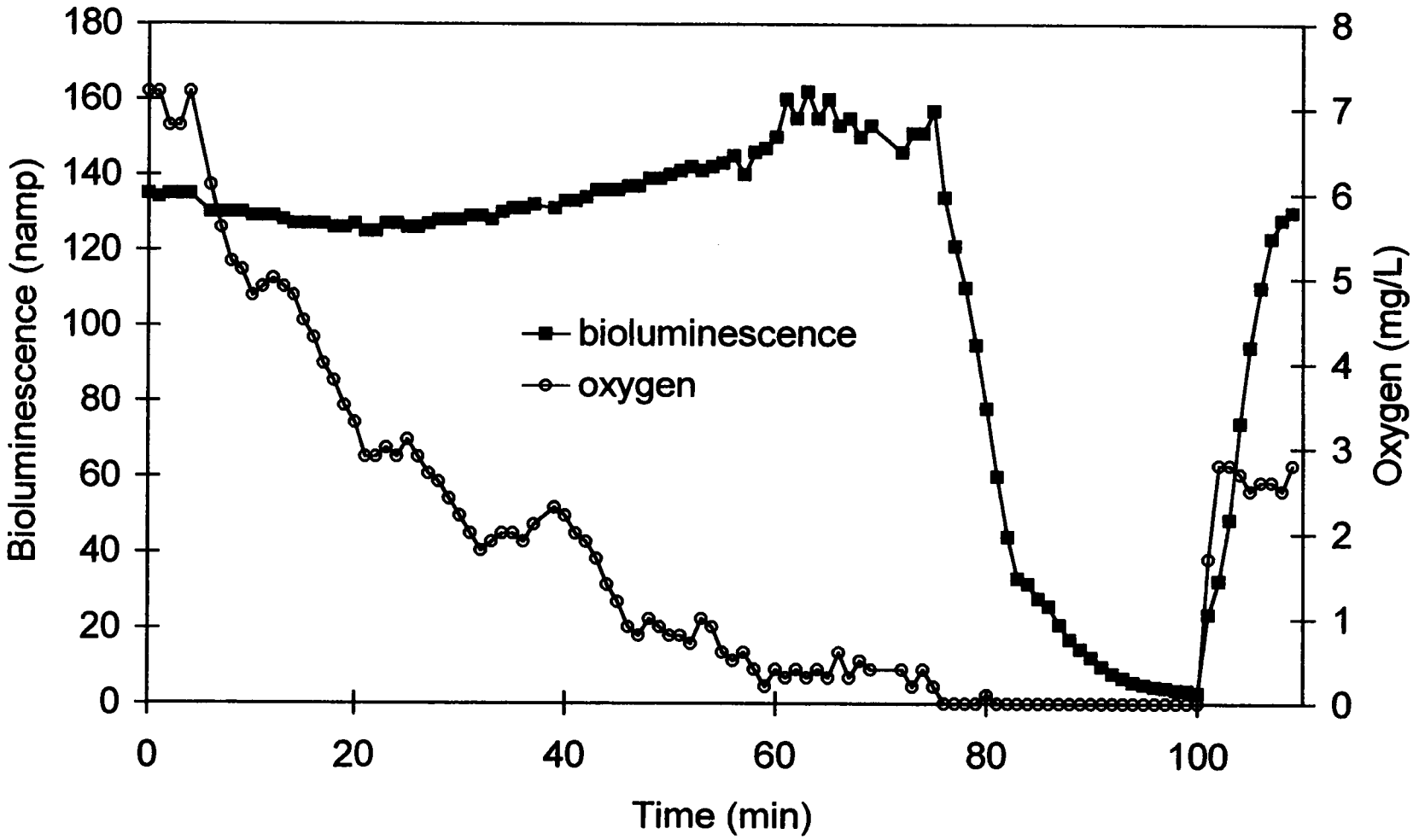

Figure 2-5. Bioluminescent response of Shk 1 to decreasing oxygen concentration.

namp/min. These results indicate future experiments could be designed with sufficient experimental mass transfer characteristics (mixing or shaking) so bioluminescence would not be limited by oxygen concentration.

Effect of Kanamycin on Growth Rate

Methodology

Three overnight cultures were grown to serve as inoculum for growth rate experiments. These cultures consisted of *P. putida* B2 with 25 mg/L kanamycin, B2 without kanamycin, and F1 without kanamycin. These were the growth conditions of the inoculum as indicated in Table 2-6. Each of these inoculum cultures was centrifuged and resuspended in minimal media with no carbon source and no antibiotic. A specific volume of each culture was used to inoculate flasks containing succinate media with various concentrations of kanamycin (Table 2-6). Cell optical density (OD_{600}) was measured intermittently from each of these flasks for eleven hours.

Table 2-6. Effect of kanamycin batch growth experimental conditions.

Inoculum growth conditions	F1 without kanamycin	B2 with kanamycin	B2 without kanamycin
batch growth conditions	0, 10 mg/L kanamycin	0, 25, 50 mg/L kanamycin	0 mg/L kanamycin

Results

The F1 inoculated culture increased in cell density at the highest rate, followed by B2 with 0 mg/L kanamycin (Figure 2-6). Because there was no difference in growth rate between the two methods of inoculum preparation (antibiotic and no antibiotic), there seemed to be no reversion of B2 back to F1 in an overnight culture without selective pressure. The 25 mg/L kanamycin containing culture grew significantly slower than the culture containing 0 mg/L kanamycin, while the 50 mg/L kanamycin culture grew even slower (Figure 2-6). The F1 culture containing 10 mg/L kanamycin did not grow. Because growth rates were affected by the presence of kanamycin, it is possible that toluene degradation rates would be affected also. Therefore, subsequent experiments to determine degradation kinetics were performed without the addition of kanamycin.

Stability of the *tod-lux* Construct

To ensure experiments performed without kanamycin would retain the genetic element responsible for bioluminescence, the stability of this element under similar experimental conditions was examined.

Methodology

An overnight culture of *P. putida* B2 grown with kanamycin was centrifuged, and resuspended in minimal media without kanamycin and used to inoculate kanamycin free medium. This culture grew for approximately 5 cell divisions. Dilution

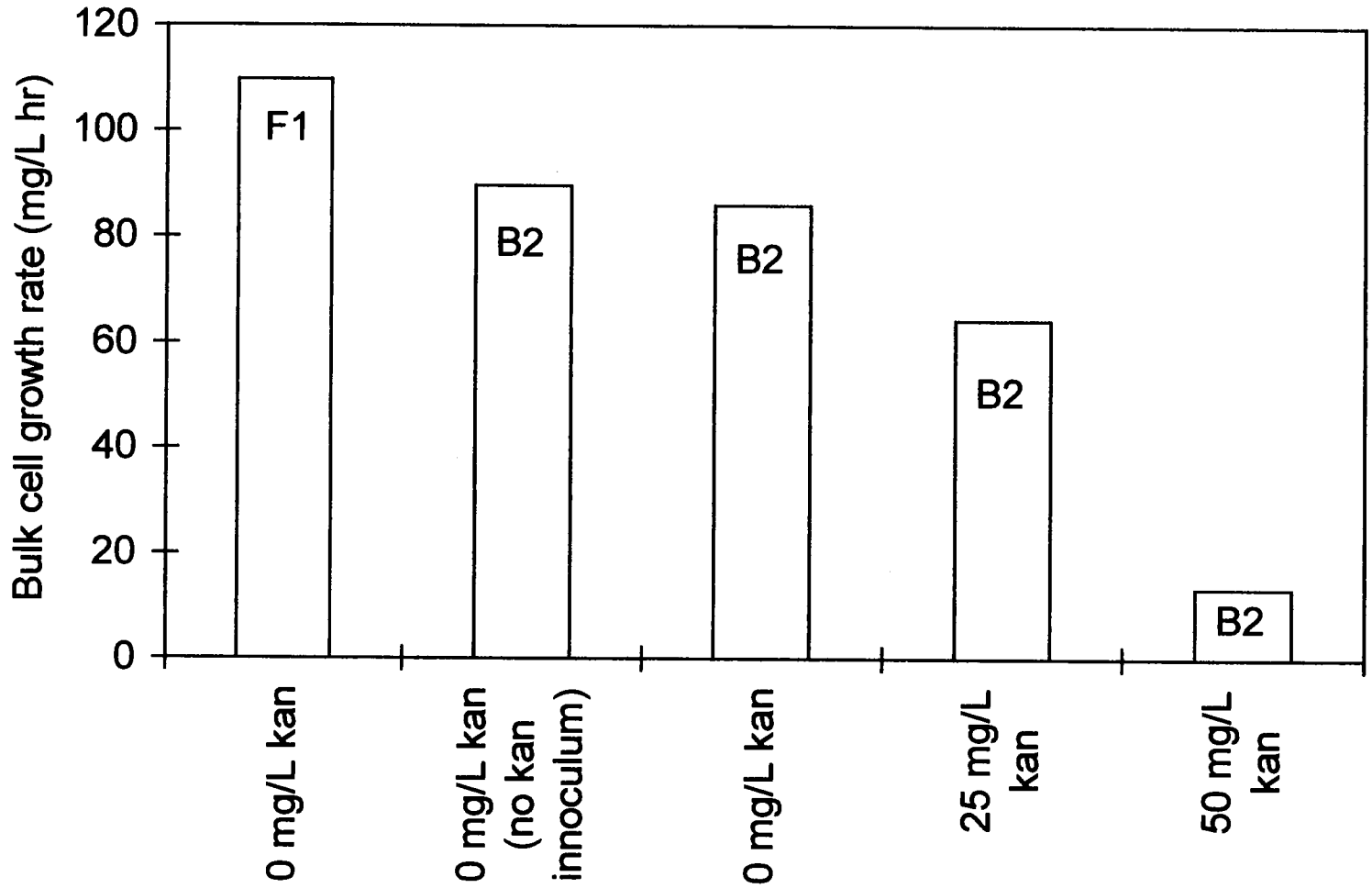

Figure 2-6. Growth rate of B2 at different kanamycin concentrations.

platings of this culture were made on selective (containing kanamycin) and non-selective LB plates. A new flask was inoculated from this culture and grew for approximately 5 cell divisions. Again, dilution platings were performed on selective and non-selective LB plates.

Results

In every case, there were no significant differences in the number of colonies between the selective plates and the non-selective plates (Figure 2-7). This indicated the construct responsible for bioluminescence was stable over two batch growth periods of 5 divisions without kanamycin. This amount of growth is in excess of the amount of growth in the batch experiments performed with this reporter. Because kanamycin was found to influence growth rates, and the construct was stable without kanamycin, batch experiments were performed without selective pressure.

Comparison of Parent Strain F1 and Bioreporter B2

Methodology

Pseudomonas putida B2 and F1 were grown in succinate minimal media with 25 mg/L kanamycin to a cell optical density of 0.9 OD_{600}, centrifuged, and resuspended in minimal media without kanamycin to a cell optical density of 0.5 OD_{600}. Four mL of the 0.5 OD_{600} culture were dispensed to vials. The culture was then starved for 18 to 26 hours. Water saturated with toluene was added to the vials to

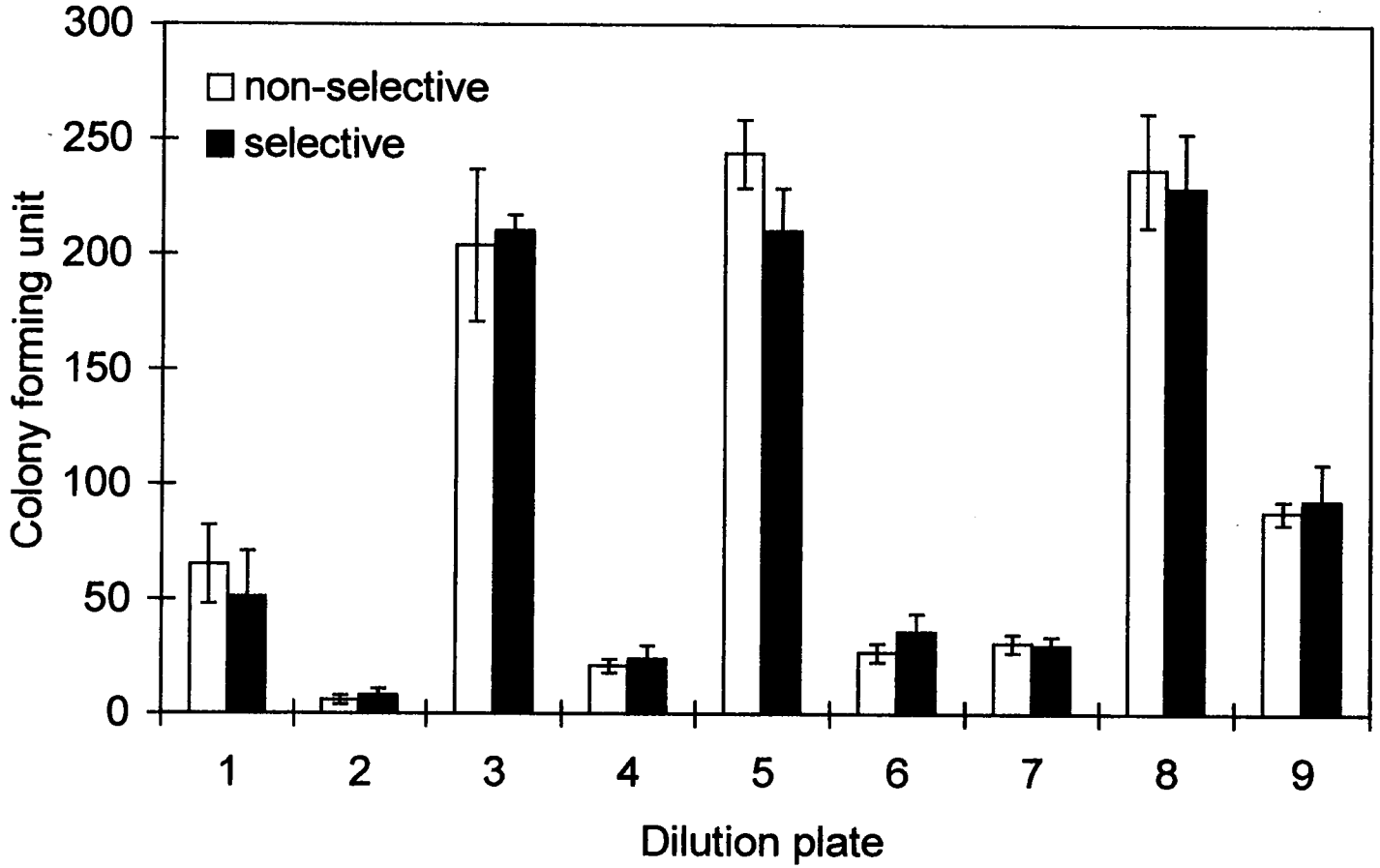

Figure 2-7. Colony forming units on selective and non-selective plates assessing the stability of the *tod-lux* construct in B2.

achieve 50 and 100 mg/L toluene concentration. An amount of minimal medium was added to make the addition of the aqueous solution to each vial equal to one mL. Therefore, the vials had a final volume of 5 mL, with a density of 0.4 OD_{600}. Toluene concentration was measured with time.

Results

The parent strain *P. putida* F1 grew faster and degraded toluene more quickly than the reporter (Figure 2-8). At present the basis of this difference is unknown. Whether there are any implications for use of this reporter for process control will depend on the specific application.

Discussion

Subsequent experiments to ascertain bioluminescence and degradation kinetics were characterized by different mixing regimes; for example they included well shaken vials, well stirred vials, shaken flasks, and stirred reactors. As indicated by Figure 2-5, bioluminescence diminished only at very low oxygen levels, and subsequent experiments were designed to maintain sufficient mass transfer rates to remain in the region where bioluminescence was not limited by oxygen concentration.

Both bioreporters contain antibiotic resistant markers: the *tod-lux* reporter contains the kanamycin resistance genes, while the Shk 1 reporter contains the tetracycline resistance genes. Inclusion of antibiotics in the growth medium would be helpful in maintenance of the genetic element responsible for bioluminescence and

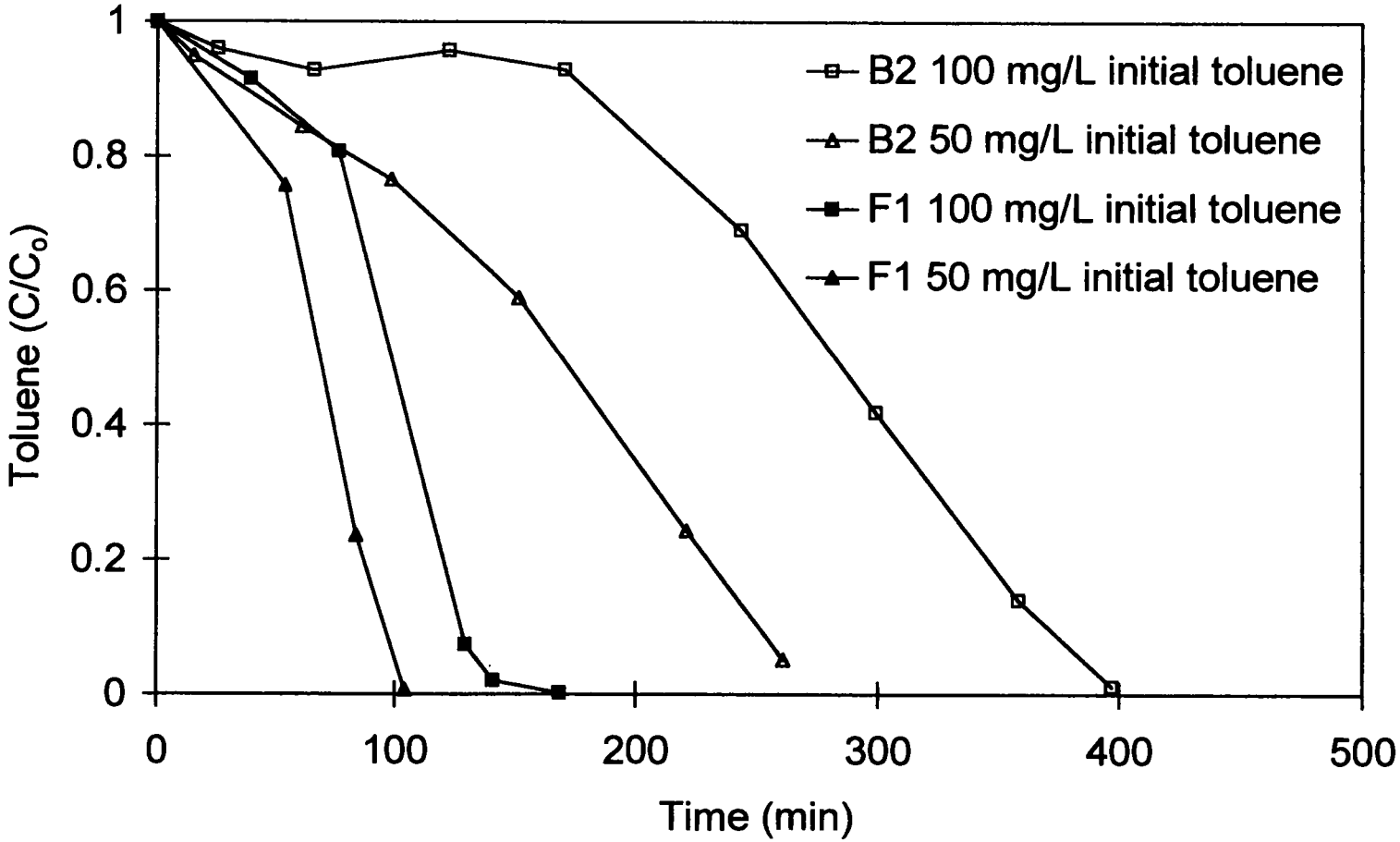

Figure 2-8. Comparison of toluene degradation betweeen B2 and F1.

exclusion of competitors. However, antibiotics may affect kinetic parameters. Therefore, antibiotics were not included in experiments where kinetics were to be measured. This includes most of the *tod-lux* experiments. Sterile techniques were maintained in these experiments. The genetic construct was shown to be stable over the course of batch rate experiments. In continuous experiments, plating on selective and non-selective media was performed to verify that a pure culture of bioreporter was maintained.

The bioreporter *Pseudomonas putida* B2 was intended to be a surrogate for the indigenous soil bacterium *Pseudomonas putida* F1. Light output may be correlated with expression of TCE degradative enzymes, and may be used for control of amendments in remediation schemes. However, the reporter grew and degraded toluene much slower than the parent strain. A new *tod-lux* reporter was constructed, *Pseudomonas putida* TVA8, to alleviate this problem, and was used for the continuous studies. However, the qualitative and mechanistic knowledge gained from the experiments with B2 can be directly applied to TVA8, as the same construct for light production is in both strains.

CHAPTER 3

CHARACTERIZATION OF THE *tod-lux* BIOREPORTER IN BATCH CULTURE

It is possible that bioreporters may increase the efficiency and productivity of bacterial processes. However, to use the bioreporter for control in an industrial process, the bioluminescent response kinetics to the conditions relevant to the reporter application need to be well understood. This chapter discusses (1) the bioluminescent response of the TVA8 reporter to batch growth conditions, (2) the bioluminescent and degradative response of B2 to multiple exposures of toluene, and (3) bioluminescent and degradative response of B2 in batch experiments to a range of initial toluene concentrations. These experiments are beginning steps in the complete characterization of process variables important in the application of this bioreporter.

Growth Curve and Bioluminescent Response

The bioluminescent response of the TVA8 bioreporter during batch growth was examined. Examining the bioluminescence under a variety of environmental conditions (batch, continuous cultivation) ensures that a specific characteristic of a single experiment does not incorrectly influence mechanistic interpretations.

Methodology

Three 250 mL flasks with 50 mL of mineral salts medium and toluene vapor feed were inoculated with two mL of a 1.7 OD_{600} overnight culture of *P. putida* TVA8. Cell density and bioluminescence were measured intermittently for 10 hr. Bioluminescence was measured by placing a glass vial with 1 mL of culture in a light tight sampling cell equipped with a light guide and photomultiplier.

Results

The maximum growth rate of TVA8 was determined to be 18 day^{-1} (Figure 3-1). Bioluminescence increased at a rate (370 namp/hr) greater than cell growth for about 5 hours, reached a maximum value of 1300 namp, then decreased to background levels at 520 namp/hr in about two hours (Figure 3-2). Maximum bioluminescence occurred at an approximate cell density of 450 mg/L (Figure 3-2).

The cell density data were fitted to an empirical logistic curve (Equation 3-1) (Bailey, 1986) with the parameters x_o=0.0075 OD_{600}, β=1.25, and k=0.2 (Figure 3-2).

$$x = \frac{x_o e^{kt}}{1 - \beta x_o \left(1 - e^{kt}\right)} \qquad (3\text{-}1)$$

The derivative of cell density with respect to time (bulk cell growth rate) (Equation 3-2) was determined to be,

$$\frac{dx}{dt} = kx(1-\beta x) \qquad (3\text{-}2)$$

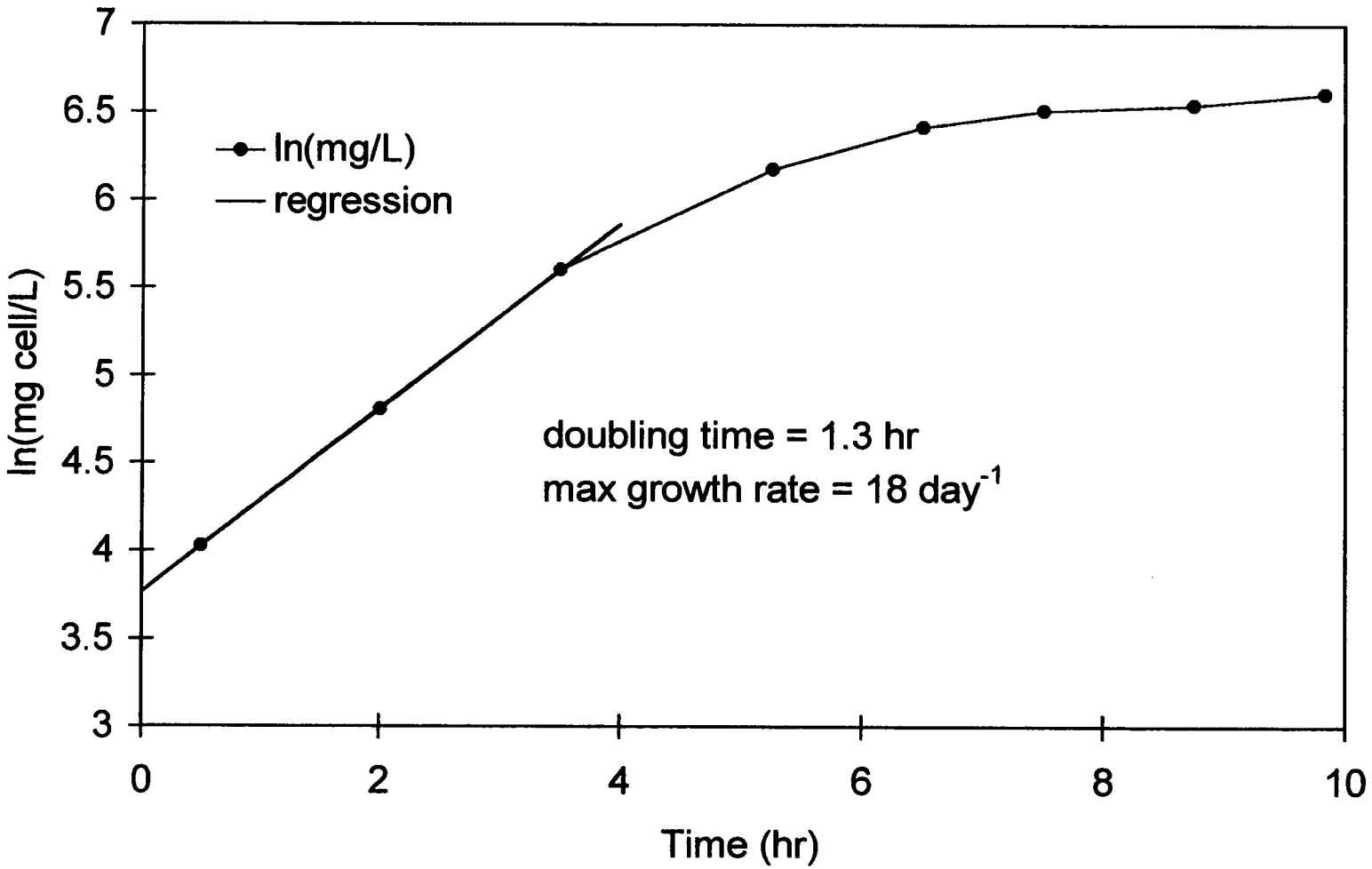

Figure 3-1. Determination of exponential growth rate for *Pseudomonas putida* TVA8.

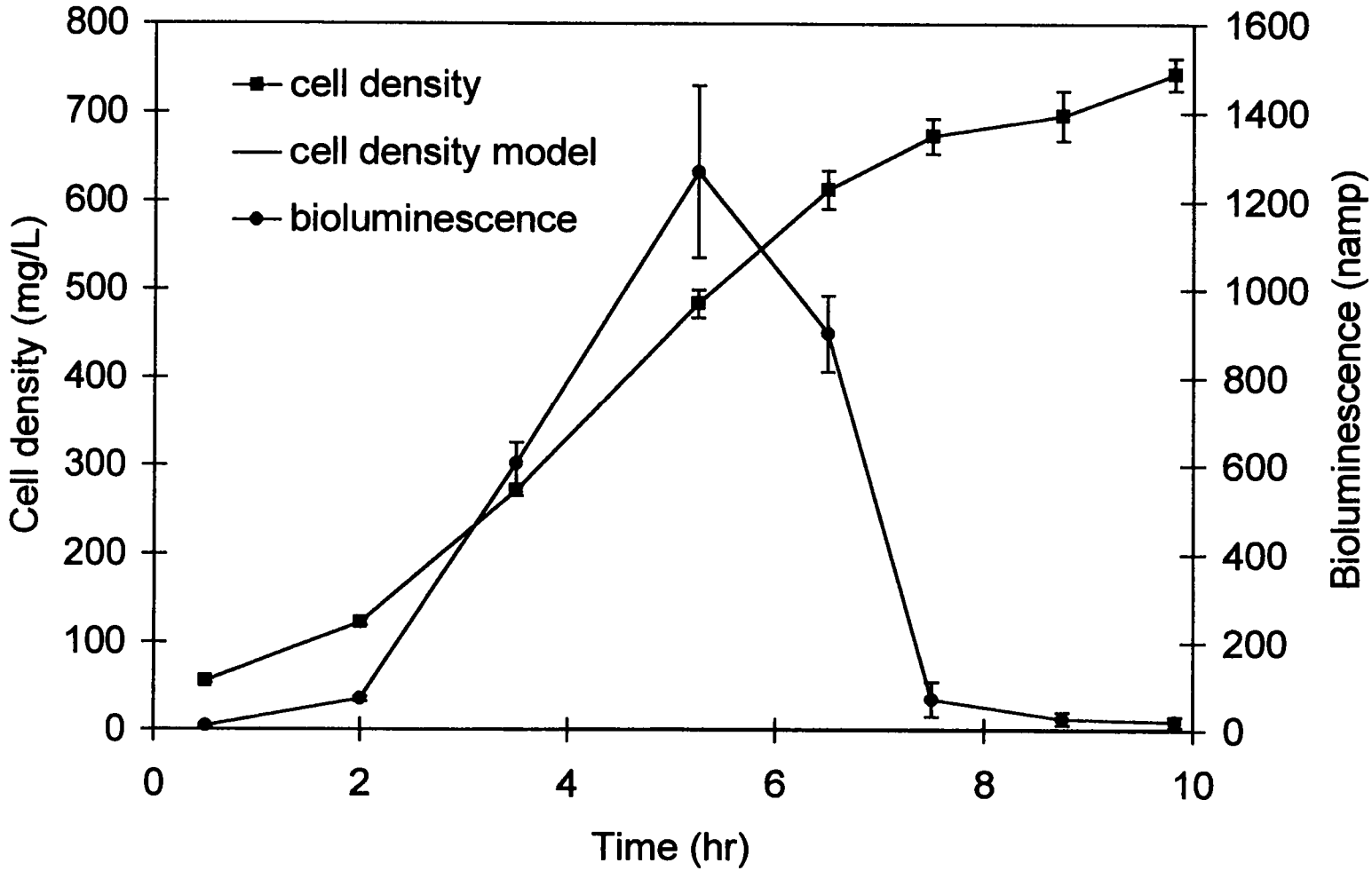

Figure 3-2. TVA8 batch growth curve: experimental cell density, logistic curve fit cell density, and bioluminescence with time.

in which x was the cell optical density (OD_{600}) and t was time (hour). The bulk growth rate, specific bioluminescence and bulk bioluminescence reached a maximum at approximately the same time (3-5 hr) (Figure 3-3).

tod-lux Bioreporter Cellular Yield

Methodology

An overnight culture of *Pseudomonas putida* B2 was centrifuged and resuspended in minimal media without succinate to approximately 0.5 OD_{600}, and 18 vials with 5 mL aliquots of culture were prepared. 100 mg/L of toluene was added to 9 vials, while 50 mg/L toluene was added to the remaining 9 vials. The initial OD_{600} was measured, and the vials were stirred until they stopped producing light (approximately 10 hours for the 100 mg/L, and 5 hours for the 50 mg/L) and then the final cell optical density was measured (Table 3-1).

Results

The yield from each replicate was calculated based on the increase in cellular mass and the mass of toluene added. The highest and lowest two values for each initial concentration were discarded, and the remaining cellular yields were averaged to obtain a cellular yield of 0.62 ± 0.08 mg cells/mg toluene.

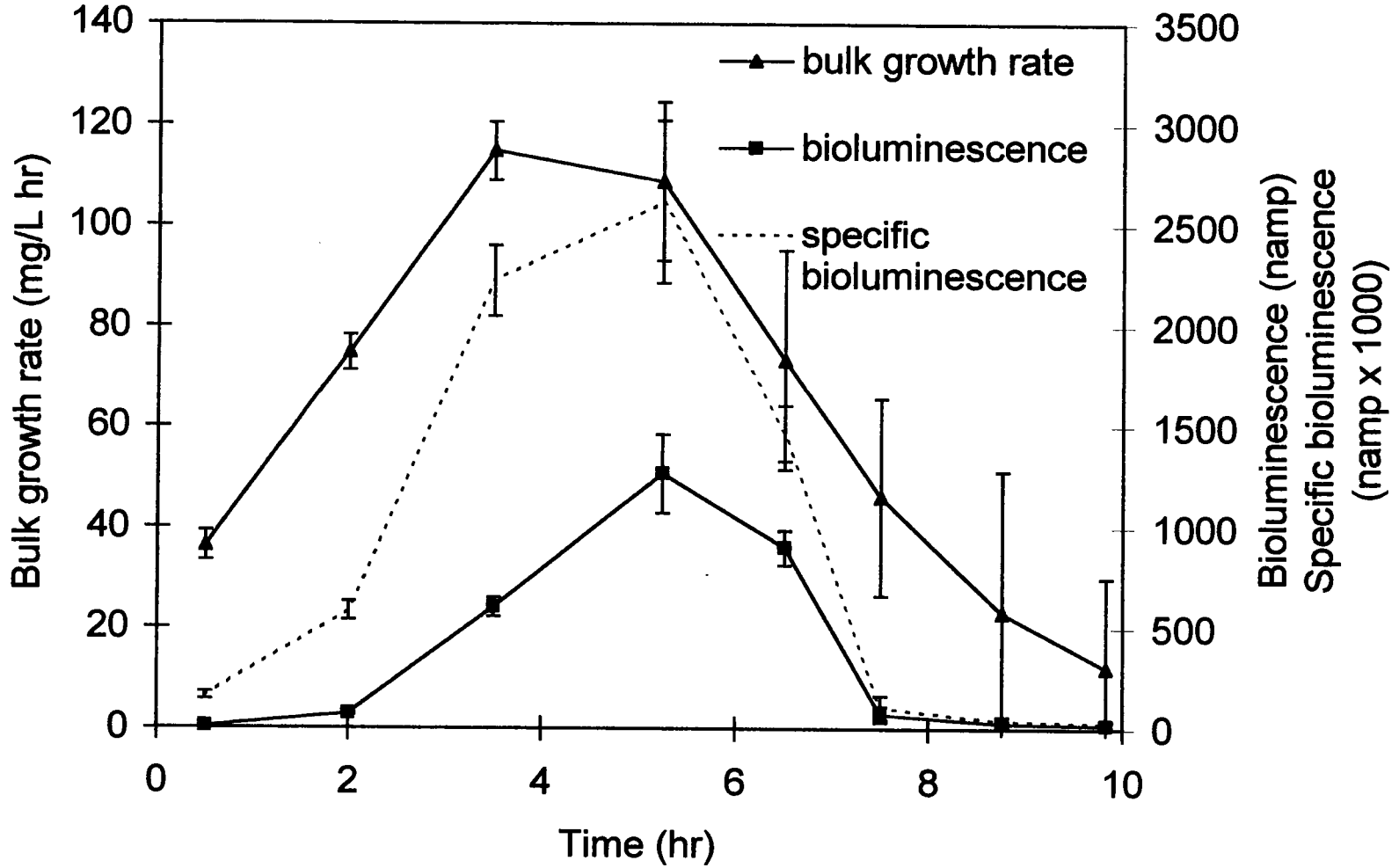

Figure 3-3. Bulk growth rate from logistic curve, bioluminescence and specific bioluminescence for batch *Pseudomonas putida* TVA8.

Table 3-1. Experimental yield results

initial OD_{600} (50 mg/L toluene)	final OD_{600} (50 mg/L toluene)	yield mg cell/mg toluene	initial OD_{600} (100 mg/L toluene)	final OD_{600} (100 mg/L toluene)	yield mg cell/mg toluene
0.48	0.50	-	0.46	0.59	0.67
.049	0.53	0.49	0.47	0.60	0.63
0.49	0.56	-	0.47	0.61	0.68
0.48	0.53	0.54	0.46	0.60	0.67
0.47	0.54	0.73	0.46	0.58	-
0.47	0.53	0.54	0.47	0.60	0.61
0.50	0.53	-	0.47	0.59	-
0.49	0.56	0.64	0.52	0.73	-
-	0.55	-	0.47	0.61	-

Discussion

During batch growth, the bioluminescent response of the reporter increased from background levels, reached a maximum and then declined to background levels as cell density continued to increase. On first consideration, it would seem that because growth rates changed in batch culture, the maximum bioluminescence may have been related to cellular growth rate. However, cellular maximum growth rate did not coincide with bulk mass growth rate, so there was no individual cellular growth rate significance to the inflection point on the cell density versus time curve. Increasing bioluminescence was probably not related simply to growth rate.

Bioluminescence increased initially in batch growth at a rate greater than cell division. It is hypothesized that this was due to an *in vivo* accumulation of the active luciferase-aldehdye complex. The luciferase oxidation of aldehyde has one of the

longest enzyme relaxation rates measured; so intuitively this step would be the rate limiting step of all the reactions involved in the production of bioluminescence.

Toluene was continuously vapor fed to the batch culture throughout the growth cycle, so the decline in bioluminescence was probably not due to growth substrate or inducer limitation. The point of maximum bioluminescence coincided approximately with the point of maximum cell mass production. A this point, the rate of increase in oxygen consumption rate was the greatest. Perhaps, at cell densities less than this point (450 mg/L), the rate of oxygen consumption was less than the rate of oxygen transfer to the cells. At about 450 mg/L oxygen transfer rates might have become limiting. Either oxygen limitation, or the on-set of stationary phase brought about by oxygen limitation might have caused the decrease in bioluminescence in batch growth cultures.

Pre- and Multiple Exposure to Toluene

Methodology

Bioluminescence

An overnight culture (minimal salts with succinate) of *P. putida* B2 was harvested at approximately 0.7 OD_{600}. The cells were centrifuged at 10,000 rpm for 10 min, and resuspended in minimal salts medium to 0.5 OD_{600} . Four mL of culture

was added to each of six 26 mL vials with Mininert® valves (Dynatech) with stir bars. One vial was used for multiple toluene exposures, while the remainder were used for single exposures. The vials were magnetically stirred in a light-tight sampling cell. Toluene-saturated water and medium alone were added to yield 0.4 OD_{600}, and 10 mg/L toluene was injected 6 times over a 130 hr period to the multiple-exposure vial. At the same time points, a single-exposure vial was injected with 10 mg/L toluene. The light response was recorded every 3 min with a photomultiplier connected to a data acquisition computer.

Degradation

Two vials were prepared with 4 mL of resuspended culture. Ten mg/L toluene was added to one of the vials to pre-expose the cells to toluene. After bioluminescence returned to background for this vial, 10 mg/L toluene was added to each vial, and toluene concentrations were measured with time.

Results

Bioluminescence

The bioluminescent response to single exposures of toluene was rapid and reproducible (Figure 3-4). The initial injection to the multiple exposure vial showed the same characteristic light response as each single exposure vial. However, compared with the response of cells previously exposed to toluene, there was a slower

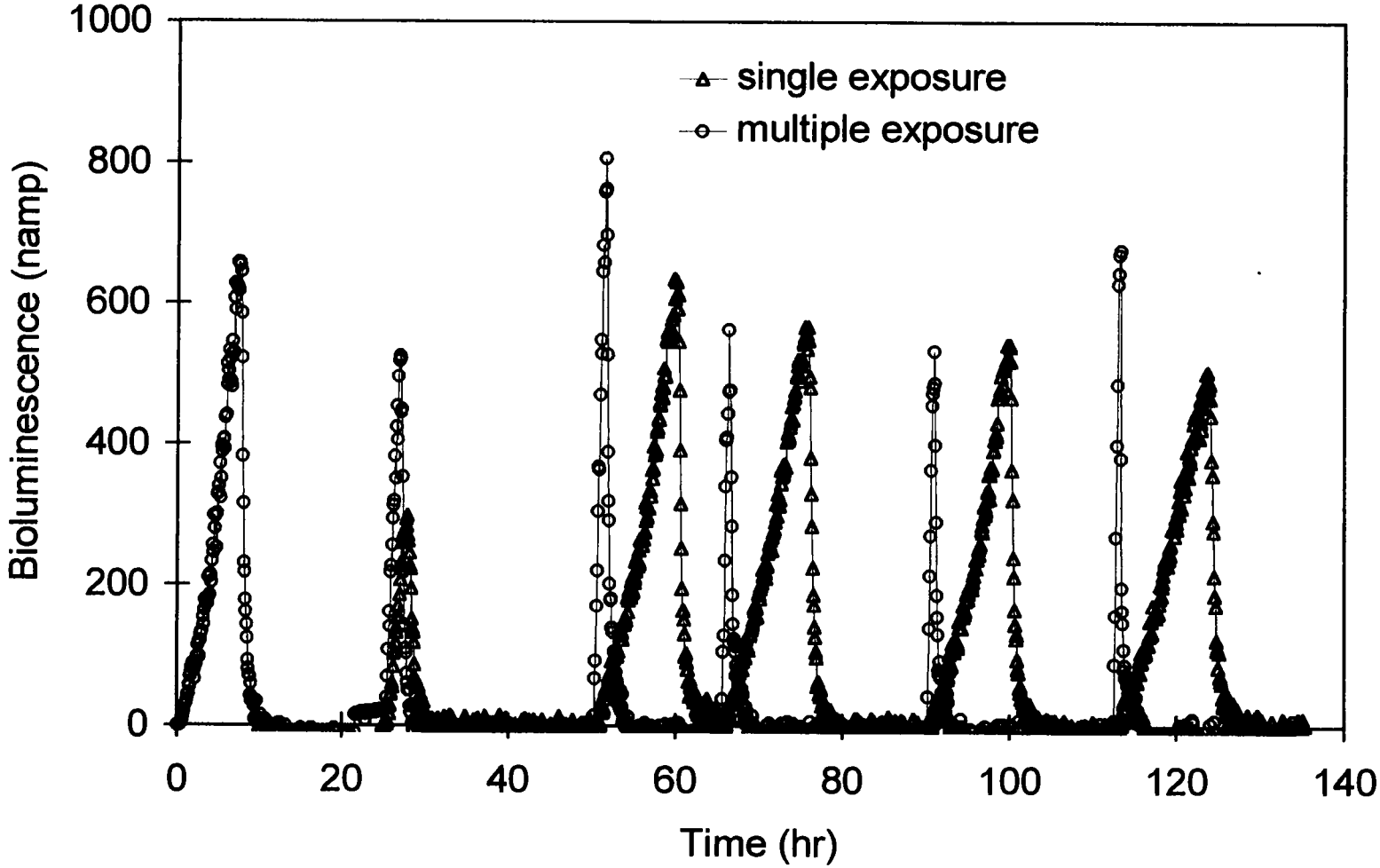

Figure 3-4. Bioluminescent response to multiple and single exposures of toluene.

response rate (the rate of increase in bioluminescence, namp/hr) by the single exposure culture upon initial exposure to toluene. The response rate of the multiple-exposure culture increased with each exposure to toluene (Table 3-2). However, the maximum bioluminescent response for both the single and multiple exposures was statistically similar at 573 ± 127 namp.

Table 3-2. Bioluminescent response rate (namp/hr) for multiple and single exposures of 10 mg/L toluene[a].

Time point	Multiple exposure vial[b]	Single exposure vials[c]
1	95	n/a
2	321	137
3	642	67
4	768	60
5	737	60
6	973	49

[a] Response rate is defined as rate of bioluminescence increase with time.
[b] A single vial, with multiple additions of toluene.
[c] A new vial, previously unexposed to toluene, injected with toluene at each time point.
n/a, not applicable.

Degradation

The cells that were pre-exposed to toluene degraded toluene at a faster rate than the cells unexposed to toluene (Figure 3-5). The rate of degradation for the pre-

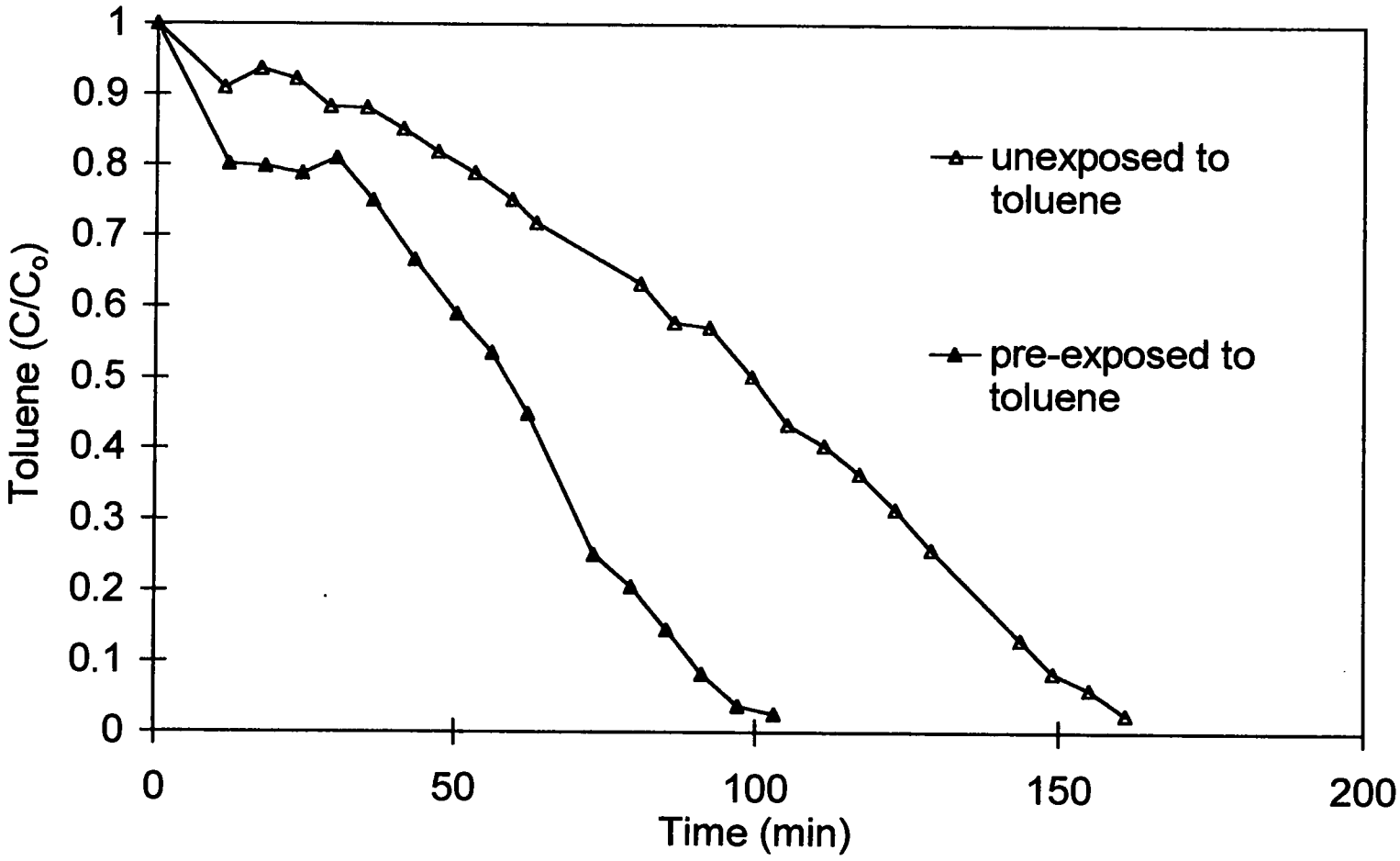

Figure 3-5. Influence of pre-exposure to toluene on degradation (initial 10 mg/L toluene).

exposed cells was 0.030 mg toluene/L min mg cell, while the unexposed cell degraded toluene at 0.019 mg toluene/L min mg cell.

Discussion

The bioluminescent response by B2 to intermittent multiple and single exposures of growth substrate spikes was reproducible for at least 5 days. Although exposure to toluene did affect the response rate, the maximum bioluminescence level remained constant. When the aromatic hydrocarbons (such as toluene) partition into the cytoplasmic membrane, membrane fluidity changes. Bacteria have shown to produce major phospholipid shifts in composition of the membrane (Pinkart, 1996) to compensate for the change in membrane fluidity when exposed to solvents. When the bioreporter is exposed to toluene, delays in cellular activity such as degradation and bioluminescence could occur until the toxicity effect of the toluene is overcome by a shift in phospholipid concentrations in the cell membrane. Possibly, the composition change had already occurred in cells pre-exposed to toluene or grown in toluene; so degradation and bioluminescence could occur more rapidly in pre-exposed cultures.

Bioluminescent Response to a Range of Inducer Concentrations

Experiments were conducted with bioreporter B2 to ascertain the effect of inducer concentration on degradation and bioluminescence kinetics.

Methodology

Glass vials (26 mL, equipped with mininert tops) were charged with cells, liquid media, toluene, and 5 mg/L TCE. Each vial contained a small stir bar and was placed on a multi-plate magnetic stirrer so that all vials were agitated at the same rate (100 rpm). The experiments were performed in a constant temperature (25 °C) incubator. The TCE concentration was selected because the rate of degradation of TCE by *Pseudomonas putida F1* was shown to be linear in the range of 1-10 mg/L, above which toxicity effects have been suggested (Wackett and Gibson, 1988). Bioluminescence and toluene and TCE concentration were then monitored until these three variables stopped changing. In addition, the initial and final cell optical density was measured.

Controls

Control experiments were also performed. The controls consisted of treatments without cells, without toluene, and with killed cells.

Bacterial analysis and preparation

Reporter cells were grown by adding 1.5 mL of freezer stock to 500 mL of mineral salts medium with toluene vapor supplied as the carbon and energy source. The culture was allowed to grow for about 24 hours, reaching a final cell density of 0.6-0.8 OD_{600}, then was centrifuged at 10,000 rpm for 10 minutes, and the cell pellet

was resuspended in 50 mL of media. This culture was shaken at room temperature for 24 hours to allow bioluminescence to cease before inducer was added.

For light measurements, a concentrated amount of cells was added (0.5-0.75 mL/5 mL of total solution) to minimal media to result in an initial OD_{600} of 0.5. Then, TCE and toluene were added, and light was measured every 3 minutes for initial toluene concentrations of 50, 75, and 100 mg/L, and every 1 minute for initial toluene concentrations of 10 and 25 mg/L. For degradation monitoring experiments, the TCE and toluene were added initially, and the vials were allowed to stir for about 15 minutes to obtain equilibrium between head-space and liquid. The initial toluene and TCE concentrations were measured before addition of 0.5-0.75 mL of cells to bring the initial cell density to 0.5 OD_{600}.

Mathematical Model Development

Because there was no feed or effluent from the batch vial, the change in substrate concentration was equal to the degradation rate by the bacteria (Equation 3-3)

$$V\frac{dC_{tol}}{dt} = -V(v_R) \qquad (3\text{-}3)$$

Three simultaneous ordinary differential equations and an algebraic equation for bioluminescence were proposed to describe bioluminescence and degradation in the batch system. They included an equation describing (1) the change in toluene

concentration, (2) the change in TCE concentration, and (3) the change in the number of luciferase molecules per cell.

The degradation rate equations consisted of terms to account for cellular growth (Chang and Alvarez-Cohen, 1995a), and enzymatic substrate degradation. Toluene and TCE degradation was described with a Michaelis-Menten expression (Baily and Ollis, 1986) for the degradation of two substrates that compete for a single enzyme (Equation 3-4 and 3-5). The traditional transformation capacity term (Chang and Alvarez-Cohen, 1995b) indicating a toxicity effect on biomass from TCE degradation was not included in this analysis.

$$\frac{dC_{tol}}{dt} = -k_{tol}\,(X_i + Y_{X/S}(C_{tol,i} - C_{tol}))\left[\frac{C_{tol}}{K_{tol}(1+\frac{C_{TCE}}{K_{TCE}}) + C_{tol}}\right] \quad (3\text{-}4)$$

$$\frac{dC_{TCE}}{dt} = -k_{TCE}\,(X_i + Y_{X/S}(C_{tol,i} - C_{tol}))\left[\frac{C_{TCE}}{K_{TCE}(1+\frac{C_{tol}}{K_{tol}}) + C_{TCE}}\right] \quad (3\text{-}5)$$

Liquid/vapor partitioning

Toluene and TCE are both volatile solvents, and they partition into liquid and vapor phases based on an equilibrium condition. For low solute concentrations, the partitioning can be represented by Henry's law (Equation 3-6 and 3-7).

$$C_{tol} = \frac{C^{v}_{tol}}{H_{tol}} \quad (3\text{-}6)$$

$$C_{TCE} = \frac{C^{v}_{TCE}}{H_{TCE}} \quad (3\text{-}7)$$

Chang and Alvarez-Cohen (1995a) reported the Henry's law coefficient for toluene to be 0.27, and for TCE 0.36. Concentrations in equations 3-4 and 3-5 are liquid phase concentrations. However, the data presented here reports concentrations as if all solute was in the liquid phase. Equation 3-8 and similar equation for TCE coupled with Henry's Law was used to calculate the equilibrium partitioning concentrations.

$$C^{overall}_{tol} = \frac{C_{tol}V + C^{v}_{tol}V^{V}}{V} = C^{v}_{tol}\left(\frac{1}{H_{tol}} + \frac{V^{V}}{V}\right) \quad (3\text{-}8)$$

Bioluminescence Modeling

The photomultiplier measured light from a constant (but unknown) volume in front of the liquid light guide face. The photomultiplier converted light, which is the number of photons per second striking the photoemissive material in the photomultiplier, to an electric current (namp). The unit of light that a photomultiplier measured was photon per time per volume sampled.

Bioluminescence was proposed to be proportional to cell density (X), the number of active luciferase complex molecules (C_{lucif}), and the cellular energy available for the bioluminescent reaction (E')(Equation 3-9). The active luciferase molecules were each relaxing, releasing photons for a period of about 10 s. Although light was a rate (photons/second), it was proportional to the concentration of luciferase

molecules. An equilibrium is assumed to exist between the active complexed form of luciferase molecules and the uncomplexed form; therefore, the active number is proportional to the total number of luciferase molecules.

$$\text{bioluminescence} = \frac{\text{namp}}{L_{sv}} = k_{light} X C_{lucif} E' \quad (3\text{-}9)$$

The total luciferase molecules are a function of the cell density in the reactor. In deriving an equation for light, a unit analysis is warranted to describe the incorporation of several constant terms into one overall light proportionality constant. There are four constants defined below.

1. M, mass per cell, mg cell/ cell
2. F_{sv}, the fraction of reactor volume sampled by the photomultiplier. L sample/L_R
3. K_{luc}, mg active luciferase/mg luciferase.
4. L_{luc}, the proportionality constant between active luciferase and the photon/sec released, photon sec^{-1}/mg active luciferase.
5. PM, the proportionality constant between photon per second entering the photomultiplier and magnitude of the induced electric current, namp sec/L_{sv} photon

The overall light constant was composed of these constant according to Equation 3-10 with the units displayed in Equation 3-11.

$$k_{light} = \frac{PM\, K_{luc}\, L_{luc}}{M\, F_v} \equiv \frac{\text{cell L namp}}{L_{sv}\ \text{mg cell mg lucif}} \quad (3\text{-}10)$$

$$k_{light} \equiv \left(\frac{namp}{L_{sv}\ photon\ sec^{-1}}\right)\left(\frac{cell}{mg\ cell}\right)\left(\frac{L_R}{L_{sv}}\right)\left(\frac{mg\ active\ lucif}{mg\ lucif}\right)\left(\frac{photon\ sec^{-1}}{mg\ active\ lucif}\right) \qquad (3\text{-}11)$$

A differential equation describing the luciferase complex in the cell was written where the luciferase complex was produced as function of toluene due to the transcriptional dependence on the inducer (Equation 3-12). In addition, a lag-time between the initial exposure to toluene and the production of luciferase was included in the solution of Equation 3-12.

$$\frac{dC_{lucif}}{dt} = \frac{k_{lucif}C_{tol}}{K_{lucif} + C_{tol}} \qquad (3\text{-}12)$$

As discussed in Chapter 1, the production of bioluminescence required ATP, $NADH_2$ and $FMNH_2$. These co-factors were related to the energy source available to the cell. Internal cellular regulation maintained the energetics of the cell at constant levels if the system was not growth substrate limited. Only when the growth substrate source concentration was low did these co-factors become limiting. Therefore, a saturational form of dependence on the energy source available to the cell was suggested (Equation 3-13).

$$light = k_{light}XC_{lucif}\left(\frac{C_{tol}}{K_{light} + C_{tol}}\right) \qquad (3\text{-}13)$$

Equations 3-4, 3-5, 3-12, and 3-13 were solved simultaneously using the parameters listed in Table 3-2.

Nomenclature:

C_{lucif}	effective cellular luciferase concentration, mass/cell
C_{tol}	liquid toluene concentration, mg/L
C^{v}_{tol}	vapor phase toluene concentration, mg/L
$C_{tol,i}$	batch initial toluene concentration, mg/L
$C^{overall}_{tol}$	toluene concentration as if all toluene was in the liquid phase, mg/L
C_{TCE}	liquid TCE concentration, mg/L
C^{v}_{TCE}	vapor phase toluene concentration, mg/L
E'	term representing energy availability to the cell, dimensionless
F_{sv}	fraction of volume sampled by the photomultiplier, L/L_R
H_{tol}	Henry's constant for toluene, dimensionless
H_{TCE}	Henry's constant for TCE, dimensionless
k_{tol}	maximum toluene degradation rate, mg toluene/L day
k_{TCE}	maximum TCE degradation rate, mg toluene/L day
K_{tol}	half-saturation constant (dissociation constant) for toluene, mg/L
K_{TCE}	half-saturation constant (dissociation constant) for TCE, mg/L
k_{light}	overall light proportionality constant
k_{lucif}	maximum luciferase production rate, mg/cell day
K_{light}	half-saturation constant (dissociation constant) for bioluminescence dependence on toluene, mg/L
K_{lucif}	half-saturation constant (dissociation constant) for luciferase dependence on toluene, mg/L
K_{luc}	mg active luciferase/mg total luciferase
L_R	liters of reactor volume
L_{sv}	liters of volume sampled by the photomultiplier
L_{luc}	the proportionality constant between active luciferase and the photon per second released, photon sec^{-1}/mg active luciferase
M	mass per cell, mg cell/cell
t	time, day
t_{lag}	lag time, day
V	liquid volume, L
V^{V}	vapor volume, L
v_R	reaction rate, mg/L day
X	cell density, mg/L
X_i	batch initial cell density, mg/L
$Y_{X/S}$	cellular yield, mg cell/mg toluene

Method of solution. These equations were solved simultaneously via a Runge Kutta fourth order routine (Cheney and Kincaid, 1985). At each time step the

partitioning of the toluene and TCE to the vapor and liquid phases was calculated. Constants were determined from a best visual fit and least squares regression to the experimental data.

Results

Toluene and TCE did not leak out of the vials, and the disappearance of toluene and TCE was not due to adsorption to the cells or vials because toluene and TCE concentrations in the no cell and killed cell control vials remained at approximately initial levels. Bioluminescence did not increase in the control vials with cells and TCE only indicating that the light response was not due to TCE (data not presented).

At each initial toluene concentration examined, bioluminescence corresponded with the presence of toluene. When toluene was added to the medium, bioluminescence increased, and as toluene was degraded, bioluminescence decreased (Figure 3-6). For each initial toluene concentration examined, the TCE concentration remained close to the initial concentration until most of the toluene was degraded, and then declined (Figure 3-7). TCE degradation rates were approximately constant for each initial toluene concentration examined. Based on initial biomass concentration TCE, degradation rates were 0.001 mg TCE/L mg cell (Figure 3-8), compared to toluene degradation rates on the order of 0.05 mg toluene/L mg cell.

Bioluminescence increased at the same rate for 25 and 50 mg/L initial toluene concentrations, but increased more slowly at a higher initial toluene

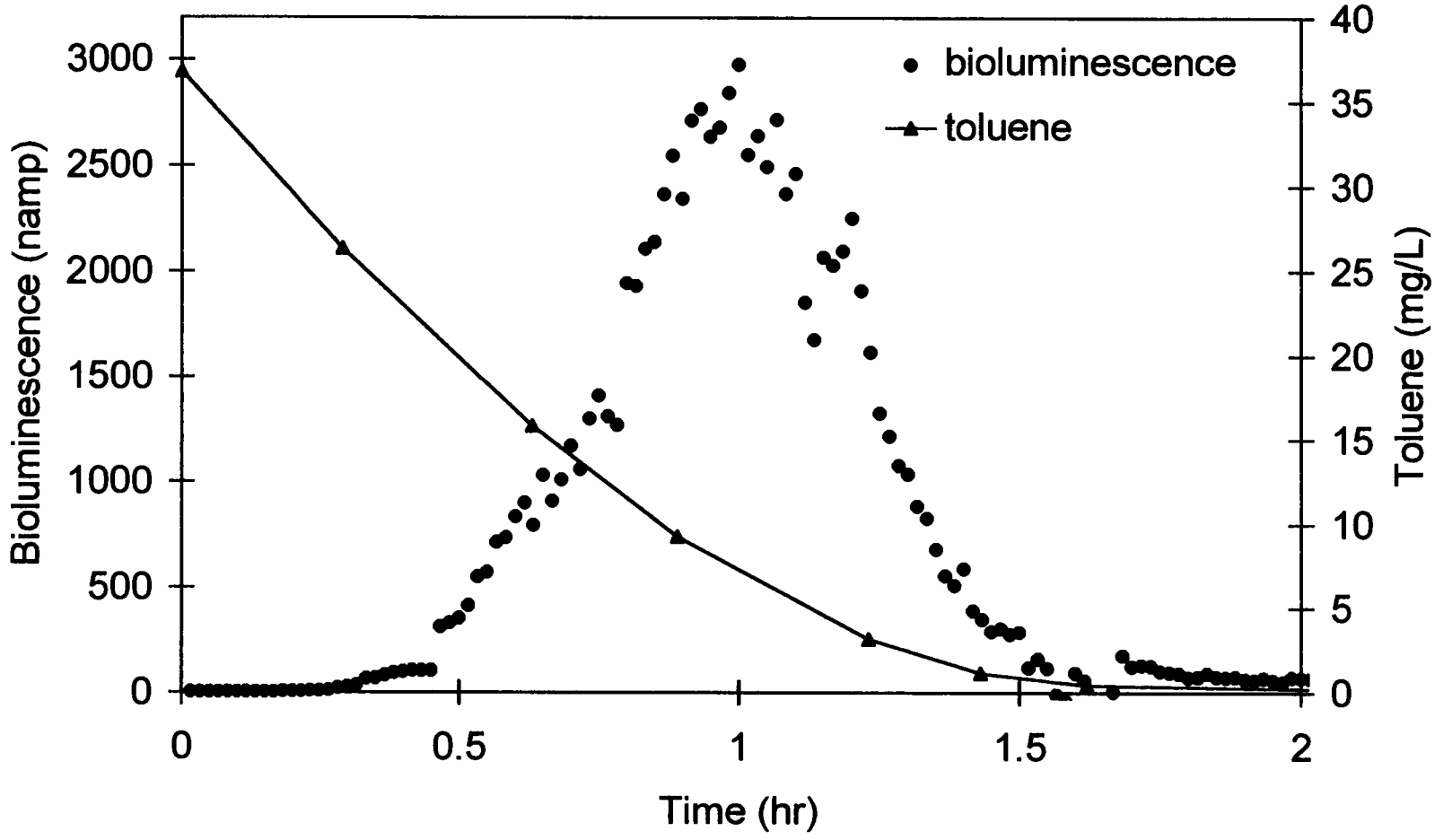

Figure 3-6. Bioluminescence and toluene concentration for an initial toluene concentration of 25 mg/L.

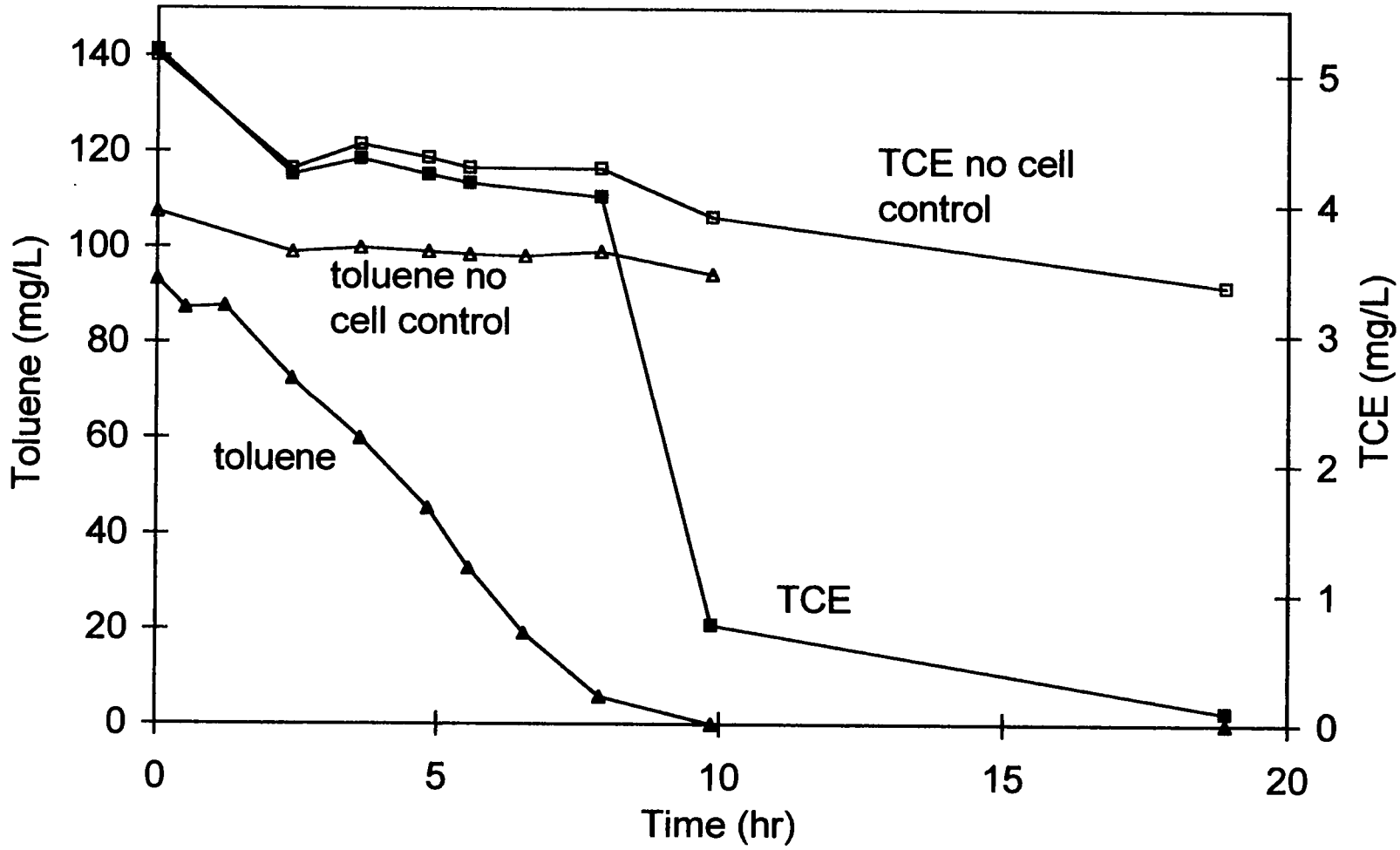

Figure 3-7. Comparative toluene and TCE co-degradation as a function of time. As was observed with other initial toluene concentrations, the TCE concentration declined only after the toluene was degraded.

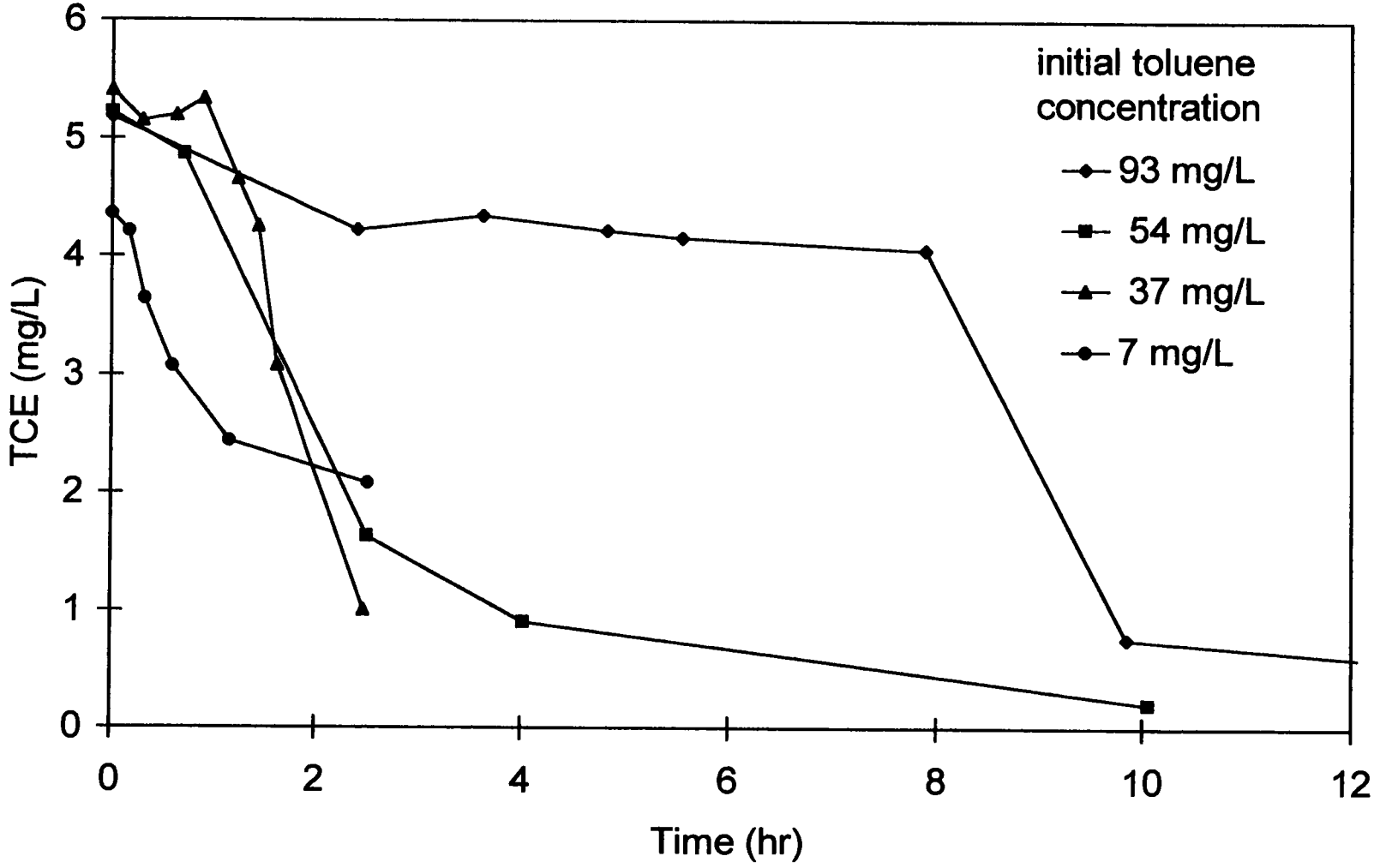

Figure 3-8. TCE degradation by B2 with a range of initial toluene concentrations.

concentrations (Figure 3-9).

Modeling parameter determination

The yield coefficient for degradation modeling was determined from replicates of 50 and 100 mg/L initial toluene concentrations was determined to be 0.62 mg cell/mg toluene. Toluene and TCE maximum degradation rates and Michaelis-Menten constants from this study along with previous literature values are reported in Table 3-3. The Chang, and Alvarez-Cohen (1995) study reports values for a mixed culture of toluene oxidizers, while the Robertson and Button (1987) study used *P. putida* F1, and finally the Chang et al. (1992) study used two unidentified *Pseudomonas* isolates. Table 3-4 includes the bioluminescent modeling parameters.

Table 3-3. Comparison of model parameters with previous studies.

Parameter	**symbol**	**units**	**this study**	**Chang, H-S[a]**	**Robertson[b]**	**Chang, M-K[c]**
bacteria examined			B2	toluene oxidizers	*P. putida* F1	2 *Pseudo-monas*
maximum specific toluene degradation rate	k_{tol}	$\frac{\text{mg tol}}{\text{d mg cell}}$	4.0	0.44	0.48	13.03 10.84
maximum specific TCE degradation rate	k_{TCE}	$\frac{\text{mg TCE}}{\text{d mg cell}}$	1.3	0.17	-	-
toluene Michaelis-Menten constant	K_{tol}	mg/L	2.7	1.02	0.06	1.96 1.88
TCE Michaelis-Menten constant	K_{TCE}	mg/L	6.4	8.64	-	-
yield	$Y_{x/s}$	$\frac{\text{mg cell}}{\text{mg tol}}$	0.62	0.29	-	1.22 0.99

[a] Chang and Alvarez-Cohen, 1995a
[b] Robertson and Button, 1987
[c] Chang et al., 1992

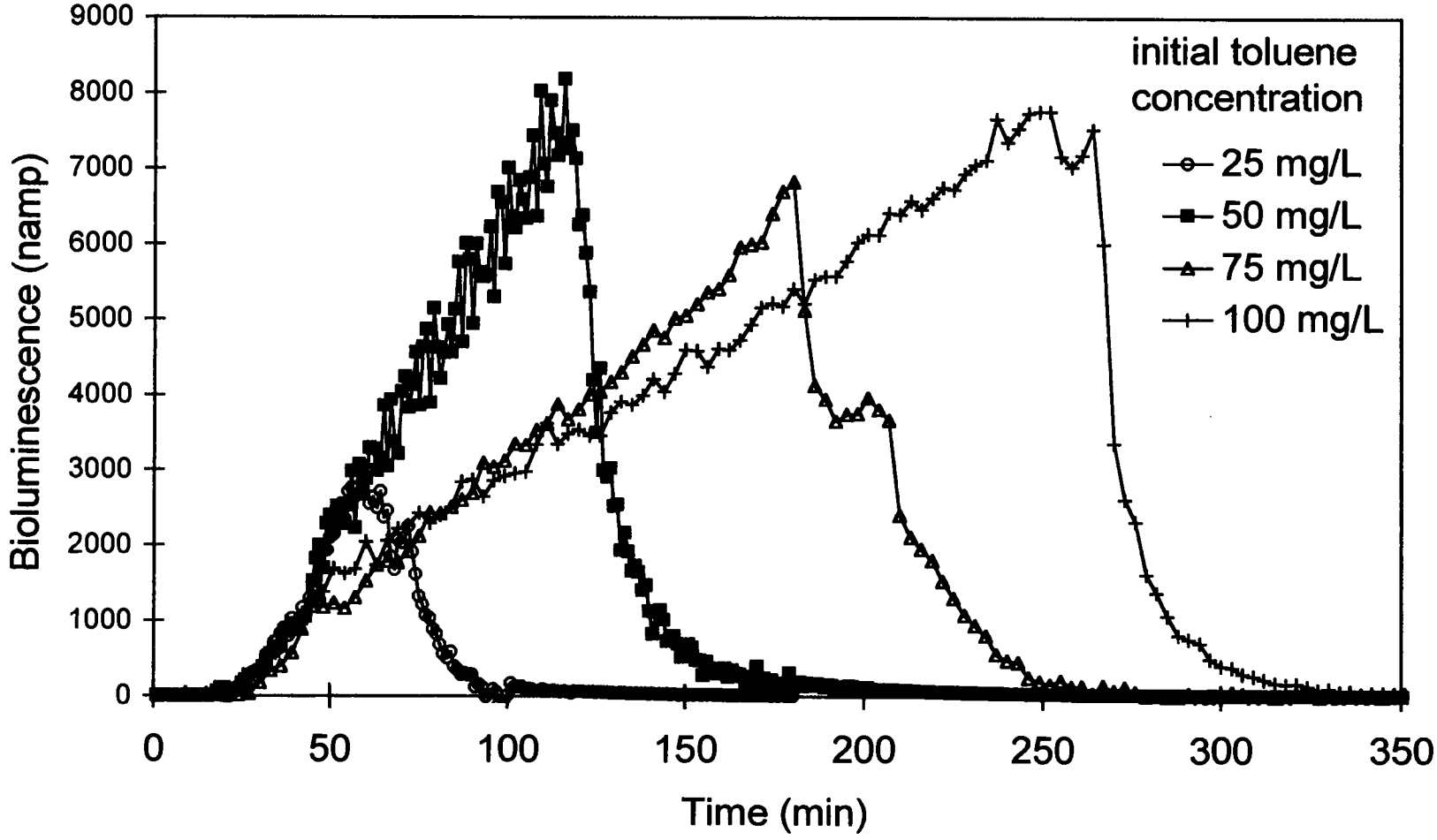

Figure 3-9. Bioluminescent response by *Pseudomonas putida* B2 to different initial toluene concentrations.

Table 3-4. Remaining modeling parameters used in simulation.

Parameter	symbol	value
maximum rate of light production	k_{light}	$650 \frac{\text{cell L namp}}{L_{sv}\ \text{mg cell mg lucif}}$
half-saturation constant for luciferase production	K_{light}	$0.2 \frac{\text{mg}}{\text{L}}$
bioluminescence lag time	t_{lag}	0.02 day

Simulation of both toluene and TCE degradation fit the lower initial toluene concentration data well (Figures 3-10 and 3-11). However, at 100 mg/L initial toluene concentration the model predicts faster degradation than observed (data not shown). Similarly, the bioluminescence model fit the data well at 25 and 50 mg/L initial toluene concentration (Figure 3-12), but predicted a faster bioluminescence response for initial toluene concentrations of 75 and 100 mg/L (data not shown).

Discussion

Batch experiments were performed using the *tod-lux* bioreporter *Pseudomonas putida* B2 to characterize its bioluminescent response and degradation kinetics with different initial concentrations of toluene.

Toluene had a higher affinity for the *tod* enzyme than TCE, as indicated by the fact that TCE degradation did not occur until the toluene had almost been completely degraded. Any TCE remediation design must incorporate the fact that toluene out-competes TCE for the *tod* enzyme.

The rate of TCE degradation was statistically constant regardless of the initial toluene concentration (10 mg/L to 100 mg/L). This possibly indicated that the toluene concentration required for full induction was less than 10 mg/L. If this was the case, toluene concentrations above 10 mg/L might not result in increased TCE degradation. Although bioluminescence reached a higher maximum with greater initial toluene

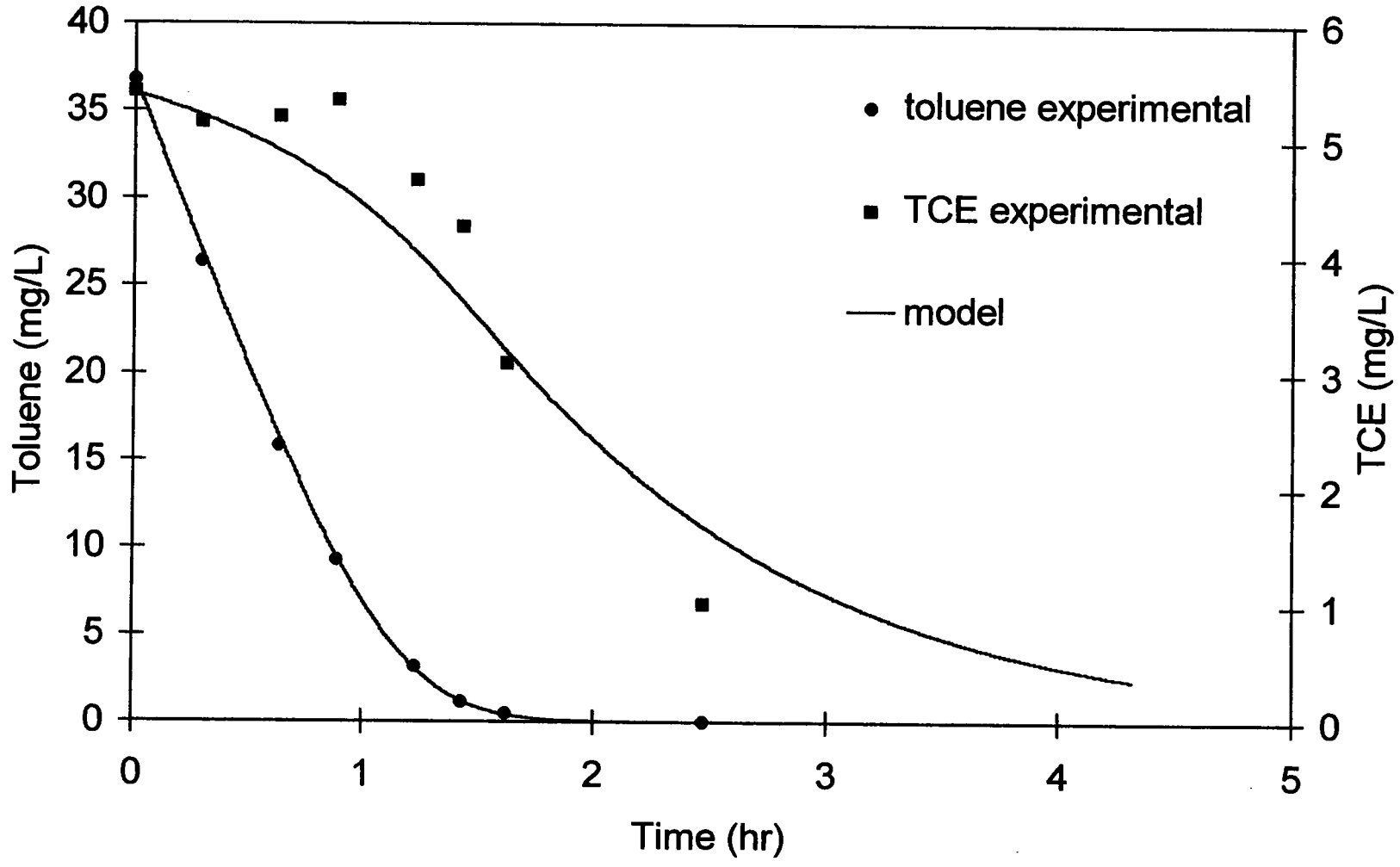

Figure 3-10. Toluene and TCE degradation (experimental and model) for an initial toluene concentration of 37 mg/L.

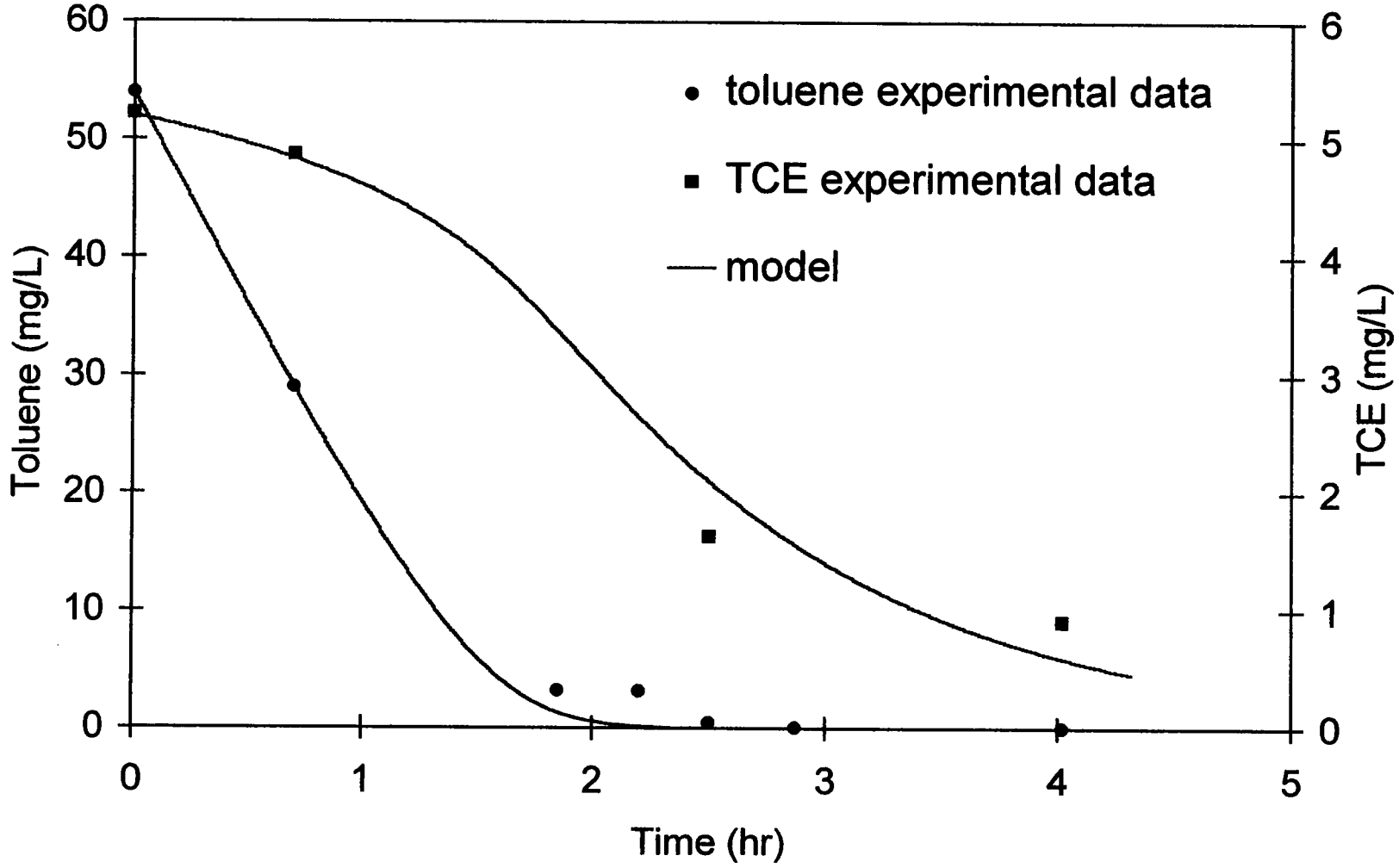

Figure 3-11. Toluene and TCE degradation (experimental and model) for an initial toluene concentration of 54 mg/L.

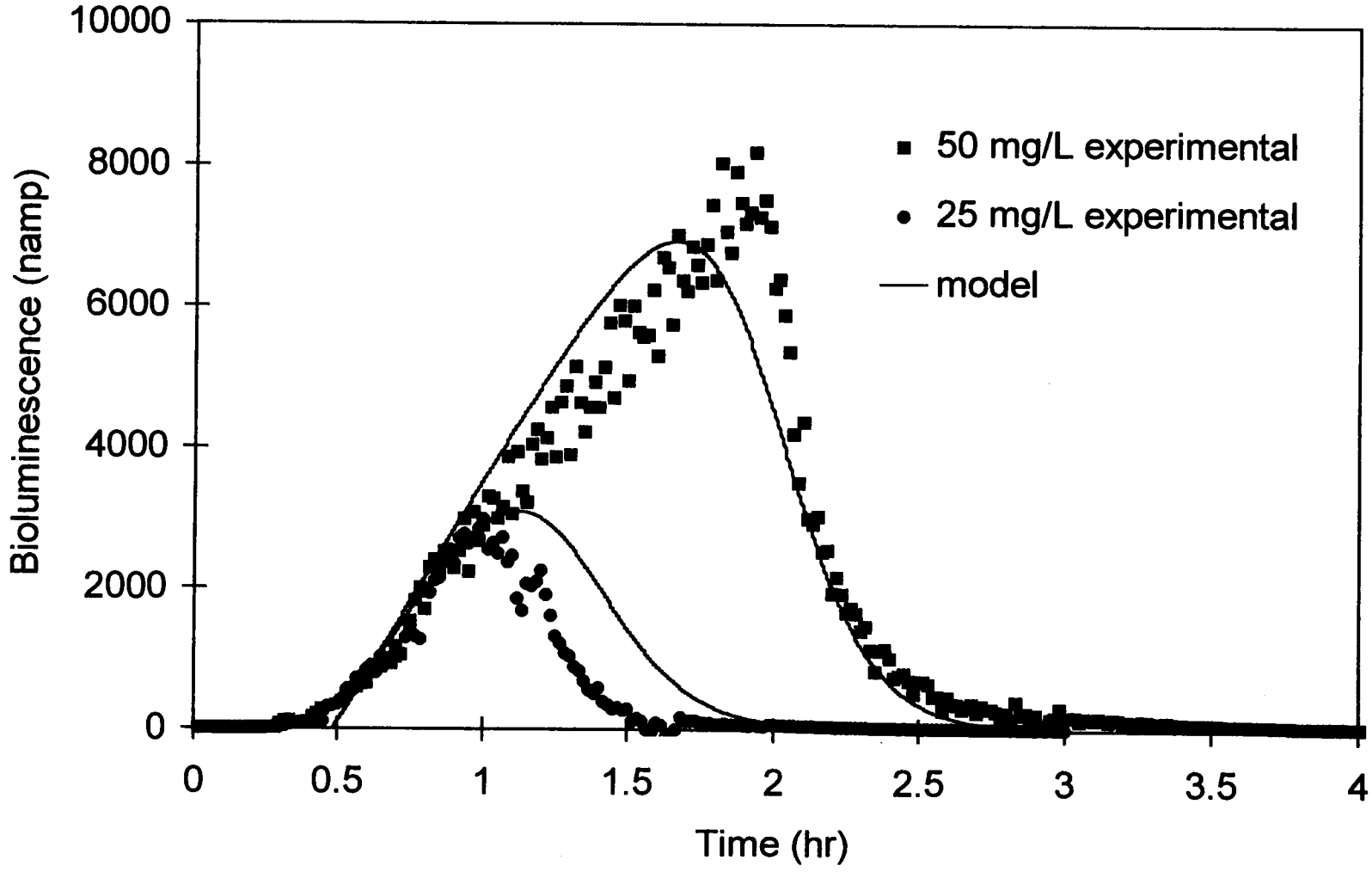

Figure 3-12. Bioluminescence for initial toluene concentrations of 25 and 50 mg/L (experimental and model).

concentration, the rate of increase for 10, 37 and 54 mg/L initial toluene was the same. The constant rate of bioluminescence increase could indicate that the *tod* promoter was transcribed at maximum levels at each of these concentrations. The toluene was present longer at the higher concentration, so the active luciferase molecules which were being transcribed at a constant rate could accumulate for a longer time period, thereby reaching higher *in vivo* concentrations. However, at greater than 50 mg/L initial toluene concentrations, a decline in rate of increase in bioluminescence and degradation is observed. This could be due to increased solvent toxicity.

Bioluminescence increased upon exposure to toluene after a 20-30 minute lag time. Heitzer (1992) also observed a lag time (15 min) with the HK44 bioluminescent reporter. This could be the lag time for induction in these reporter systems.

The increase in bioluminescence at a rate greater than cell growth was attributed to the accumulation of active luciferase molecules. But, the cause of the decrease in bioluminescence as toluene is completely degraded can not be explicitly determined from these experiments. The decrease could be explained by either lack of induction or limitation of energy available for reactions involved in bioluminescence. A lack of induction would result in a net decline in *lux* enzymes as degradation rate of *lux* enzymes would be greater than their production rate. Energy is provided for the light reactions from the metabolism of toluene, so when the toluene is completely degraded the cell becomes energy limited.

CHAPTER 4

CHARACTERIZATION OF THE *tod-lux* BIOREPORTER IN A CHEMOSTAT

Experiments were performed with continuous culture to ascertain fundamental parameters affecting bioluminescence. Bioluminescent responses to changes in feed toluene concentration were examined with the TVA8 bioreporter in a chemostat reactor.

Methodology

A chemostat was used to investigate the effects of toluene feed concentration on bioluminescence and degradation rates with the reporter strain *Pseudomonas putida* TVA8. The reactor consisted of a 1 L glass vessel with an overflow port that resulted in 300 mL of liquid volume and 700 mL of vapor volume (Figure 4-1). The reactor was fed with 80% strength mineral salts medium, toluene, TCE, and air. The mineral salts medium was fed via a peristaltic pump through a glass drip tube. The drip tube prevented back contamination from the reactor to the feed reservoir, and extended into the liquid volume of the reactor. TCE and toluene were fed from separate no-head space piston pumps. The piston pump reservoirs held water saturated with toluene and TCE, respectively. Air was fed from an aquarium type air pump through a 0.2 *um* filter and a flow meter. The reactor was equipped with a marine type impeller operated at 250 rpm, and four stainless steel 1/2" wide baffles.

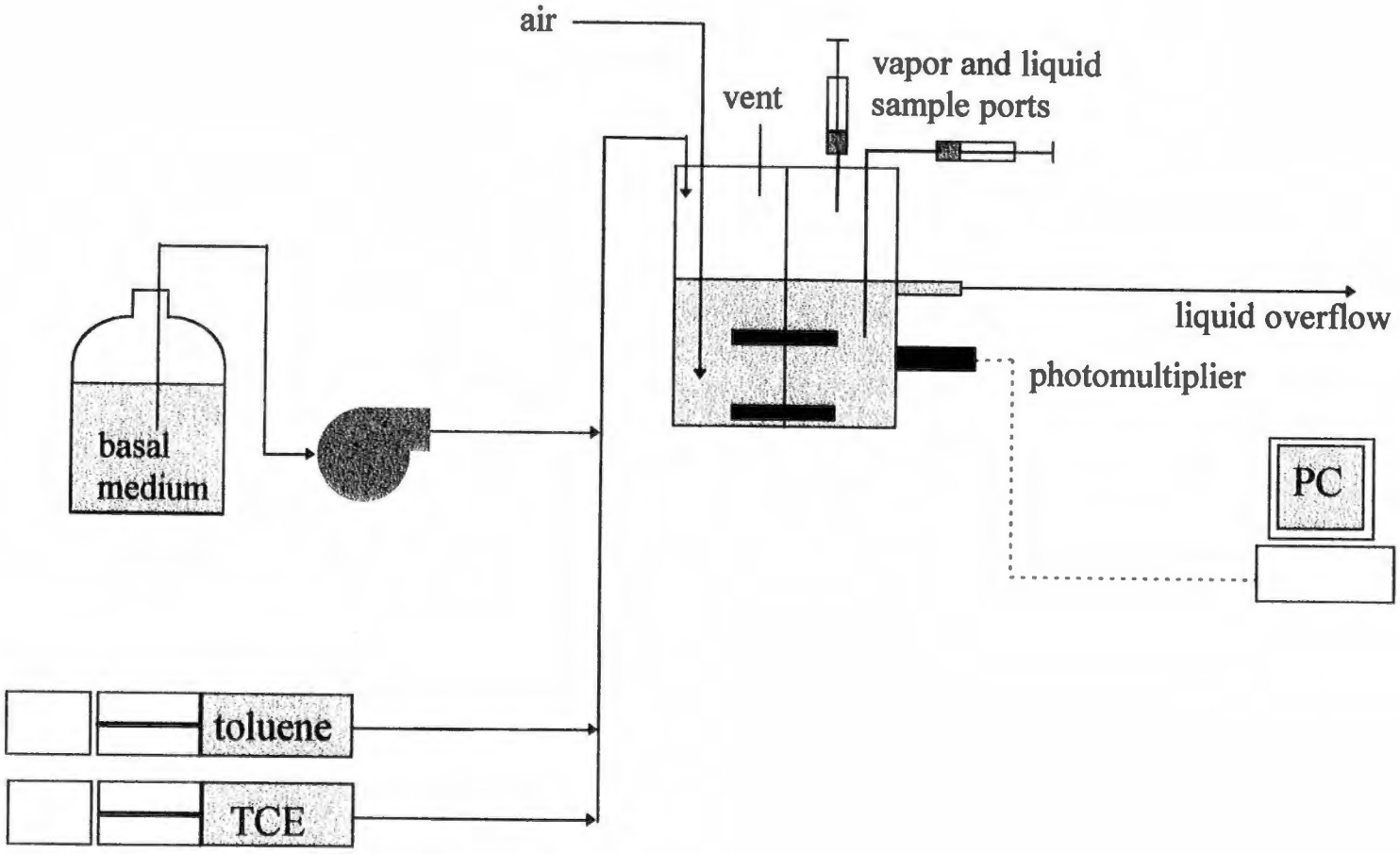

Figure 4-1. TVA8 chemostat schematic.

The entire glass reactor was placed in a light-tight wooden box. A liquid light guide was placed against the glass wall of the reactor about an inch from the bottom of the reactor. All feed lines were stainless steel except for the silicon tubing of the peristaltic pump, and the effluent line was a combination of stainless steel and silicon tubing. The reactor was operated at room temperature, which varied from 25-29 °C.

Reactor Analysis

The reactor was equipped with a 1/16" stainless steel line for liquid sampling from the reactor. Vapor was sampled from a septum port in the top of the reactor. Two methods were employed to sample toluene and TCE from the reactor. (1) A 0.5 mL liquid reactor sample was taken with a syringe and injected into a sealed 1.9 mL amber vial. The vial was shaken 15 minutes and then 25 *u*l head-space samples were injected onto the GC column for toluene and TCE analysis. (2) A 10 mL vapor sample was taken from the head-space of the reactor with a gas-tight glass syringe. The 10 mL of vapor was injected into a sealed 1.9 mL amber vial equipped with a needle through the septum for venting, replacing the existing gas with vapor from the reactor. Head-space samples were immediately analyzed on the GC for toluene and TCE. Method (2) yielded the more consistent and repeatable results. One mL samples were withdrawn from the reactor for cell density quantification by optical density. Light was transferred from the reactor, through the liquid light pipe to a photomultiplier, where it was converted to an electrical current signal which was recorded automatically every 10 minutes on a data acquisition computer. The sample

averaging period of the data acquisition software was on the order of 1-3 seconds. Effluent samples were periodically plated on LB and R2A selective and non-selective media to determine loss of the genetic element responsible for bioluminescence and contamination by other organisms.

Experimental Description

Two chemostat experiments were performed. The first consisted of stepping up and then down the feed toluene concentration, while the second consisted a closer examination (toluene and cell density measurements taken more often) of an increase in toluene feed concentration (Table 4-1).

Table 4-1. TVA8 chemostat experimental conditions.

Exp. #	toluene feed (mg/L)	TCE feed (mg/L)	feed rate (mL/min)	air flow (mL/min)
1	10, 28, 69, 125, 188, 0, 125, 69, 28	5.6	0.68	3.2
2	13, 94	4.5	0.82	3.8

Chemostat Mathematical Modeling

Chemostat Cellular Yield

The steady-state cellular yield in a chemostat could be different than in batch system due to growth substrate availability conditions. The yield can be defined as the

mass of cells obtained in the chemostat effluent divided by the amount of toluene consumed in the reactor. This relationship is defined in equation (4-13).

$$Y_{X/S} = \frac{X^{ss}}{C_{tol}^{f} - C_{tol}^{overall\ ss}} \qquad (4\text{-}13)$$

Reactor Mass Balance

Biomass, toluene, and TCE mass balances were performed on the reactor volume to obtain three simultaneous differential equations describing the reactor variables. In addition, a differential equation describing the luciferase dependence on toluene concentration, and an equation relating bioluminescence to luciferase and growth substrate concentrations were proposed. These four simultaneous differential equations and single algebraic equation were solved using a 4th-order Runge-Kutta routine.

The cellular mass balance on the chemostat volume resulted in Equation 4-1.

$$V\frac{dX}{dt} = FX_o - XF + V\mu X - Vk_dX \qquad (4\text{-}1)$$

Assuming a sterile feed, a negligible death rate, and Monod cell growth kinetics Equation 4-1 simplified to Equation 4-2.

$$\frac{dX}{dt} = -X\frac{F}{V} + Y_{X/S}(v_R) \qquad (4\text{-}2)$$

An unsteady-state mass balance on toluene and TCE was performed on the reactor volume resulting in Equation (4-3) and (4-4).

$$V\frac{dC_{tol}}{dt} = C^{f}_{tol}F - C_{tol}F - C^{v}_{tol}A - V\left(v_R^{tol}\right) \qquad (4\text{-}3)$$

$$V\frac{dC_{TCE}}{dt} = C^{f}_{TCE}F - C_{TCE}F - C^{v}_{TCE}A - V\left(v_R^{TCE}\right) \qquad (4\text{-}4)$$

Michaelis-Menten rate expressions for the competition of two substrates for a single enzyme (Equations 4-6 and 4-7) were used as in the batch model development.

$$\left(v_R^{tol}\right) = k_{tol}\,X\left[\frac{C_{tol}}{K_{tol}\left(1+\frac{C_{TCE}}{K_{TCE}}\right)+C_{tol}}\right] \qquad (4\text{-}6)$$

$$\left(v_R^{TCE}\right) = k_{TCE}\,X\left[\frac{C_{TCE}}{K_{TCE}\left(1+\frac{C_{tol}}{K_{tol}}\right)+C_{TCE}}\right] \qquad (4\text{-}7)$$

The overall, liquid and vapor phase concentrations were related to the reactor volumes and Henry's Law coefficients for small solute concentrations, and equilibrium vapor and liquid concentration were determined at each time step in the solution.

Bioluminescence Modeling

Chemostat bioluminescence modeling followed the same development as batch bioluminescence modeling, except a term accounting for *in vivo* degradation of the luciferase enzyme was proposed. Equation 4-8 is a differential equation describing the luciferase complex in the cell, where luciferase was degraded at a rate proportional to the luciferase concentration.

$$\frac{dC_{lucif}}{dt} = \frac{k_{lucif} C_{tol}}{K_{lucif} + C_{tol}} - K_d C_{lucif} \qquad (4\text{-}8)$$

As in batch bioluminescence modeling, light was proposed to be proportional to biomass, luciferase, and a term accounting for the energy available to the cell (Equation 4-9).

$$light = k_{light} X C_{lucif} \left(\frac{C_{tol}}{K_{light} + C_{tol}} \right) \qquad (4\text{-}9)$$

Nomenclature:

μ	cellular growth rate, day^{-1}
A	air flow rate, L/min
F	feed and effluent liquid flow rate, L/min
C_{lucif}	effective cellular luciferase concentration, mass/cell
C_{tol}	reactor liquid toluene concentration, mg/L
C^v_{tol}	reactor vapor toluene concentration, mg/L
C^f_{tol}	feed toluene concentration, mg/L
$C^{overall\ ss}_{tol}$	steady-state reactor toluene concentration expressed as if all toluene was in the liquid phase, mg/L
C_{TCE}	reactor liquid TCE concentration, mg/L
C^v_{TCE}	reactor vapor TCE concentration, mg/L
C^f_{TCE}	feed TCE concentration, mg/L
F	chemostat feed rate, L/day
k_{tol}	maximum toluene degradation rate, mg toluene/L day
k_{TCE}	maximum TCE degradation rate, mg TCE/L day
K_{tol}	Michaelis-Menten constant for toluene, mg/L
K_{TCE}	Michaelis-Menten constant for TCE, mg/L
k_{light}	overall light proportionality constant, $\frac{\text{cell L namp}}{L_{sv}\ \text{mg cell}\ \text{mg lucif}}$
k_{lucif}	maximum luciferase production rate, mg/cell day
K_{light}	half-saturation constant for bioluminescence dependence on toluene, mg/L
K_{lucif}	half-saturation constant for luciferase dependence on toluene, mg/L
k_d	cellular death rate, day^{-1}
K_d	luciferase *in vivo* decay rate, day^{-1}
t	time, day

ν_R reaction rate, mg/L day
ν_R^{tol} toluene reaction rate, mg/L day
ν_R^{TCE} TCE reaction rate, mg/L day
V reactor liquid volume, L
X biomass concentration, mg/L
X_o chemostat feed cell density, mg/L
X_{ss} chemostat steady-state cell density, mg/L
$Y_{X/S}$ cellular yield, mg cells/mg substrate

Results

Chemostat Cellular Yield

The first experiment examined 8 periods of specific toluene feed concentration. However, at the greatest concentration (188 mg/L) the toluene feed pump was left off before cell densities were measured, so there were 7 pseudo-steady-state feed concentration points available for analysis. Although several of the feed concentrations were examined twice, the pseudo- steady-state cell density was different at each concentration. Table 4-2 illustrates, for example, that at 128 mg/L the pseudo-steady-state cell optical density was 0.145 OD_{600} for the first period, and 0.56 OD_{600} for the second period at 128 mg/L. The calculated yield decreased with each feed concentration examined until the last two periods and then remained approximately constant. This could have been due to biofilm formation on walls or feed tubes. A biofilm would consume toluene while not being accounted for in the biomass quantification of suspended cells, causing a lower calculated yield. Also, there appears to be a high yield grouping (before the toluene was turned off) and a

lower yield grouping (after the toluene was turned off). Perhaps the biomass had not recovered from washing out of the reactor to a lower cell density when the toluene was off. However, the chemostat yield values bracket the yield determined in batch culture (0.62 mg biomass/mg toluene).

Table 4-2. Biomass yield in TVA8 chemostat.

feed concentration (mg toluene/L)	cell density (OD_{600})	yield (mg biomass/mg toluene)
10	0.025	1.23
28	0.062	1.10
69	0.145	1.05
125	0.225	0.90
125	0.135	0.54
69	0.056	0.41
28	0.027	0.48

Bioluminescence

Both bioluminescence and cell density in the chemostat increased with increasing toluene feed concentration (Figure 4-2, Figure 4-3). However, after the initial increase, bioluminescence declined until the next step change in toluene feed concentration (Figure 4-2). When the toluene feed concentration dropped to 0 mg/L, bioluminescence quickly decreased. As soon as toluene was reintroduced to the reactor, bioluminescence increased. At steady-state for all feed toluene

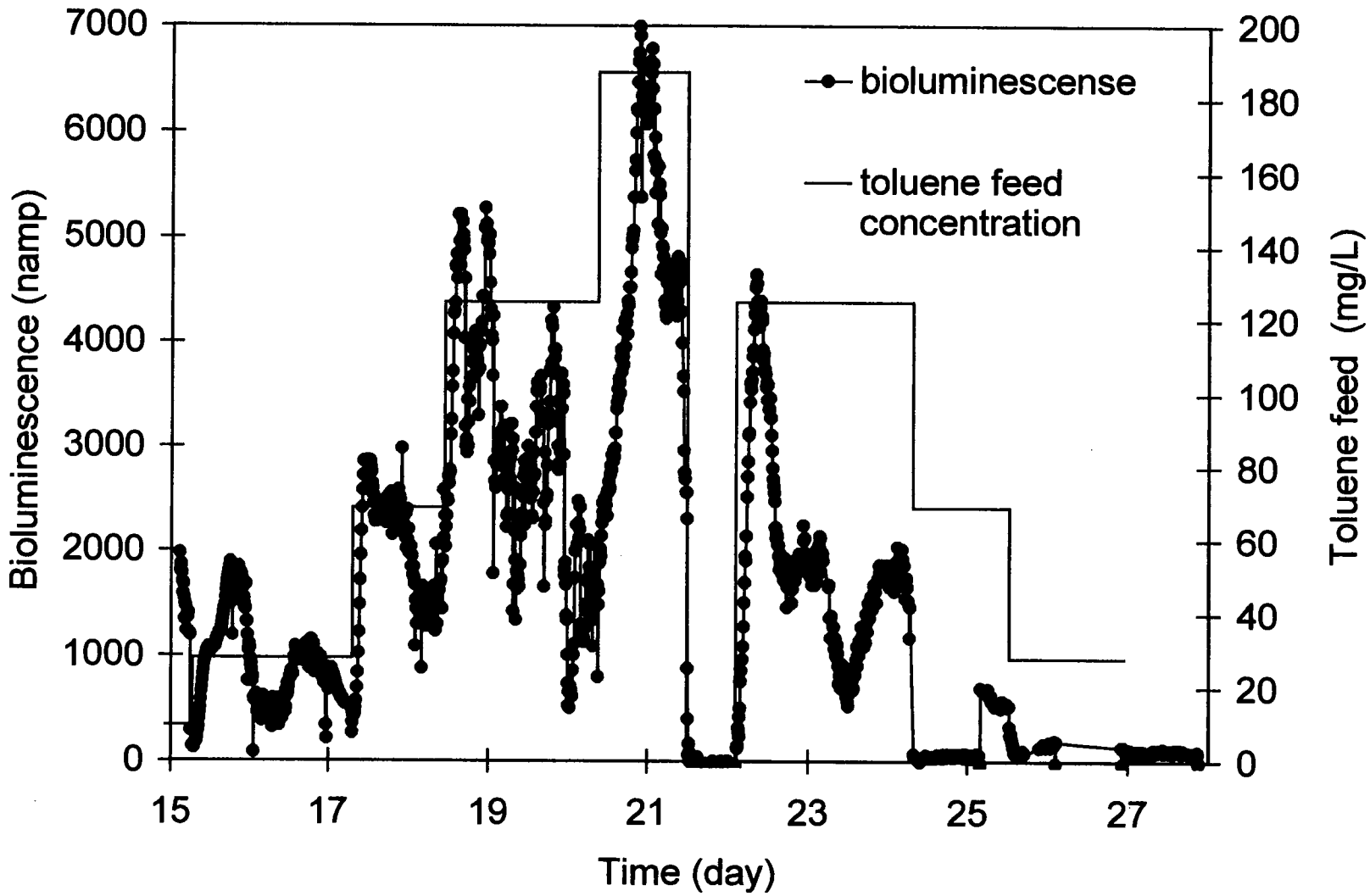

Figure 4-2. Bioluminescence from a TVA8 chemostat with feed concentration step changes.

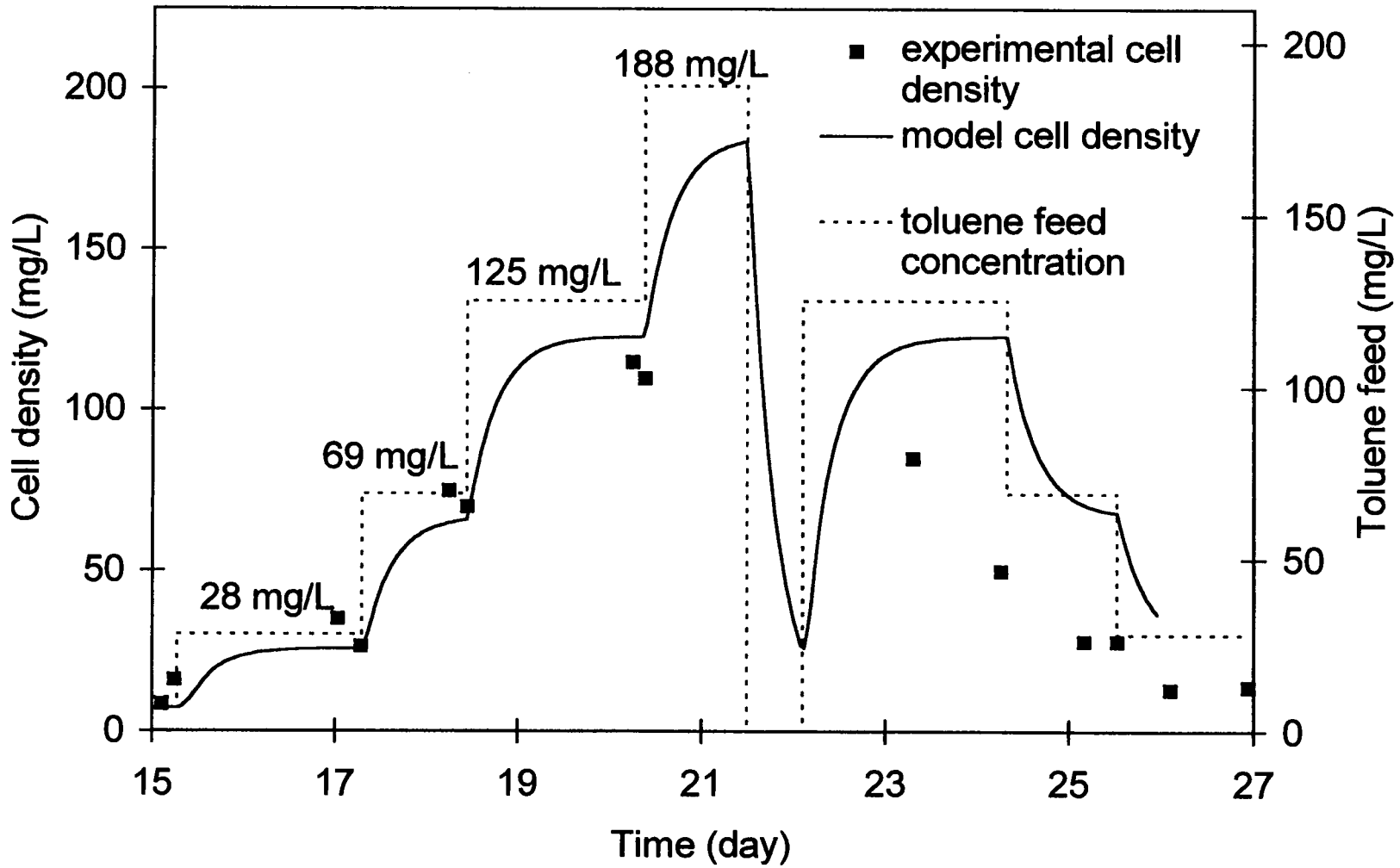

Figure 4-3. TVA8 chemostat cell density (model and experimental) and step feed toluene concentrations with time.

concentrations examined, all of the toluene was degraded by the cells in the reactor, while none of the TCE was degraded (data not shown).

The chemostat model was used to estimate the cell density profile with time in the reactor (Figure 4-3). Values for the parameters k_{TCE}, K_{tol}, K_{TCE} were the same as the batch model (Table 4-2), while k_{tol} was adjusted to fit the measured steady-state cell density. The yield of cells per mass of toluene is expected to be higher under carbon limited continuous culture than batch cultures because the cells channel available carbon to biosynthesis. A yield of 1.0 for chemostat model solution was selected because the yield determined from the steady-state cell density values approached 1.0 for the first half of the experiment (Table 4-2) and Chang (1992) reported yields of 1.22 and 0.99 for *Pseudomonas* on toluene.

The specific bioluminescence per mass of cell was determined by dividing the experimental bioluminescence by the model calculated cell density (Figure 4-4). Although the maximum transient bioluminescence increased with increasing feed concentration, the actual bioluminescence per cell decreased with higher feed concentrations. The bioluminescence increases were reflecting an increase in cell density as opposed to a increased level of transcription. The transient toluene concentration in the reactor was determined from the chemostat model (Figure 4-4). Upon an increase in feed toluene concentration, the reactor toluene concentration would increase slightly (to less than 1 mg/L), then decrease as cell densities reached steady-state values. The specific bioluminescence seemed to correlate well with the calculated reactor toluene concentration (Figure 4-4).

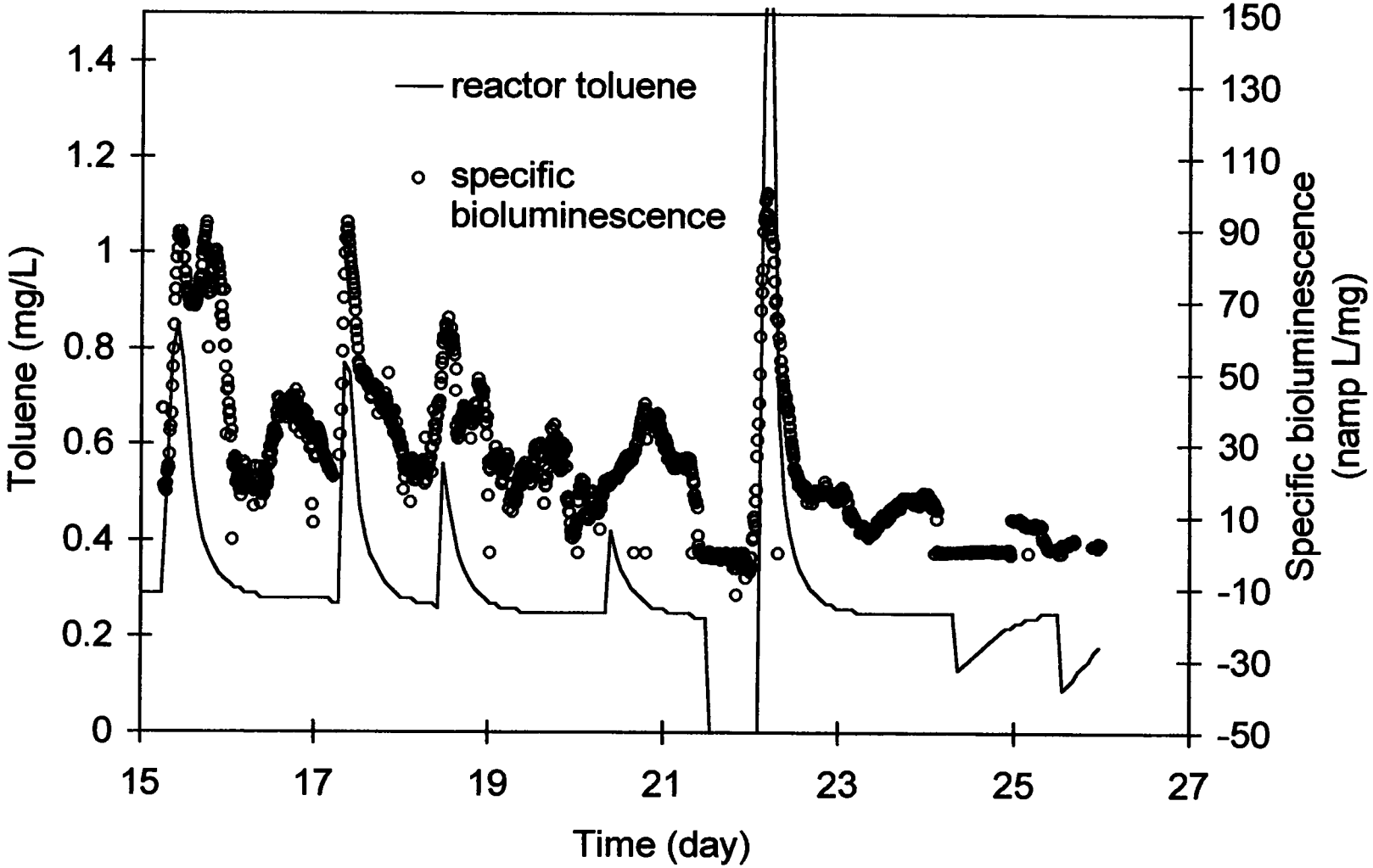

Figure 4-4. TVA8 chemostat specific bioluminescence and calculated reactor toluene concentration.

Model Parameters

Using the degradation parameters discussed above and the bioluminescence model parameters (k_{light}, K_{light}) determined from the batch experimental data, the model for bioluminescence did not fit chemostat bioluminescence data well (Figure 4-5). However, using higher values for the K_{light} and K_{lucif} parameters, and including a term to account for *in vivo* enzyme degradation, the model better fit the chemostat bioluminescent data (Figure 4-5). Table 4-3 lists the parameters used in the chemostat mathematical simulation, their values, and how they were determined.

Transient Response to a Step Change

In the second *tod-lux* chemostat experiment, the transient portion of the step change in feed toluene concentration was examined. Steady-state light output was stable around 300 namp with a toluene feed concentration of 13 mg/L toluene (Figure 4-6).

Reactor concentrations of TCE remained constant and equal to abiotic concentrations. The feed toluene concentration was increased to 94 mg/L for about 3 hr. Reactor cell density increased soon after the toluene feed concentration was increased, while bioluminescence began to increase 2.5 hr after the toluene feed concentration was increased. The reactor toluene concentration increased immediately after the increase in feed toluene concentration.

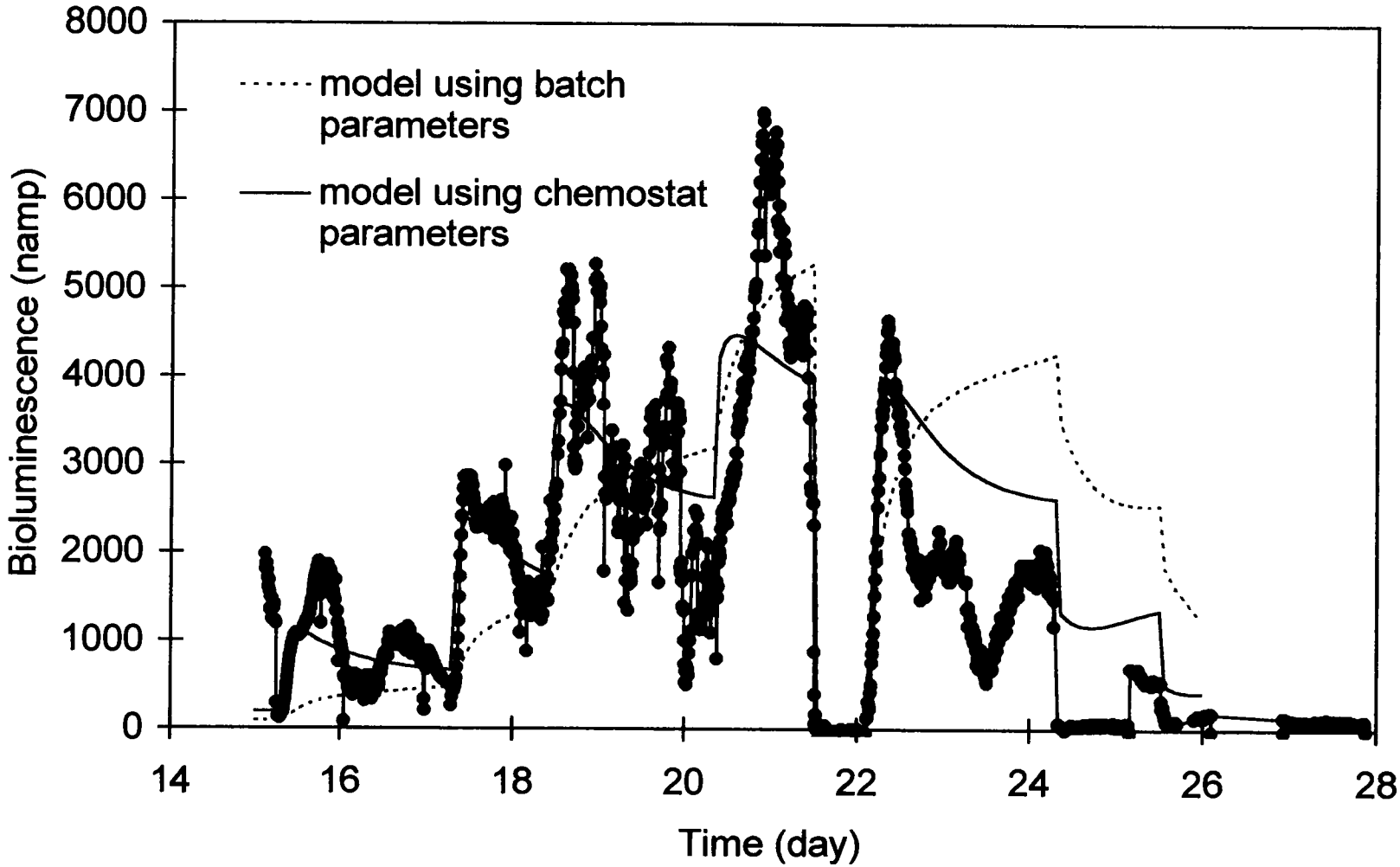

Figure 4-5. Bioluminescence (model and experimental) from a TVA8 chemostat with feed concentration step changes.

Table 4-3. Chemostat model parameter values and method of determination.

Parameter	symbol	value	obtained from
toluene yield coefficient	$Y_{X/S}$	1.0	steady-state chemostat cell density
maximum specific substrate degradation rates	k_{tol}	$14.0 \frac{\text{mg tol}}{\text{day mg cell}}$	steady state chemostat cell density
	k_{TCE}	$1.3 \frac{\text{mg TCE}}{\text{day mg cell}}$	inducer varied batch experiments
half saturation substrate degradation constants	K_{tol}	$2.7 \frac{\text{mg}}{\text{L}}$	inducer varied batch experiments
	K_{TCE}	$6.4 \frac{\text{mg}}{\text{L}}$	
Henry's law coefficient	H_{tol}	0.27	literature
	H_{TCE}	0.36	
light half saturation constant	K_{light}	$5.0 \frac{\text{mg}}{\text{L}}$	approximate value from batch experiment
luciferase half saturation constant	K_{lucif}	$5.0 \frac{\text{mg}}{\text{L}}$	approximate value from batch experiments
luciferase decay constant	K_d	$2\ \text{day}^{-1}$	chemostat decay in bioluminescence as steady-state is approached
light proportionality constant	k_{light}	$1750 \frac{\text{cell L namp}}{L_{sv}\ \text{mg cell mg lucif}}$	magnitude of bioluminescence in transient part of chemostat experiment

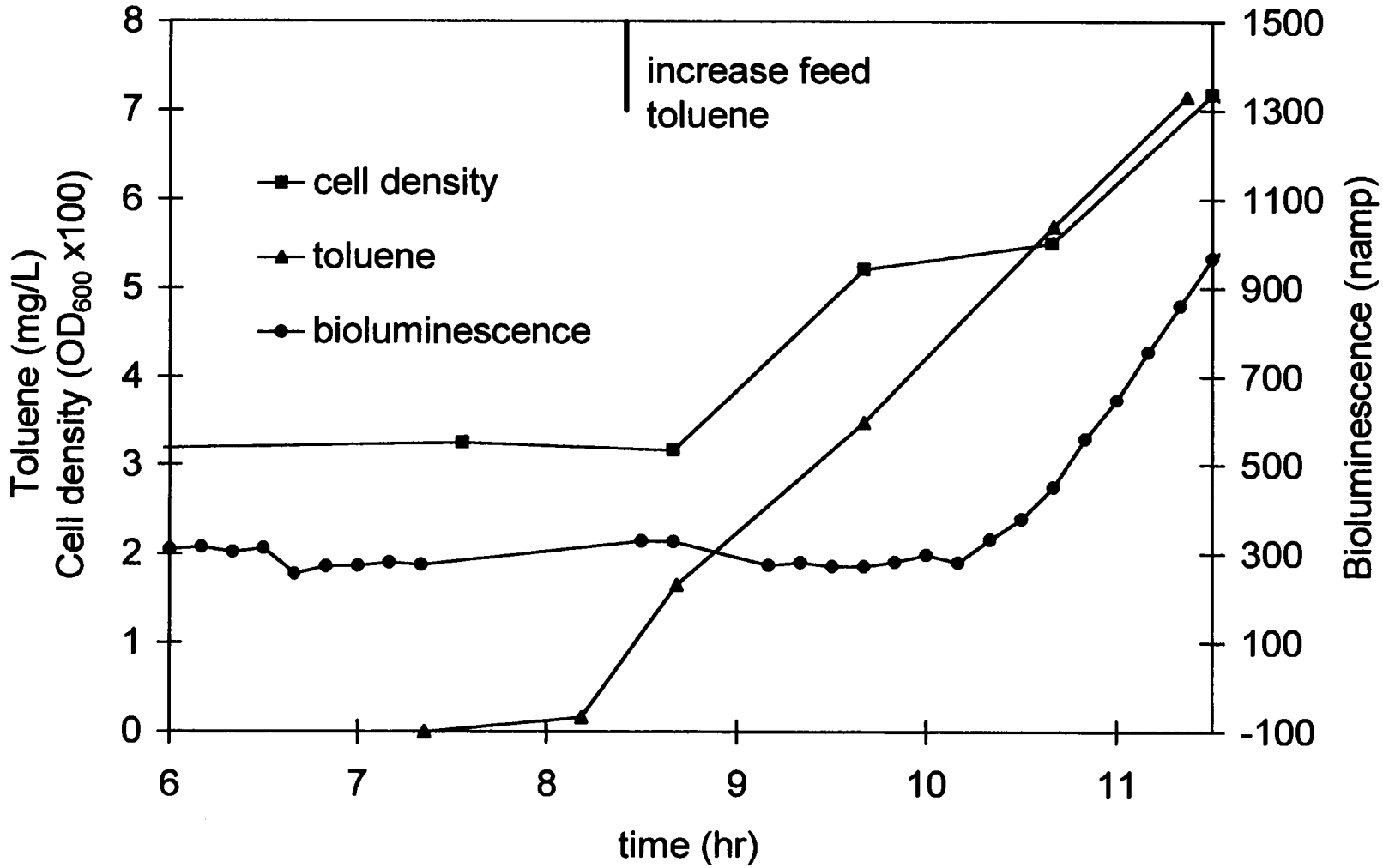

Figure 4-6. Bioluminescence, cell density and toluene concentration from a TVA8 chemostat with an increase in toluene feed concentration.

Discussion

In the *tod-lux* chemostat experiments, bioluminescence increased initially with and increase in toluene feed concentration, and then declined to a steady-state level. This occurred for each subsequent increase in feed concentration. When a chemostat is operated under steady-state conditions, the reactor growth substrate (in this case toluene) concentration is close to zero. The growth substrate that enters the reactor is distributed and immediately consumed by the cells in the reactor. When the feed concentration is increased, the cell mass does not increase to the steady-state value instantaneously. When the toluene feed concentration was increased, the reactor toluene concentration increased (Figure 4-4 and 4-6), resulting in an increased growth rate of cells. The cellular growth rate was increased until the cell density reached a point where the cells consumed all the growth substrate that entered the reactor and then the cell growth rate decreased to the original value. However, the cell density was higher at the new steady-state (Figure 4-3). In the transient period just after the increase in feed concentration, the cells existed in a growth substrate and inducer rich (toluene) environment. The bioluminescence spikes observed after the increase in toluene feed concentration reflected the increased growth substrate and inducer availability. In a steady-state chemostat operation the *tod* promoter might not be induced and there is probably growth substrate limitation for the production of light. These two issues (growth substrate limitation and lack of induction) are difficult to separate with a metabolized inducer such as toluene.

Parameter values that resulted in a good fit of chemostat bioluminescence were different than those for batch bioluminescence. The chemostat was operated for much longer times than the batch experiments; so intuitively, the effect from the *in vivo* decay of *lux* enzymes would be more pronounced in the chemostat. The luciferase enzyme decay rate (K_d) was used to fit the chemostat transient decline in bioluminescence after an initial bioluminescent spike. The value that caused the model to best fit the data was 2 day^{-1}, which corresponds to a molecular life of 12 hours. Chase (1950) reported declines in luciferase activity for *in vitro* luciferase for different temperatures. The lowest temperature indicated (40°C) resulted in an initial (measured for 8 hr) decline of activity, at a rate where the enzyme has lost half the activity by 12 hours. Although these were *in vitro* experiments, a decay rate of 2 day^{-1} seems reasonable.

The K_{light} and K_{lucif} parameters were increased above batch simulation values to fit the chemostat data. These terms represent the region of toluene concentration where light and luciferase production were dependent on reactor toluene concentration (saturational dependence on toluene concentration). In the growth substrate limited chemostat system, the cells probably do not have reserve storage polymers and may be more sensitive to toluene concentrations. In the batch studies, maximum induction was estimated to occur below 10 mg/L toluene, and bioluminescence peaked at about 10 mg/L toluene (Figure 3-10), so the value of the Michaelis-Menten constants (K_{light} and K_{lucif}) were chosen to be 5.0 mg/L in the chemostat. In addition, the batch

experiments were performed with the B2 reporter, while the chemostat experiments were performed with the TVA8 reporter, so specific values of parameters could be different due to strain differences.

CHAPTER 5

CHARACTERIZATION OF THE SHK 1 BIOREPORTER IN BATCH CULTURE

The constitutive bioreporter examined in this study was Shk 1, which was constructed by mating a constitutive *lux* construct into an activated sludge isolate (Kelly, 1997). The advantage of this construct over other light producing bacteria frequently used to assess toxicity is that Shk 1 is a microbial component of activated sludge. Therefore, it is expected to respond similarly to activated sludge communities. This type of reporter can be used as an early warning to plant operators that a toxic component is present in the waste stream.

The Shk 1 reporter was constructed by mating plasmid pUTK2 (Burlage, et al., 1990), containing the Tn4431 *lux* transposon with a mixed population of activated sludge microorganisms obtained from the Eastman Chemical Company wastewater treatment plant. Selection for transformants was performed on a minimal salts medium, with a chemical composition similar to the influent wastewater, containing 20 mg/L tetracycline and 2,000 mg/L ethylene glycol. Shk1 was identified as *Azospirillum* by partial sequencing of the 16S rRNA (Kelly, 1997).

Batch Bioluminescent Response

Batch Growth Curve

Methodology

Three flasks with 100 mL of simulated wastewater, 2,000 mg/L complex carbon source, and 25 mg/L tetracycline were inoculated with 200 *u*L of an overnight culture of Shk 1. Samples were withdrawn intermittently from the flask for cell density and bioluminescence measurement. The samples were then returned to the flask. Bioluminescence was measured by placing a vial containing 3 mL of culture into a light tight sampling cell equipped with a light guide and photomultiplier.

Results

The maximum growth rate of 11 day^{-1} was determined by plotting the natural logarithm of cell density (mg/L) versus time (Figure 5-1). The culture exhibited a lag time of approximately 10 hr before a significant increase in cell optical density was observed (Figure 5-2). This was due to the small inoculum of 200 *u*L. However, after 15 hours, the cell density increased linearly for 20 hours at a rate of 0.045 OD_{600}/hr. In contrast, bioluminescence increased linearly at 440 namp/hr for only 7 hours, reached a maximum, then decreased at 350 namp/hr, reaching background light levels in 8 hours. Bioluminescent behavior was similar to the TVA8 batch growth experiment. As with TVA8, maximum bioluminescence corresponded to the inflection

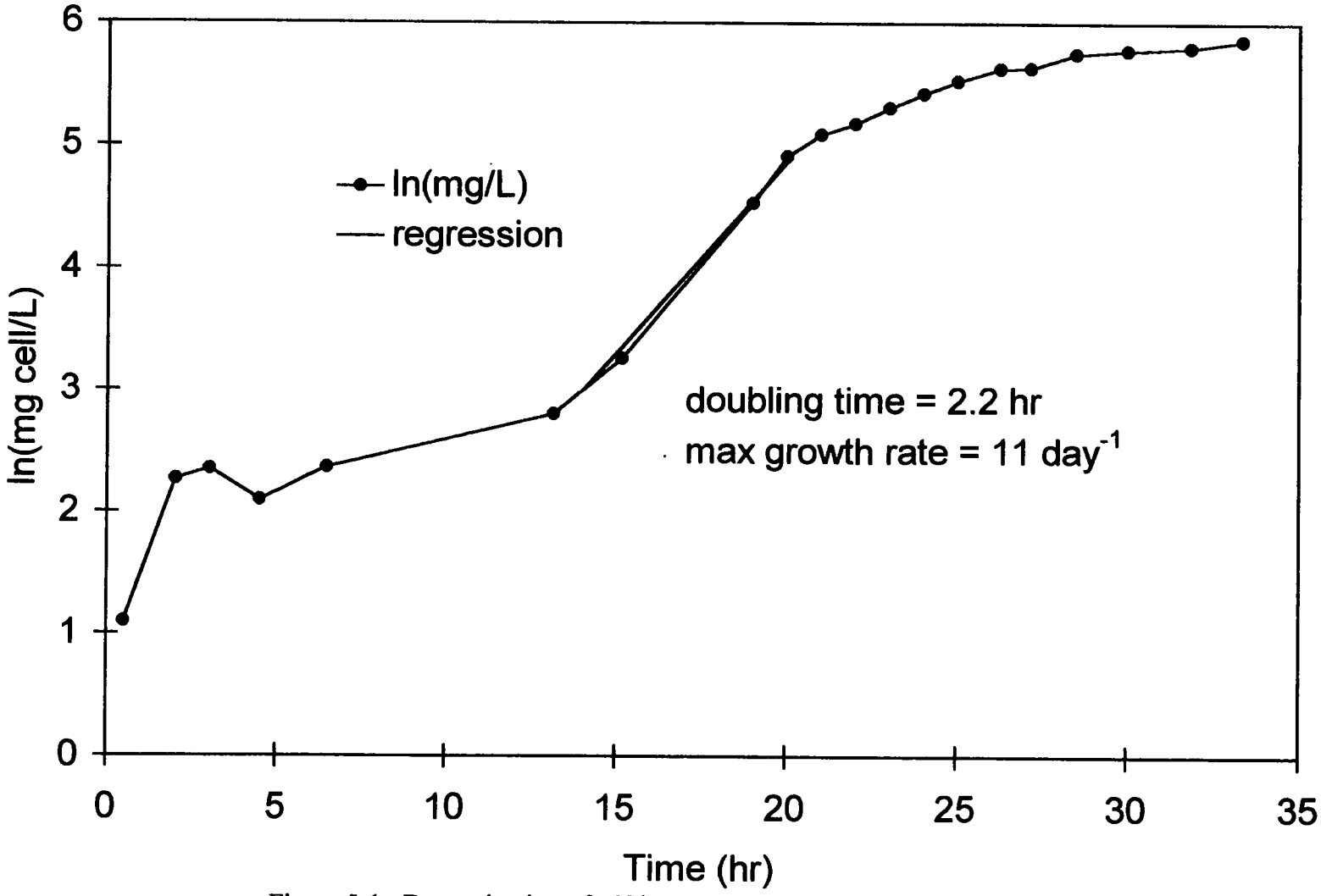

Figure 5-1. Determination of Shk 1 exponential growth rate.

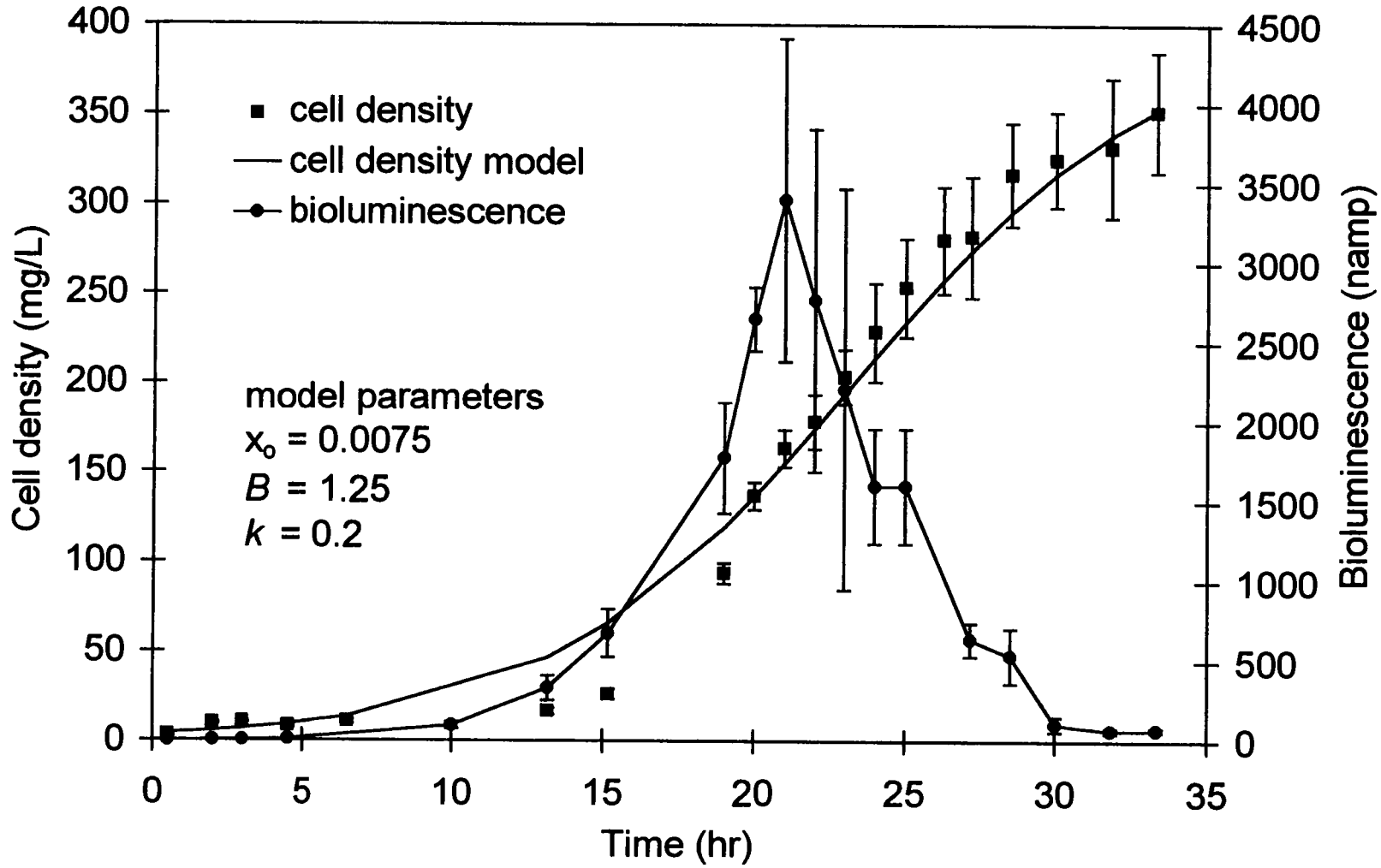

Figure 5-2. Shk 1 batch growth curve: experimental cell density, logistic curve fit cell density, and bioluminescence with time.

point of the cell density curve. The cell density data were fitted to the empirical logistic curve (Equation 3-1) with the parameters x_o=0.0075 OD_{600}, β=1.25, and k=0.2. The bulk growth rate, specific bioluminescence and bulk bioluminescence reached a maximum at approximately the same time (15-20 hr) (Figure 5-3).

Effect of Various Carbon Sources on Growth Curve

Methodology

A mid-log phase culture of Shk 1 was centrifuged, and resuspended in simulated wastewater without any carbon source. The resulting initial optical cell density was 0.11 OD_{600}. Five mL samples were dispensed to triplicate vials. Four treatments were examined. They consisted of adding (1) no carbon source, (2) 2,000 mg/L calcium acetate, (3) 2,000 mg/L ethylene glycol, and (4) 2,000 mg/L complex carbon from the simulated wastewater medium. Bioluminescence was monitored every 30 minutes for 6 hours, and the final cell optical density was measured.

Results

Each of the treatments started at approximately the same level of bioluminescence (Figure 5-4). Bioluminescence of the complex carbon source and acetate carbon source treatments increased with time, reached a maximum, then decreased. Bioluminescence of the ethylene glycol and no carbon source treatments

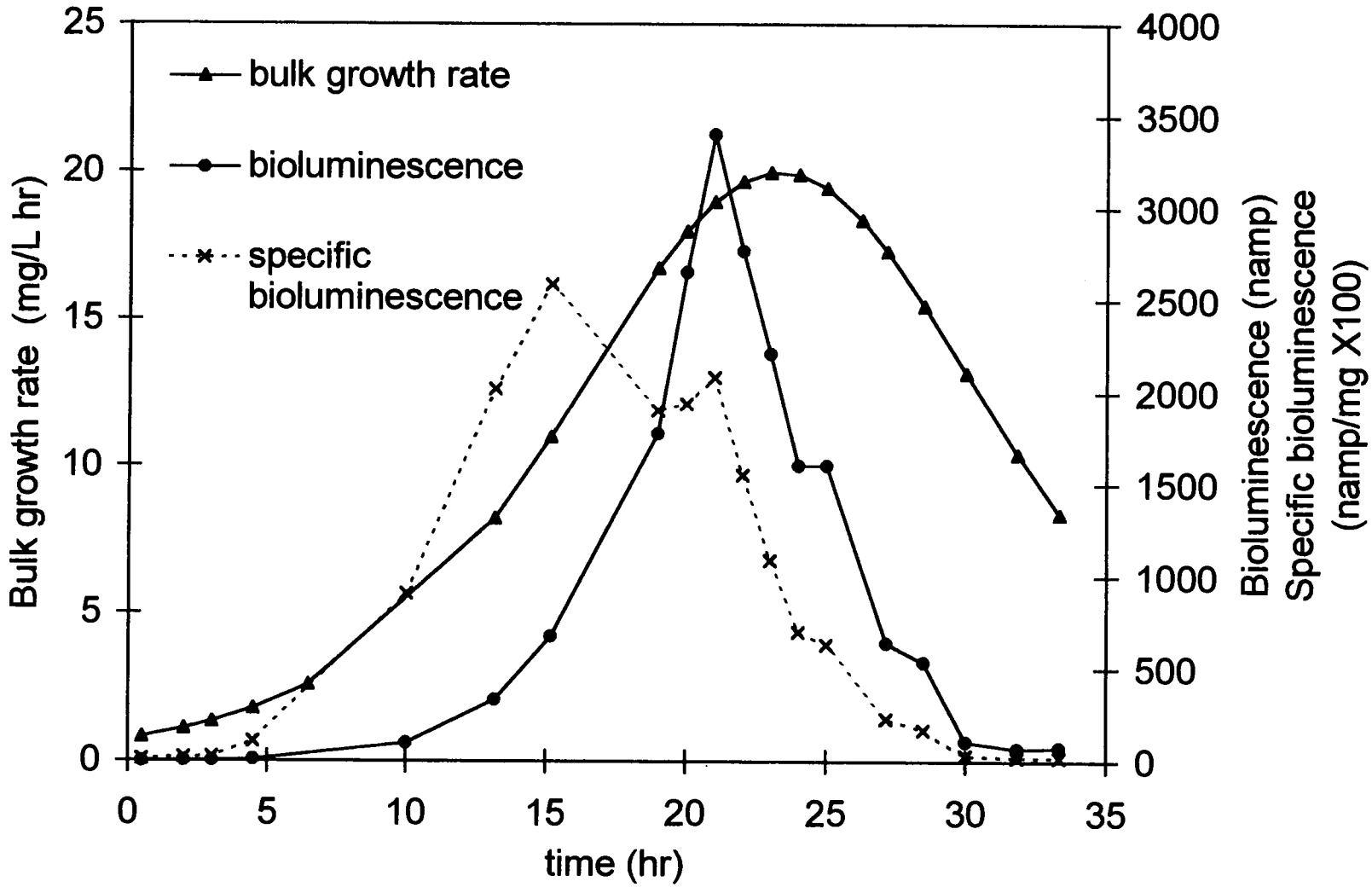

Figure 5-3. Bulk growth rate from logistic curve, bioluminescence and specific bioluminescence for batch Shk 1.

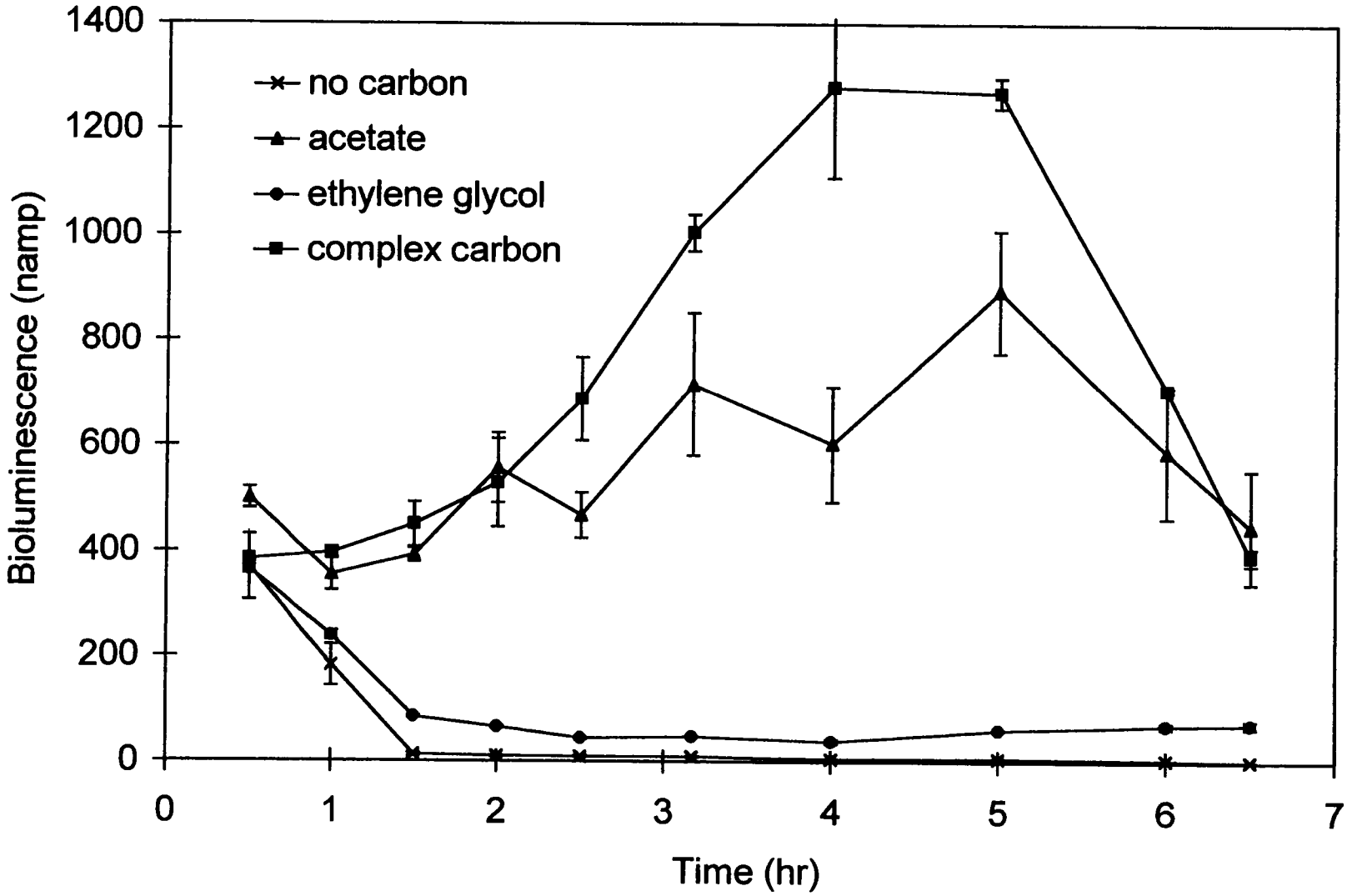

Figure 5-4. Bioluminescent response to various carbon sources.

decreased with time. However, the ethylene glycol treatment decreased more slowly than the no carbon source treatment. The final optical density of the no carbon source treatment was 0.15 OD_{600}, the ethylene glycol was 0.3 OD_{600}, the calcium acetate was 0.6 OD_{600}, and the complex carbon source was 0.7 OD_{600}. Although the bulk bioluminescence is plotted in Figure 5-4, the maximum specific bioluminescence based on the final cell density yielded the same qualitative results: complex carbon 3.6 namp/mg cell, acetate 2.9 namp/mg cell, ethylene glycol 0.54 namp/mg cell, and no carbon 0.08 namp/mg cell.

Discussion

Shk 1 batch growth bioluminescence was qualitatively similar to the bioluminescent behavior of the inducible TVA8 reporter. The interpretations of an accumulation of luciferase to describe the increasing bioluminescence and possibly oxygen limitation to explain the decrease in bioluminescence apply to this system also. The fact that the non-inducible reporter exhibited the same behavior as the inducible reporter reinforces that the changes in bioluminescence were probably not related to induction.

During batch growth, reporter cells responded and utilized various carbon sources to different extents. The Shk 1 cells utilized some carbon sources more efficiently than others. These results indicated that an easily metabolized carbon source must be provided to the reporter cells for significant light production, and a predictive

mg/L. All samples were prepared in triplicate. Hydroquinone toxicity was assessed in distilled water, simulated wastewater, and simulated wastewater with sludge from bench scale reactors.

Respirometry of Activated Sludge in Response to Hydroquinone

Oxygen consumption rates by industrial activated sludge upon exposure to hydroquinone were measured. Activated sludge was obtained from an industrial wastewater plant and placed in 500 mL flasks. The flasks were incubated overnight with 50 mL of simulated wastewater media. Three mL of the sludge solution, 1 mL of an appropriate hydroquinone solution, and 1 mL of simulated wastewater media were added to the respirometer well. The oxygen probe was immediately placed over the sample allowing no head-space in the well, and the decline in oxygen concentration was measured over time.

Results

Bioluminescent Response to Toxicants in Batch Tests

Bioluminescence of the Shk 1 reporter strain decreased in response to the toxicants cadmium, 2,4-dinitrophenol, and hydroquinone. In contrast, concentrations of ethanol up to 10,000 mg/L had no effect on bioluminescence (Figure 5-5). The bioluminescent response by the Shk 1 bioreporter was constant with pH between 6.1 and 7.9. However, at the lowest pH tested (5.5 pH), bioluminescence was depressed

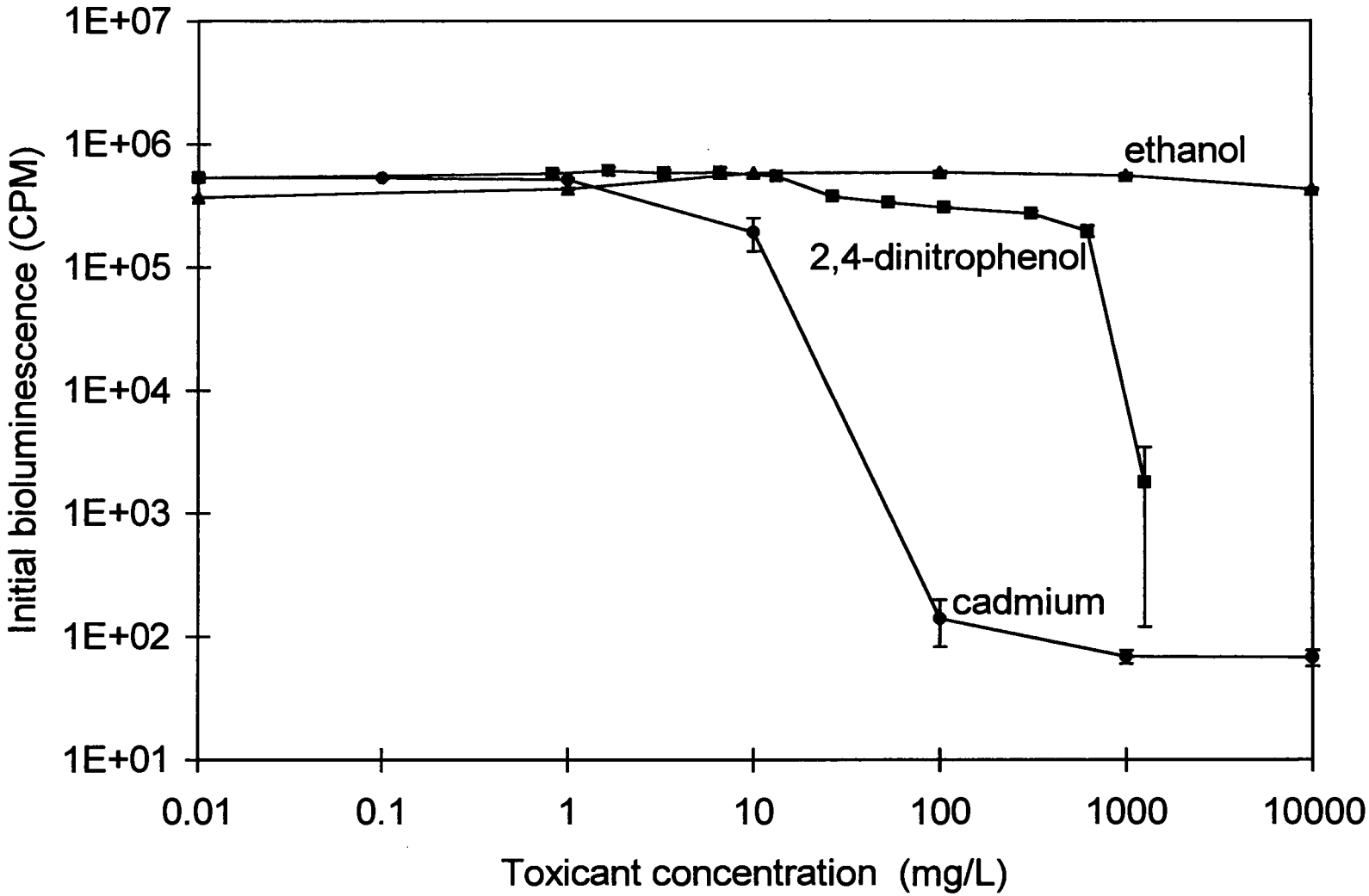

Figure 5-5. Initial bioluminescent response of Shk 1 to cadmium, ethanol, and 2,4-dinitrophenol.

slightly (data not shown). Bioluminescence decreased with increasing cadmium concentration greater than 1 mg/L (Figure 5-5). There was a significant drop in bioluminescence between 1 and 10 mg/L, and at cadmium concentrations of 100, 1,000, and 10,000 mg/L bioluminescence was completely diminished. The bioluminescent response to 2,4-dinitrophenol remained constant with increasing concentration of toxicant until approximately 1,000 mg/L, then decreased sharply (Figure 5-5).

Bioluminescence of Shk 1 and Respirometry of Activated Sludge in Response to Hydroquinone

The initial level of bioluminescence of Shk 1 decreased with increasing hydroquinone concentration in each of the matricies examined: Shk 1 with distilled water, simulated wastewater, and simulated wastewater with sludge from bench scale reactors. Data from Shk 1 with simulated wastewater and sludge is presented (Figure 5-6). However, the 1, 10, and 100 mg/L samples recovered to the 0 mg/L hydroquinone concentration bioluminescence levels while the 1,000 and 10,000 mg/L samples had not increased in four hours. In previous studies, toxicity to phenol was shown to decrease with increasing incubation time indicating recovery of bioluminescence (Dutka, 1983). Respirometry of industrial activated sludge resulted in the same general trend in hydroquinone toxicity as the bioreporter (Figure 5-7). Oxygen consumption declined with increasing hydroquinone concentration. For both bioluminescence and oxygen consumption rate, the decline was dramatic between 0, 1

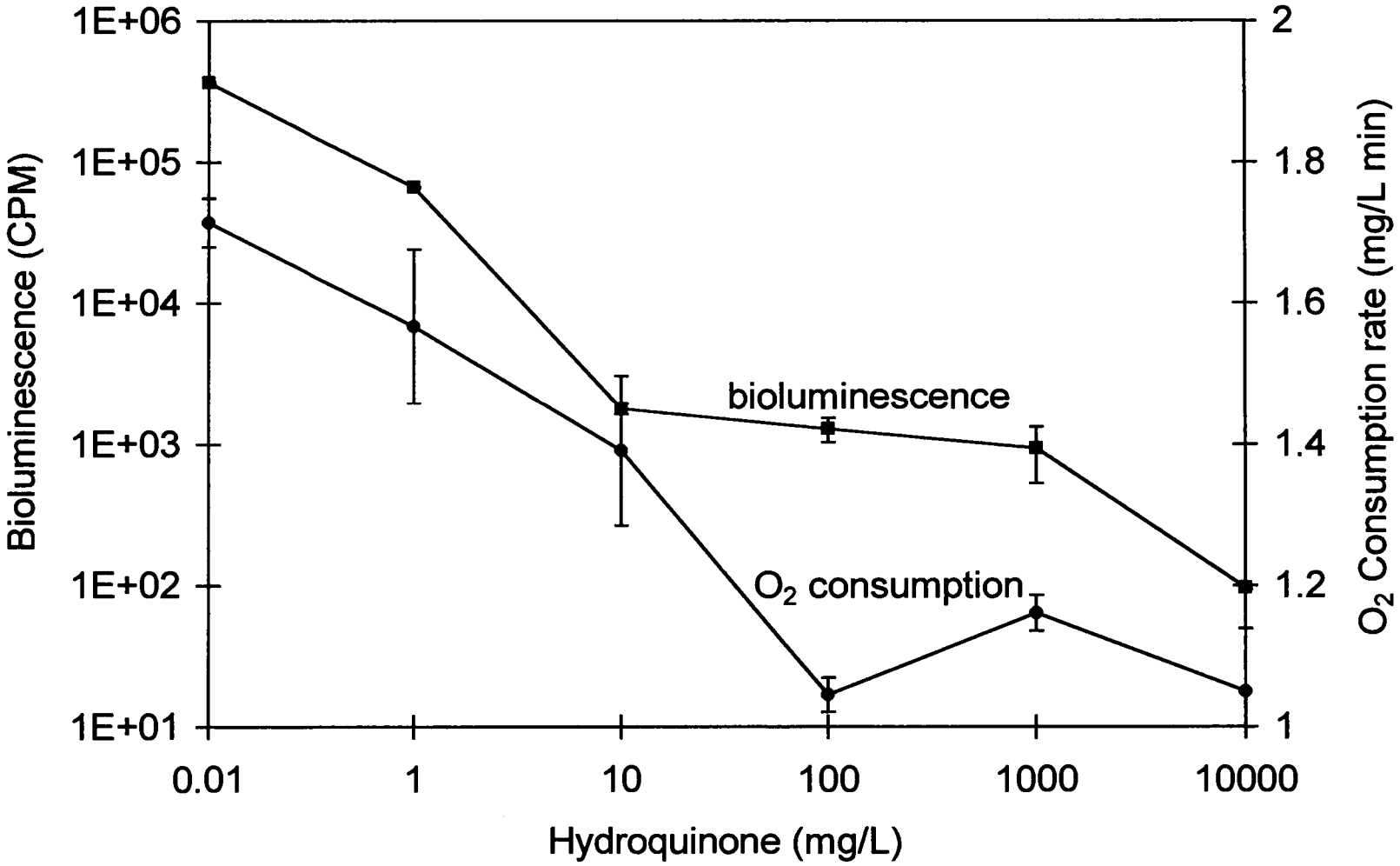

Figure 5-6. Initial bioluminescence and oxygen consumption rate of Shk 1 in response to hydroquinone.

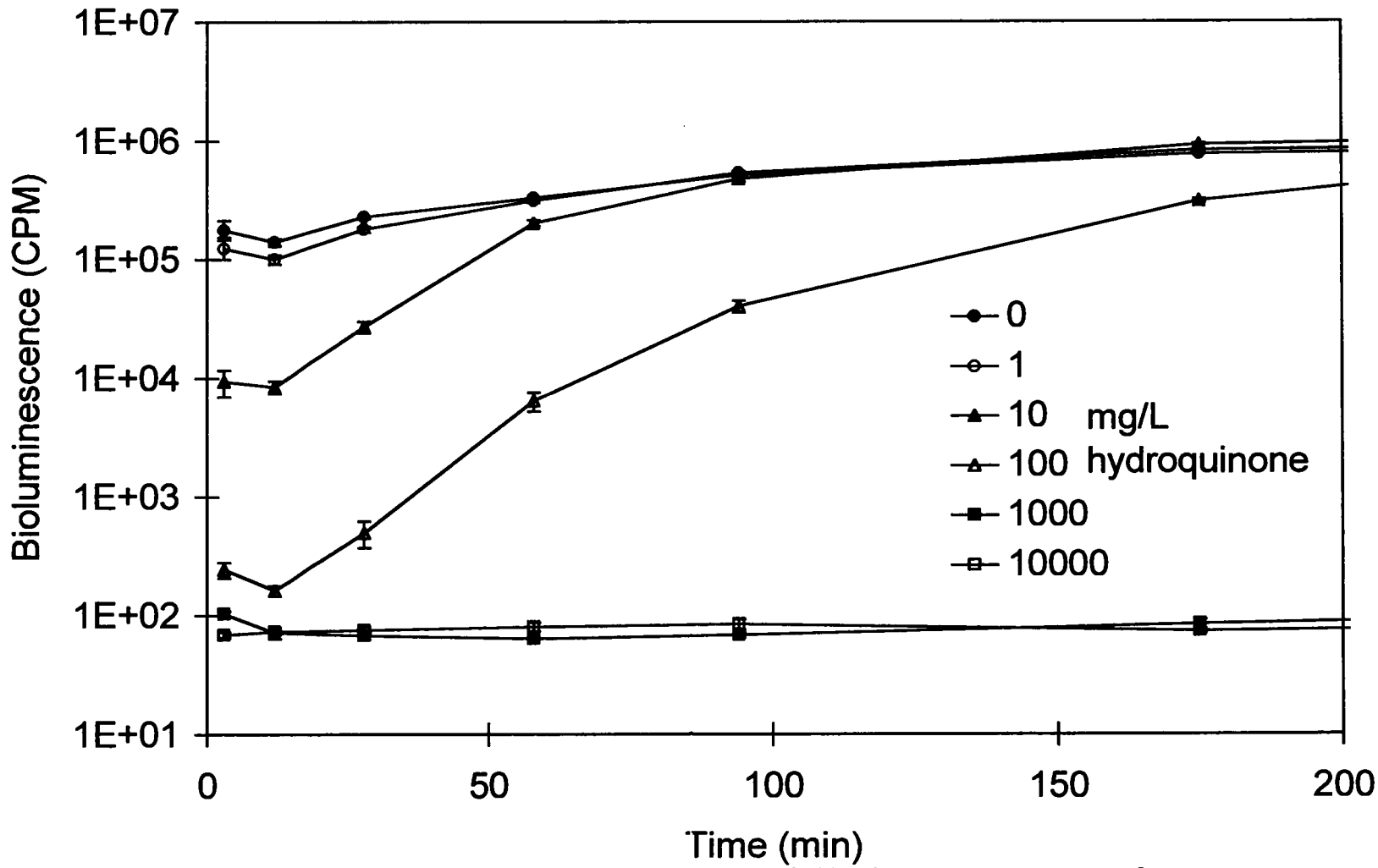

Figure 5-7. Time course bioluminescence of Shk 1 in response to a range of hydroquinone concentrations.

and 10 mg/L hydroquinone, but leveled off between 10 and 1,000 mg/L hydroquinone.

Discussion

The Shk 1 bioreporter has several characteristics desirable in a toxicity monitoring system for prescreening of new manufacturing waste chemicals, and routine on-line monitoring of influent wastewater and plant effluent. The Shk 1 reporter's high growth rate as dispersed cells are advantages for routine preparation of cultures for toxicity determinations. Shk 1 grows in full strength synthetic wastewater containing the typical carbon sources being treated at the targeted plant. Methanol, isopropanol and ethylene glycol (used in this study) have been found to be non-inhibitory to activated sludge, with respirometry based EC_{50} values ranging from 50 to 200 mL/L (Kilroy, 1992). Bioluminescence was not affected by settled activated sludge supernatant or normal influent wastewater. A decrease in bioluminescence would indicate that the strain is overly sensitive to potential toxicant effects on sludge quality. In addition, Shk 1 bioluminescence is unaffected by pH over typical influent pH ranges. A constant bioluminescence response over a wide pH range enables the bioreporter to be used at typical wastewater pH and assess toxicity with more relevance than a naturally bioluminescent marine bacterium. Toxicity monitoring is more difficult using strains with nutritional needs or toxicity responses inconsistent with the nature of the wastewater being treated.

Treatment facility specific bioreporters may be more reflective of potential toxic impacts on sludge quality than more generic strains. Light emission from Shk 1

was sensitive to cadmium, 2,4-dinitrophenol, and hydroquinone, which are toxicants known to impact sludge microbial activity (Norberg, 1983; Battistoni, 1993; Volskay, 1988; Stom, 1992). While ethanol, a common component of the influent wastewater, had no impact on light emission in the range tested. The Microtox system also indicated low ethanol toxicity, with an EC_{50} value for ethanol from 31,000 to 56,706 mg/L (Dutka, 1983). However, the EC_{50} value for 2,4-dinitrophenol varies significantly with type of toxicity assessment. This study yields an EC_{50} value of 340 mg/L, while Volskay reports EC_{50} of 110 mg/L determined from respirometry (Volskay, 1988) and Strotman (1995) reports an EC_{50} of 29 mg/L using bioluminescence with *P. phosphoreum*, and 70 mg/L via a nitrification inhibition method.

It is desirable that a luminescent strain designed for toxicity monitoring exhibit both relative (between chemicals) and absolute (concentration) toxicity comparable to potential impacts on sludge microorganisms. Previous experiments indicate poor correlation between toxicity of specific chemicals as determined by respirometry and luminescent response using the Microtox system (A.J. Meyers, personal communication). Shk 1 bioreporter toxicity assessment gave comparable results with respirometry toxicity assessment of hydroquinone to activated sludge. This suggests that this strain reflects the toxicity characteristic of activated sludge microbial populations. However, this can not be verified without more extensive comparative experiments.

The ability to insert reporter sequences in a wide array of microorganisms allows the development of bioreporters tailored for specific applications. In a municipal wastewater treatment plant with tertiary nitrogen removal, nitrifiers may be the most sensitive organisms of concern. In industrial wastewater treatment plants or municipal plants with only secondary treatment these populations may be of no concern. In these cases protection of specific degradative organisms for recalcitrant or volatile organics may be of greater importance. In other cases the only concern may be pin floc resulting from toxicant damage to floc structure. The design of effective bioreporters for toxicity monitoring should include these considerations.

CHAPTER 6

CHARACTERIZATION OF THE SHK 1 BIOREPORTER IN A CHEMOSTAT AND A TURBIDOSTAT

Methodology

Chemostat and Turbidostat Apparatus

The chemostat and turbidostat utilized the same glass reactors and associated fittings. A 50 mL, round bottom glass tube equipped with a rubber stopper at the top served as the reactor vessel. The vessel contained a magnetic stirrer and was placed in a light-tight box on a magnetic stir plate. An overflow outlet was located to maintain a 25 mL liquid volume. Air was provided with 1/16" stainless steel tubing through the rubber stopper and into the liquid. Feed entered through the top of the reactor from a drip tube to prevent back contamination of the feed reservoir. Simulated wastewater with 25 mg/L tetracycline was fed to the reactor. Light was collected from a liquid light guide and photomultiplier and automatically recorded. Cell optical density measurements were taken intermittently from the effluent.

The turbidostat was designed to maintain a constant turbidity in the reactor. A light source (light emitting diode, LED) was located just outside the glass reactor (approximately 2 inches from the bottom of the vessel). Directly across from the LED

(180°) was a light detector (photoresistor) (Figure 6-1). The photoresistor was connected to a circuit that energized the feed pump when the turbidity of the culture (as measured by the LED and photoresistor) exceeded the set-point set with a variable resistor (potentiometer) in the circuit. The circuit was modified from a Radio Shack comparator circuit design (light level indicator) (Figure 6-2).

Experimental Description

There were two reactor vessels, one of which could be operated in turbidostat or chemostat mode, while the other was operated in chemostat mode. Three separate experiments were performed. It is important to identify the timing in which the experiments were performed because (1) the feed tended to precipitate and perhaps became contaminated with time, and (2) Shk 1 tended to grow with floc and biofilm morphology after an extended time in continuous culture. Before each of these three experiments the vessels were cleaned, autoclaved, and new feed media prepared. The three experiments are described below.

(1) Vessel one was operated in chemostat mode. Additional acetate was added to the feed tank to effectively yield step changes in feed carbon concentration. The times and feed carbon concentration are listed in Table 6-1.

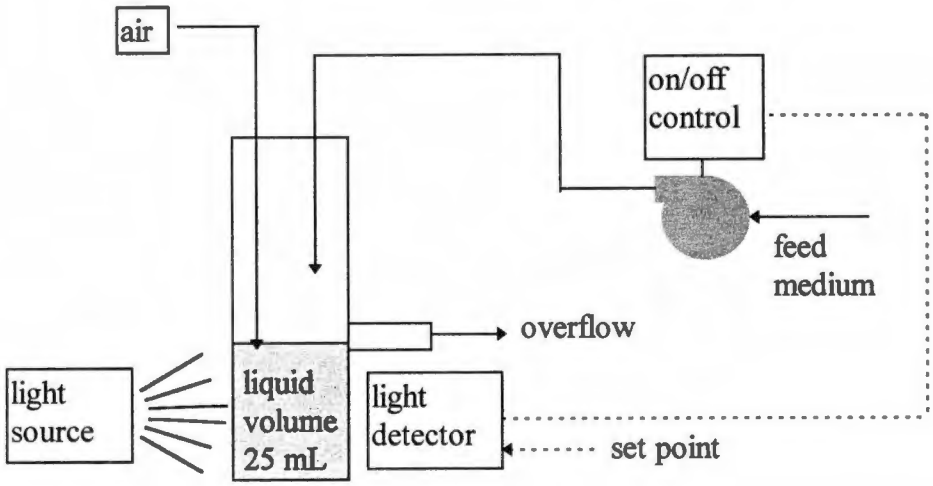

Figure 6-1. Turbidostat schematic.

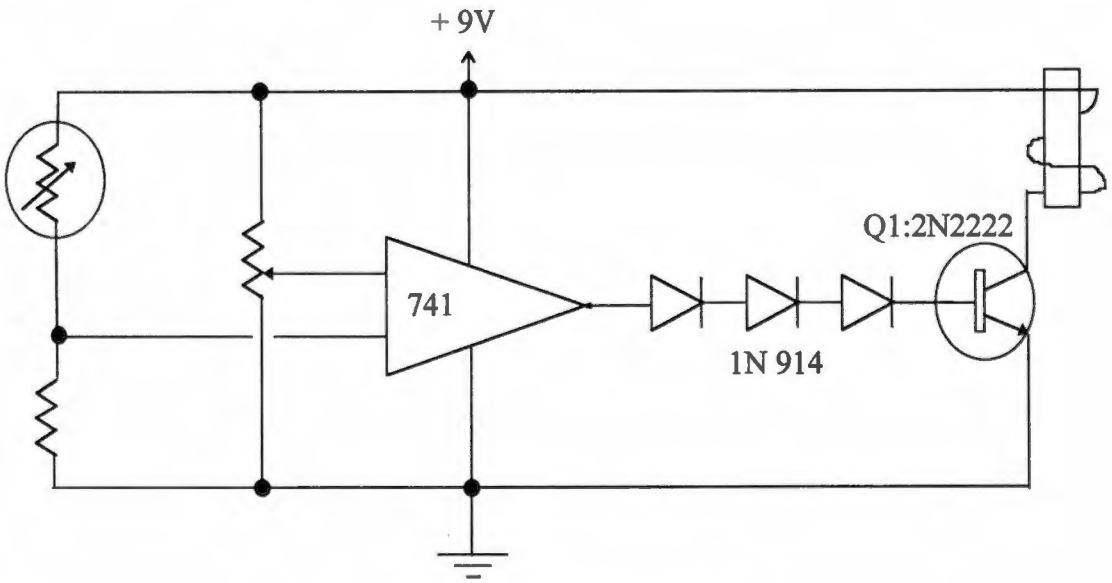

Figure 6-2. Turbidostat circuit schematic.

Table 6-1. Shk 1 chemostat feed concentration step changes.

Time (hr)	Feed Concentration (mg/L)
0 - 66.5 hr	50 mg/L
66.5 - 160 hr	250 mg/L
160 - 225 hr	750 mg/L

(2) Vessel one was operated in turbidostat mode, with 2000 mg/L acetate and 25 mg/L tetracycline in the feed. Vessel two was operated in chemostat mode and fed simulated wastewater with 1000 mg/L acetate and 25 mg/L tetracycline at 2.6 mL/hr, resulting in a dilution rate of 2.5 day^{-1}. The expected chemostat steady-state cell density (for this carbon concentration) was estimated from the previous experiment, and the turbidostat set-point was set at that value.

(3) Both vessels were operated in chemostat mode, with 1000 mg/L acetate and 25 mg/L tetracycline in the feed. Two dilution rates were examined in each chemostat.

Table 6-2 summarizes the three experiments performed.

Table 6-2. Turbidostat and chemostat operating conditions. Horizontal lines separate feed formulation.

	Vessel one			Vessel two		
#	dilution rate	cell density	mode	dilution rate	cell density	mode
1.	2.5 day^{-1}	0.03, 0.08, 0.18 OD_{600}	chemostat	———	———	———
2.	10.7 day^{-1}	0.24 OD_{600}	turbidostat	2.5 day -1	0.24 OD_{600}	chemostat
3.	6.5 day^{-1}	0.31 OD_{600}	chemostat	4 day^{-1}	0.21 OD_{600}	chemostat
	2.5 day^{-1}	0.31 OD_{600}	chemostat	8.7 day^{-1}	0.21 OD_{600}	chemostat

Results

Increasing Feed Carbon Concentration

Bioluminescence

Each time the chemostat was operated there was an initial unsteady-state period of high light output and fluctuating cell density (Figure 6-3). After the light decreased, bioluminescence remained approximately constant at 10 namp for 35 hr, then acetate was added to the feed tank to achieve a concentration of 500 mg/L (Figure 6-3). Light increased after1 hr to greater than 100 namp and then decreased back to approximately 10 namp. Light remained at this level until the feed tank was replaced with freshly prepared feed of the same concentration. A bioluminescence spike similar to the spike when acetate was added to the feed tank was observed,

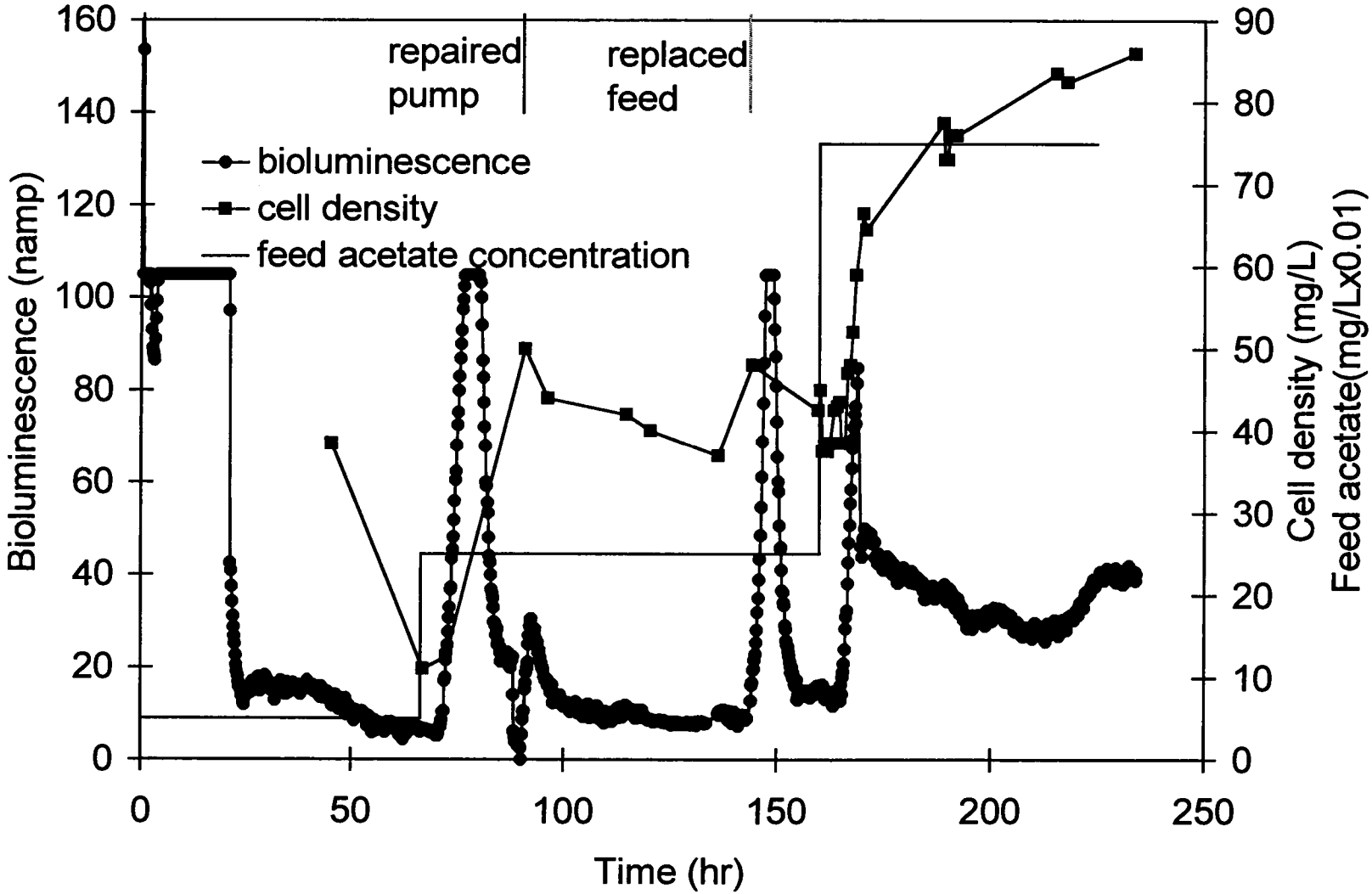

Figure 6-3. Shk 1 chemostat with step changes in feed concentration.

peaking above 100 namp. The feed acetate concentration was then increased again to 750 mg/L. A bioluminescence spike was observed again. However, bioluminescence returned to a higher steady-state level of 30 namp.

Cell Density

Cell optical density increased with each addition of acetate to the feed tank from steady-state values of 0.03 OD_{600} to 0.08 OD_{600} to a final value still increasing value of 0.18 OD_{600} at 750 mg/L feed acetate.

Chemostat Compared to Turbidostat.

A turbidostat and chemostat loaded with Shk 1 were run in a side-by-side experiments. The turbidostat cell density set-point was set at the steady-state chemostat cell density. The cell optical density in the chemostat remained approximately constant at 0.22 OD_{600}, while the turbidostat cell optical density cycled about 0.22 OD_{600} (Figure 6-4). At the initial loading time, the light output of the chemostat cells was higher than that of the turbidostat cells. However, as the reactors approached an approximate steady-state condition, bioluminescence of the chemostat decreased to about 25 namp, while the turbidostat steady-state value was 175 namp. The chemostat steady-state bioluminescence was about 7 times less than the steady-state bioluminescence of the turbidostat. The turbidostat bioluminescence light output remained approximately constant for 15 hours.

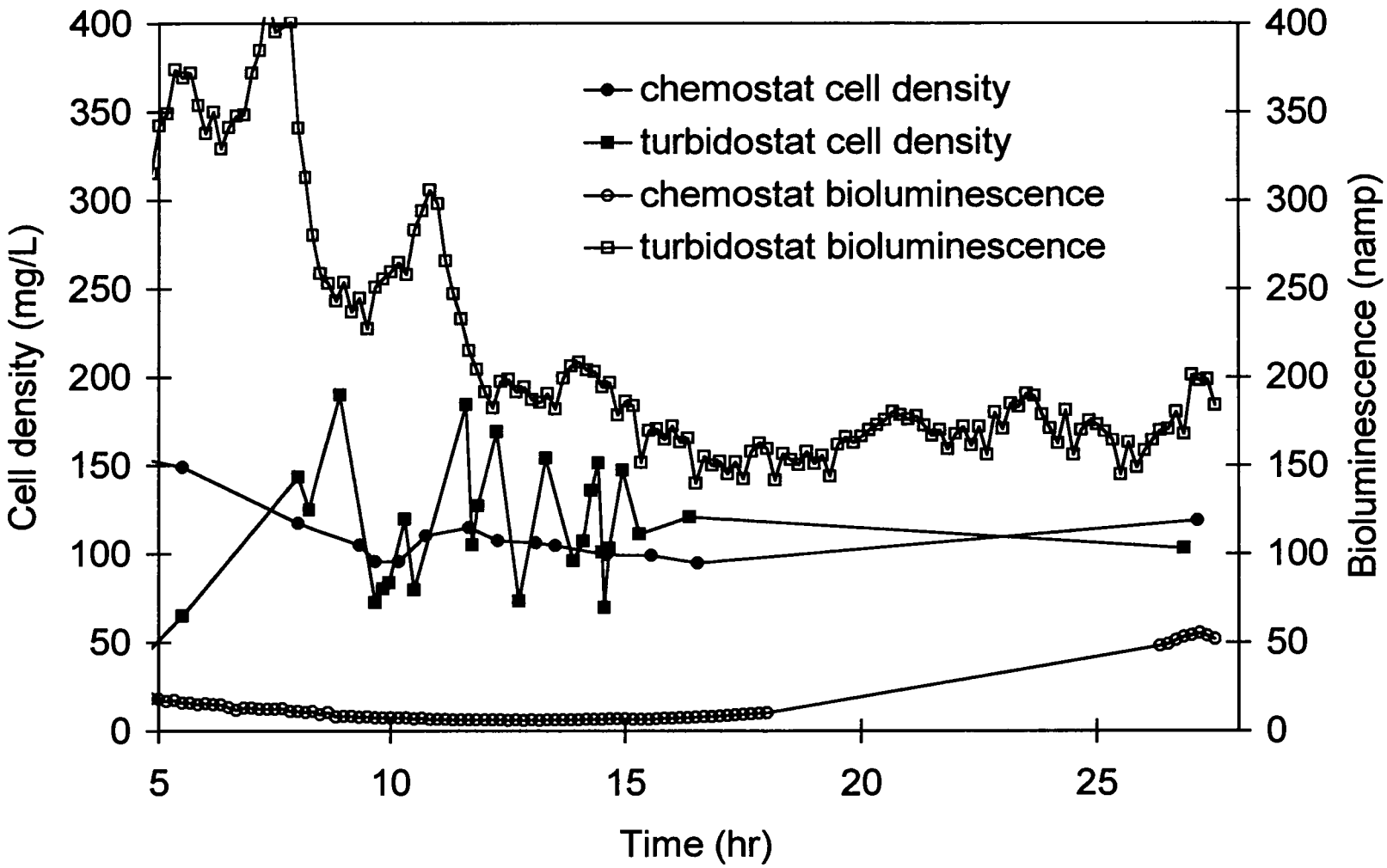

Figure 6-4. Comparison of bioluminescence in a chemostat and turbidostat loaded with the Shk 1 bioreporter.

Chemostat at Different Flow Rates

Bioluminescence

Four chemostat dilution rates were examined. The goal of this experiment was to determine if growth rate had an effect on steady-state bioluminescence. The chemostats were operated for 80 hours before the dilution rate was changed. However, bioluminescence in either chemostat did not reach a steady value (Figure 6-5). At the dilution change, it appeared that in chemostat one bioluminescence decreased in response to the change in flow rate (6.2 day^{-1} to 2.5 day^{-1} dilution rate). However, as chemostat two dilution rate was changed from 4 day^{-1} to 8.7 day^{-1}, it seemed that bioluminescence did not change (Figure 6-5).

Cell Density

The cell density of each chemostat remained relatively constant through the changes in dilution rate. The average cell optical density of chemostat one was 0.31 OD_{600}, while the cell optical density of chemostat two was 0.21 OD_{600} (average values exclude the 2 points directly after flow rate change).

Discussion

Figure 6-6 illustrates the theoretical cell density, substrate concentration and cellular doubling time for a chemostat. Over a wide range of cellular growth rates (doubling time) the cell density remains constant (for a specific feed carbon

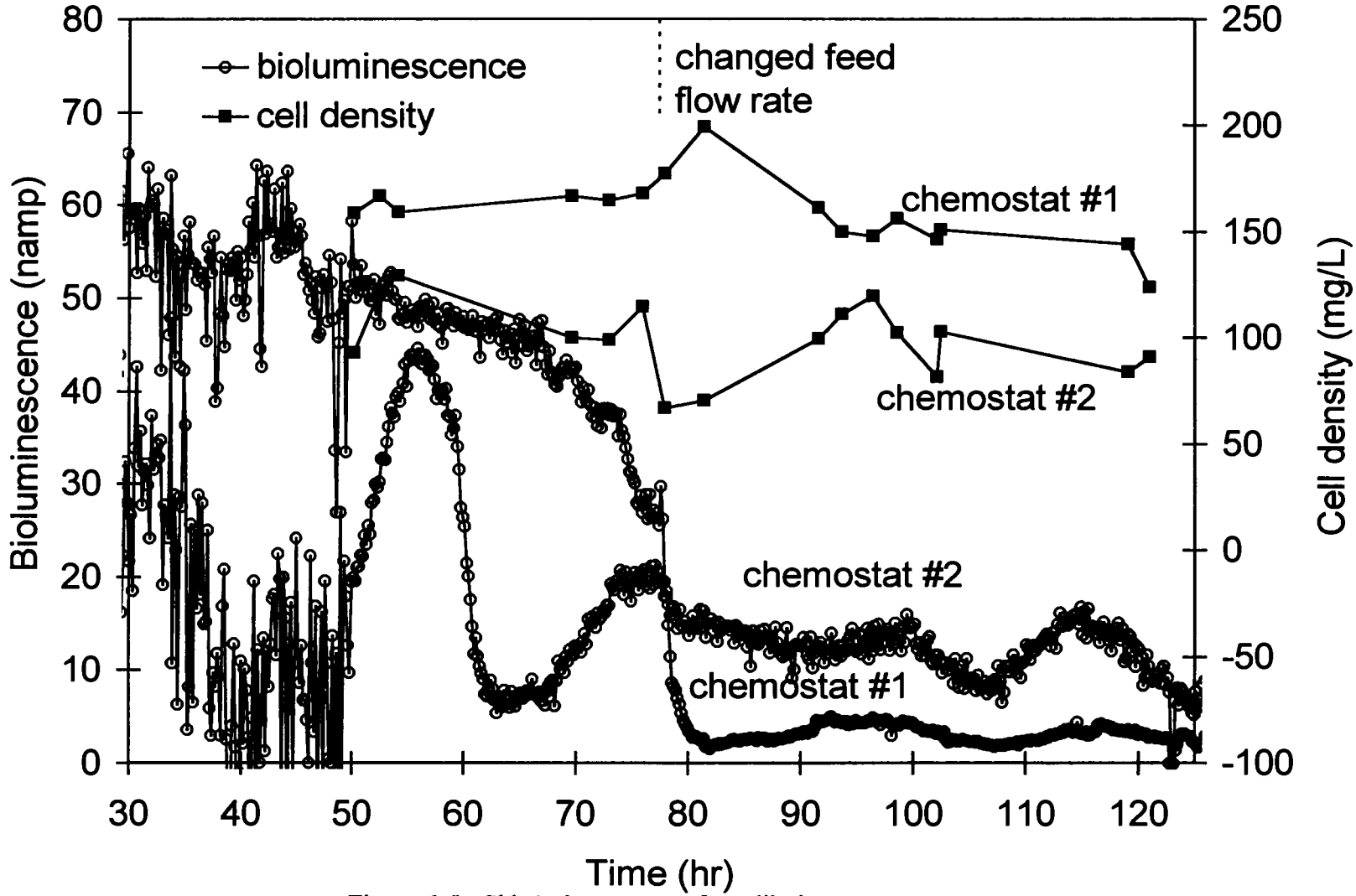

Figure 6-5. Shk 1 chemostat at four dilution rates.

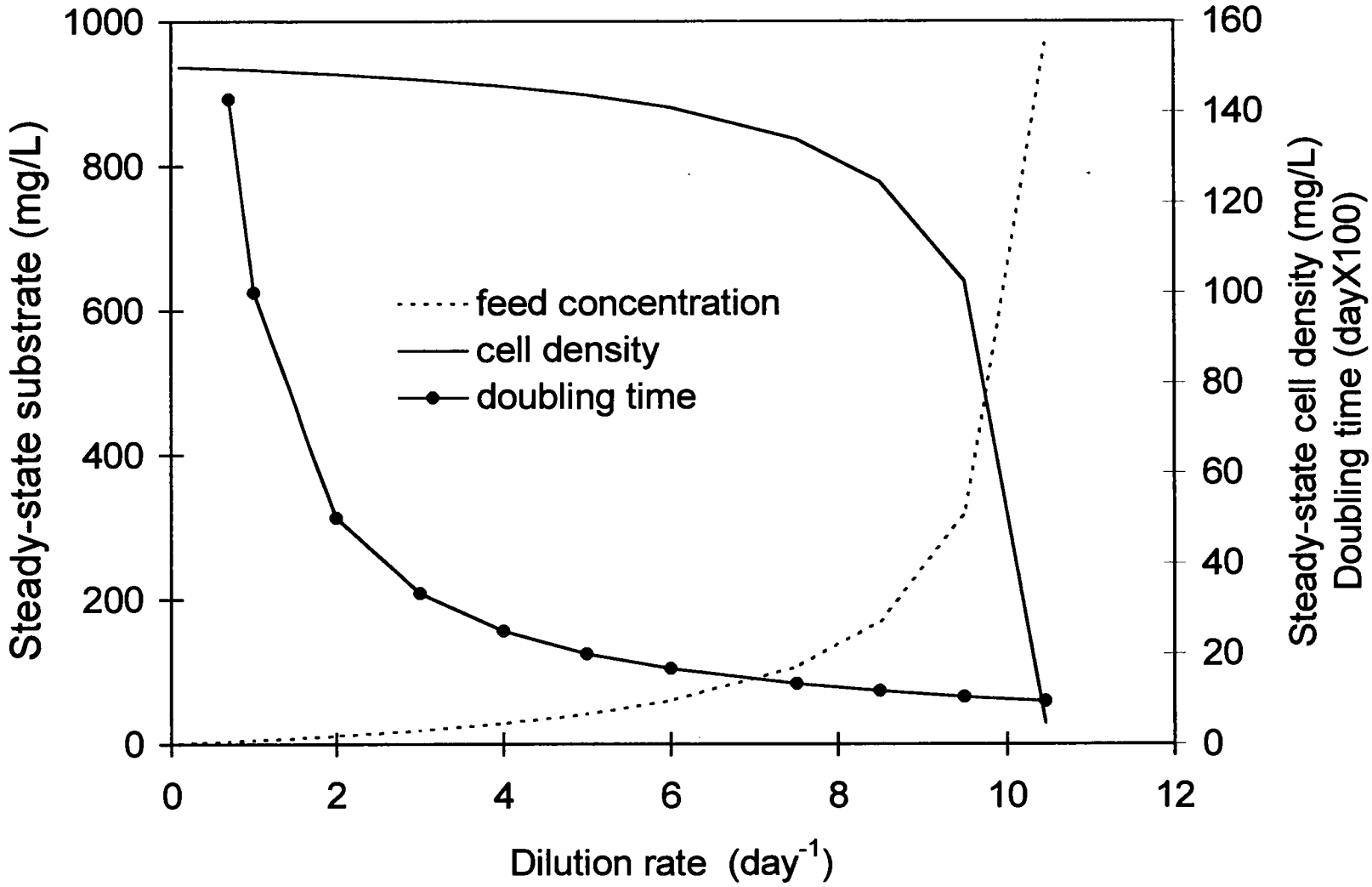

Figure 6-6. Theoretical chemostat operation.

concentration), while the vessel's carbon concentration is close to zero. At high dilution rates the chemostat becomes unstable because the washout rate of the cells is approaching the intrinsic maximum growth rate of the cells; the cell density rapidly declines, while the available substrate rapidly increases. This is the point at which a turbidostat operates. The turbidostat has a high carbon concentration in the feed, and only when the cells reach a certain density does more feed enter the reactor, diluting the cell density. So there is always available substrate, and the cells grow at their maximum growth rate.

Five chemostat dilution rates were examined, in addition to the turbidostat with the cell density set to the steady-state chemostat cell density for 1000 mg/L acetate (Figure 6-7). For the 6 experiments the cell density remained approximately constant at 0.24 OD_{600}. The differences in cell density can be attributed to error in carbon source addition to the feed, as the two high cell density experiments utilized the same feed preparation. Steady-state bioluminescence (ranging from 0 to 40 namp) were not significantly different for any of the chemostat dilution rates. In contrast, the steady-state turbidostat bioluminescence was significantly higher at 175 namp. The Shk 1 reporter constitutively produces the *lux* enzymes, so lack of induction was not the reason for lower light in the chemostat. It is proposed that low light was a result of growth substrate limitation for bioluminescence reactions. This reinforces the *tod-lux* chemostat conclusion that growth substrate limited cells are energetically limited for the production of bioluminescence.

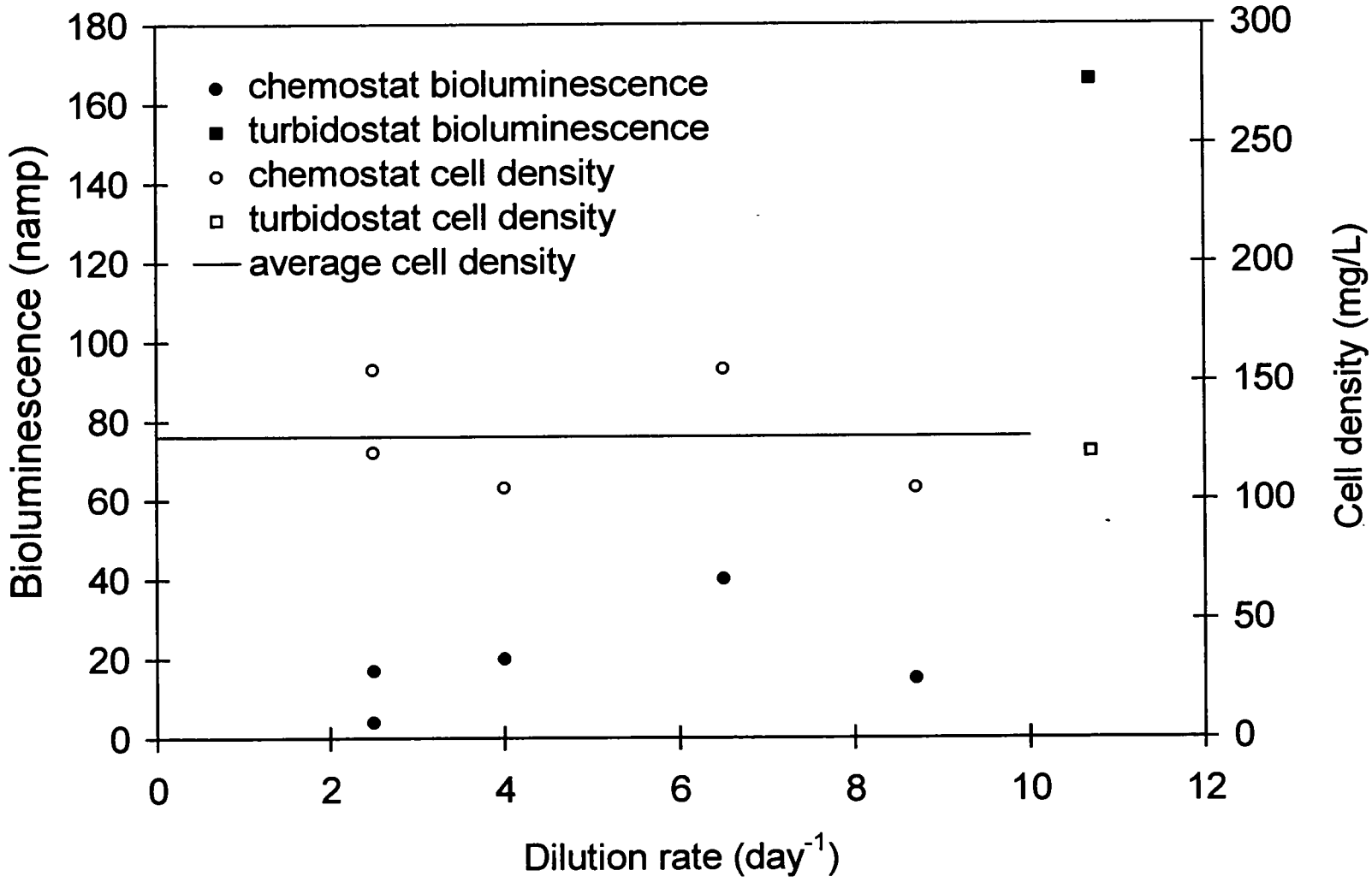

Figure 6-7. Comparison of chemostat and turbidostat with Shk 1.

Traditional continuous research reactors such as CSTRs, PFRs, and packed bed reactors rely on carbon starvation to limit cell growth. Batch growth is carbon rich before the on-set of stationary phase, which is why so many experiments with bacteria are performed with cells in mid-log phase growth. A turbidostat will provide bioreporter cells with higher steady light output than a chemostat. Relatively high light and steady output values are important for the control application of this bioreporter.

CHAPTER 7

CONTACTING DESIGN

The genetics and the proposed application of the Shk 1 reporter are less complex than the *tod-lux* reporter. For example, the *tod-lux* reporter requires an inducer for bioluminescence, while the Shk 1 reporter is intended to produce light constitutively. The Shk 1 application involves only the determination of toxicity, indicated by a reduction in bioluminescence, while the *tod-lux* reporter applications are complex and varied. However, issues involved in biosensor design such as mass transfer of oxygen and nutrients, carbon starvation, and cultivation conditions can be applied to any bioluminescent reporter system. Due to the simplicity of the Shk 1 reporter, design of systems to contact the reporter with process fluid will utilize the Shk 1 reporter. Results and conclusions can then be applied to the more complex *tod-lux* reporter.

Incorporation into a biosensor used to monitor biological systems is the goal of the technical development of bioreporters. A biosensor as a device that uses a biological mechanism for analyte detection, consisting of two parts; a biological sensing element and a signal transducer. Sensing elements can consist of enzymes, antibodies, DNA or whole cells, while transducers can be electrochemical, optical or acoustic (Rogers, 1996). Whole, living cells are the sensing element of *lux* bioreporters, light is the signal, and photomultipliers are the signal transducers.

Inherent in the development of reporter technology is the need to physically contact the bioreporter bacteria to the process fluid the reporter is designed to monitor. For example, the *tod-lux* reporter system needs to contact the bioreactor environment or aquifer waters for *in situ* degradation scenarios. The Shk 1 reporter needs to contact wastewater entering the activated sludge treatment system or the activated sludge basins.

Two systems were designed for contacting reporter strains with process fluids; (1) a continuous sampling system and (2) an in process fluid biosensor. The continuous sampling system was tested with simulated equalization basin wastewater and hydroquinone as the test toxicant. The biosensors were tested in beakers of activated sludge effluent and bench scale activated sludge reactors.

Continuous Sampling System

Methodology

A continuous sampling system was developed to assess the bioluminescent response of the Shk1 reporter to toxicants (Figure 7-1), using hydroquinone as the test toxicant. The sampling system consisted of two light tight sampling vessels with 10 mL of liquid volume, and 15 mL of air head-space. A liquid light guide was connected to the top of each vessel that transferred the light to a photomultiplier.

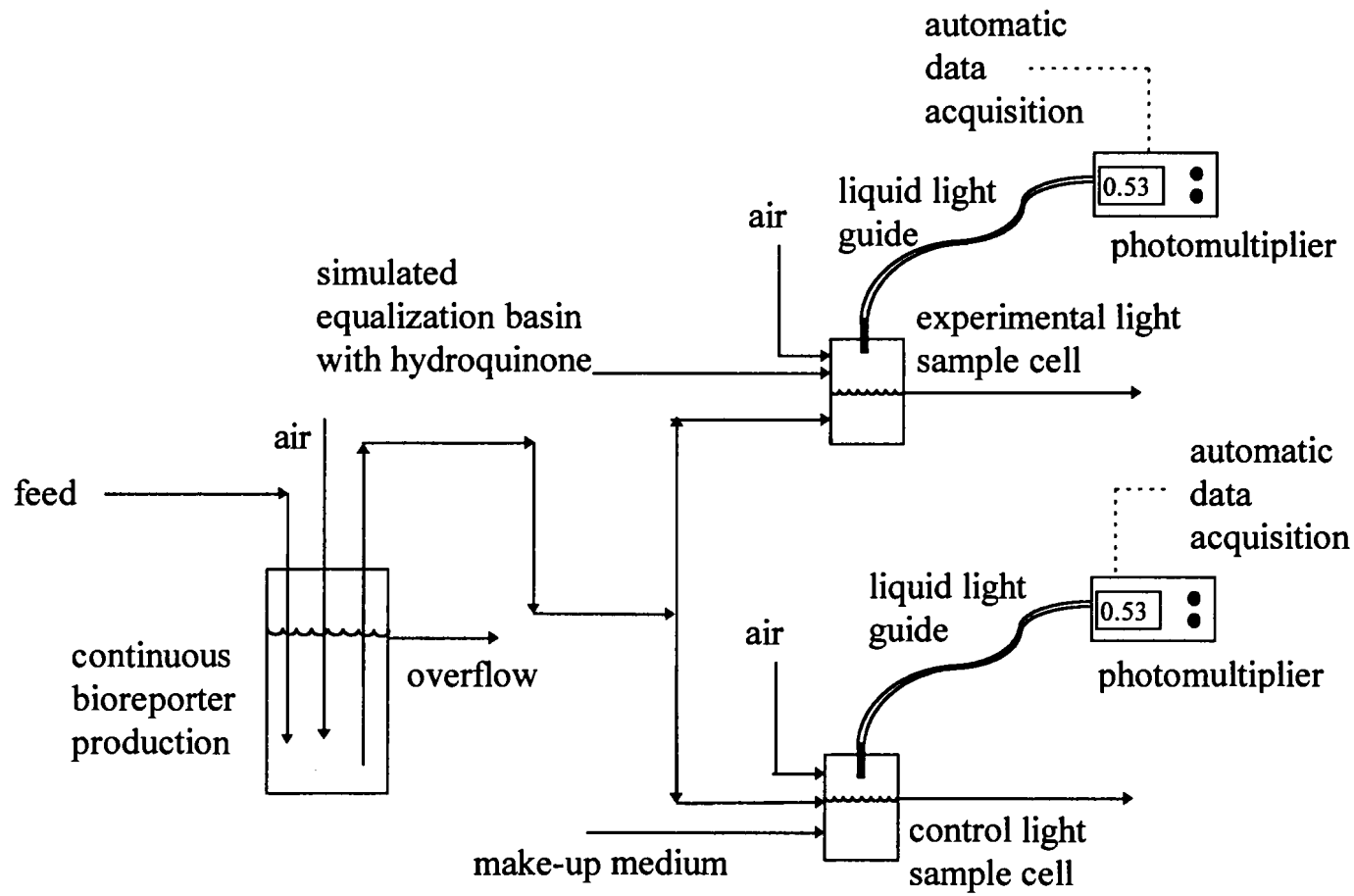

Figure 7-1. Schematic of continuous sampling system to assess wastewater toxicity to activated sludge microorganisms.

Shk 1 reporter cells were supplied to the sampling vessels continuously. A 25 mL vessel containing Shk 1 reporter cells provided cells to the sampling vessels. Medium was manually added to this vessel at a rate to attain a constant cell density as determined by periodic cell density determinations. This was essentially a manual turbidostat. These reporter cells were fed to the sampling vessels via a peristaltic pump at a rate of 0.17 mL/min. Air was also provided to each sampling vessel. The control vessel received simulated wastewater, while the experimental vessel received simulated wastewater with successive hydroquinone concentrations of 10, 100, 1,000 and 10,000 mg/L. The simulated waste water was provided at 0.17 mL/min except for directly after the 1,000 mg/L hydroquinone addition. The flow rate was increased to return the light to baseline levels more quickly by flushing the sampling cell. Table 7-1 displays the flow rates and hydroquinone concentrations fed to the sampling vessels.

Table 7-1. Conditions for continuous sampling experiment.

time (min)	flow rate from equalization basin (mL)	hydroquinone concentration in equalization basin (mg/L)
0	0.17	0
87	0.17	10
115	0.17	0
180	0.17	100
240	0.17	0
282	0.17	1,000
290	0.59	0
313	0.17	0
343	0.17	10,000
360	0.17	0

The theoretical hydroquinone concentration in the sampling vessel was calculated by performing a hydroquinone mass balance on the sampling vessel. Equations 7-1 through 7-3 show the development of this balance. There was assumed to be no degradation of hydroquinone by Shk 1.

$$\text{accumulation} = \text{in} - \text{out} + \text{generation} \qquad (7\text{-}1)$$

$$V_{samp}\frac{dC_{samp}}{dt} = v_{eqb}C_{eqb} + v_{shk1}C_{shk1} - C_{samp}(v_{eqb} + v_{shk1}) + 0 \qquad (7\text{-}2)$$

$$V_{samp}\frac{dC_{samp}}{dt} = v_{eqb}C_{eqb} - C_{samp}(v_{eqb} + v_{shk1}) \qquad (7\text{-}3)$$

Nomenclature:

C_{eqb}	concentration of hydroquinone in the feed from the simulated equalization basin, mg/L
C_{shk1}	concentration of hydroquinone in the feed from the reporter cell supply vessel, mg/L
C_{samp}	concentration of hydroquinone in the sampling vessel, mg/L
v_{eqb}	volumetric flow rate from the simulated equalization basin, mL/min
v_{shk1}	volumetric flow rate from the reporter cell supply vessel, mL/min
V_{samp}	volume of the sampling vessel, mL

Results

Although continuous production of Shk 1 reporter cells was maintained, the light signal from the control sample cell increased throughout the continuous sampling experiment. To account for this, both the signal from the control cell and the signal from the experimental cell were normalized by the control signal. The normalized light

response by the Shk 1 reporter declined during each exposure period to hydroquinone (Figure 7-2). The decline in bioluminescence corresponded to the increase of the calculated hydroquinone concentration in the sample vessel. The rate of decline in bioluminescence increased with increasing hydroquinone concentration (Table 7-2), indicating more severe toxic response to each higher concentration of hydroquinone. When the hydroquinone concentration in the feed to the sampling vessel was set to 0 mg/L, the normalized light signal increased corresponding to a dilution of the hydroquinone in the sampling vessel and a continuous addition of Shk1 cells unexposed to hydroquinone.

Table 7-2. Rate of bioluminescence decline upon exposure to hydroquinone in the continuous sampling system.

Hydroquinone concentration (mg/L)	Rate of normalized bioluminescence decline (min^{-1})
10	0.011
100	0.013
1,000	0.015
10,000	0.064

Discussion

The continuous on-line toxicity monitoring system exhibited rapid and proportional response to increasing hydroquinone concentration. However, normalization of light response using a control chamber was required. More stable Shk 1 culture conditions should yield more consistent light output, and preclude the need for a control chamber. Light monitoring of the Shk 1 culture being supplied to the

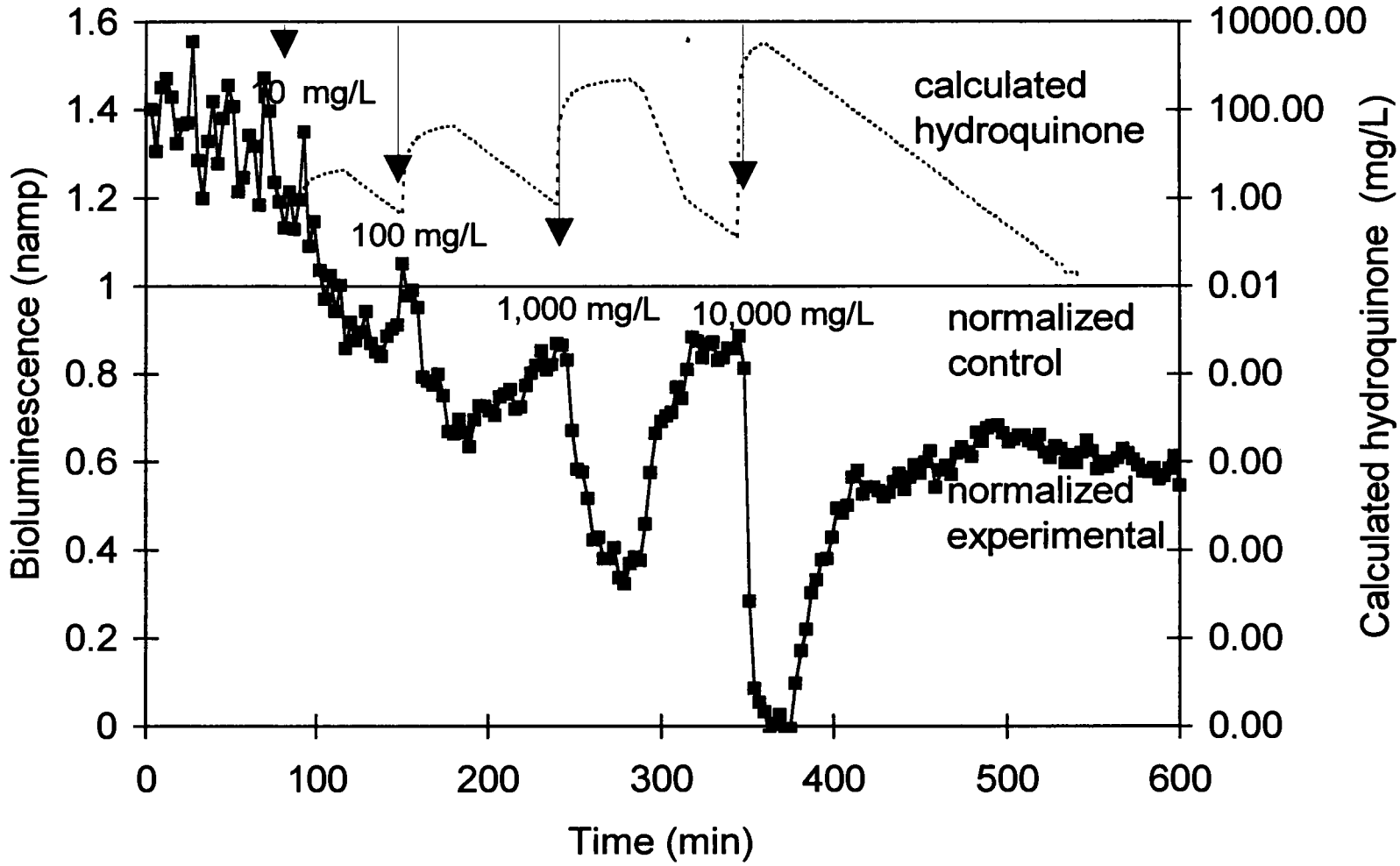

Figure 7-2. Continuous sampling system response to hydroquinone.

experimental chamber, rather than the use of a control contact vessel, would further simplify the system. The ultimate goal of a toxic shock control strategy is to minimize damage to the activated sludge rather than simply document its occurrence. Process control responses may include diversion of influent wastewater to temporary retention basins followed by gradual addition to the aeration basins at a rate sufficient to avoid toxic concentrations, increase in return activated sludge to buffer toxic effects, and changes in influent flow patterns to minimize localized high toxicant concentrations.

Biosensor Design

A biosensor design used in previous research (Heitzer, 1992) consisted a solid gel of polymerized alginate incorporating the bioreporter cells at the end of a liquid light pipe held in place by stainless steel mesh. The entire assembly was placed in a stream of media forcing the liquid to enter the alginate by convection (Heitzer, 1992). However, alginate beads held in place by the stainless steel mesh would provide better mass transfer to the cells due to the void space between the beads.

In the application of this study, the sensor is sampling liquid in a stirred vessel (activated sludge bioreactor). The alginate bead design was tested in the activated sludge reactors and no light was detected. This could have been due to low mass transfer rates of oxygen and/or nutrients. Oxygen in the reactors was maintained at only 2 mg/L, and the primary mechanism to deliver oxygen to the immobilized cells with the bead design was diffusion, as opposed to convection. Therefore, biosensors

were designed that allowed for convective mass transfer of air and nutrients to the reporter cells.

Biosensor Configurations

Air-purged, Immobilized Cell Biosensor

A sensor was designed to allow convective mass transfer of oxygen, nutrients, and aldehyde to the immobilized cells (Figure 7-3A). The sensor consisted of a tip containing alginate immobilized Shk 1 cells in the form of beads. The tip was placed over the end of a liquid light pipe. The opposite end of the sensor tip was covered with mesh that allowed air and liquid to enter and exit the tip, but retained the alginate beads. The sensor was placed into the liquid in a vessel. Air was pulsed into the cell by an air pump, a solenoid valve, and a timer. Air flowed into the cell for 10 s, forcing the reactor liquid out of the cell and convecting air across the beads, out of the cell and into the reactor. Then, when the air exited out the solenoid valve line for 10 s, the reactor liquid media entered the cell due to liquid head in the reactor, convecting the liquid to be sampled across the beads. In addition, the sensor was equipped with the ability to provide nutrients and aldehyde to the beads by pumping them into the air line to the cell. Bioluminescence was measured from the liquid light pipe by a photomultiplier.

Alginate beads were prepared by mixing a cell suspension with a cold alginate solution (28 g of alginate/L distilled water). This solution is placed into a syringe, and

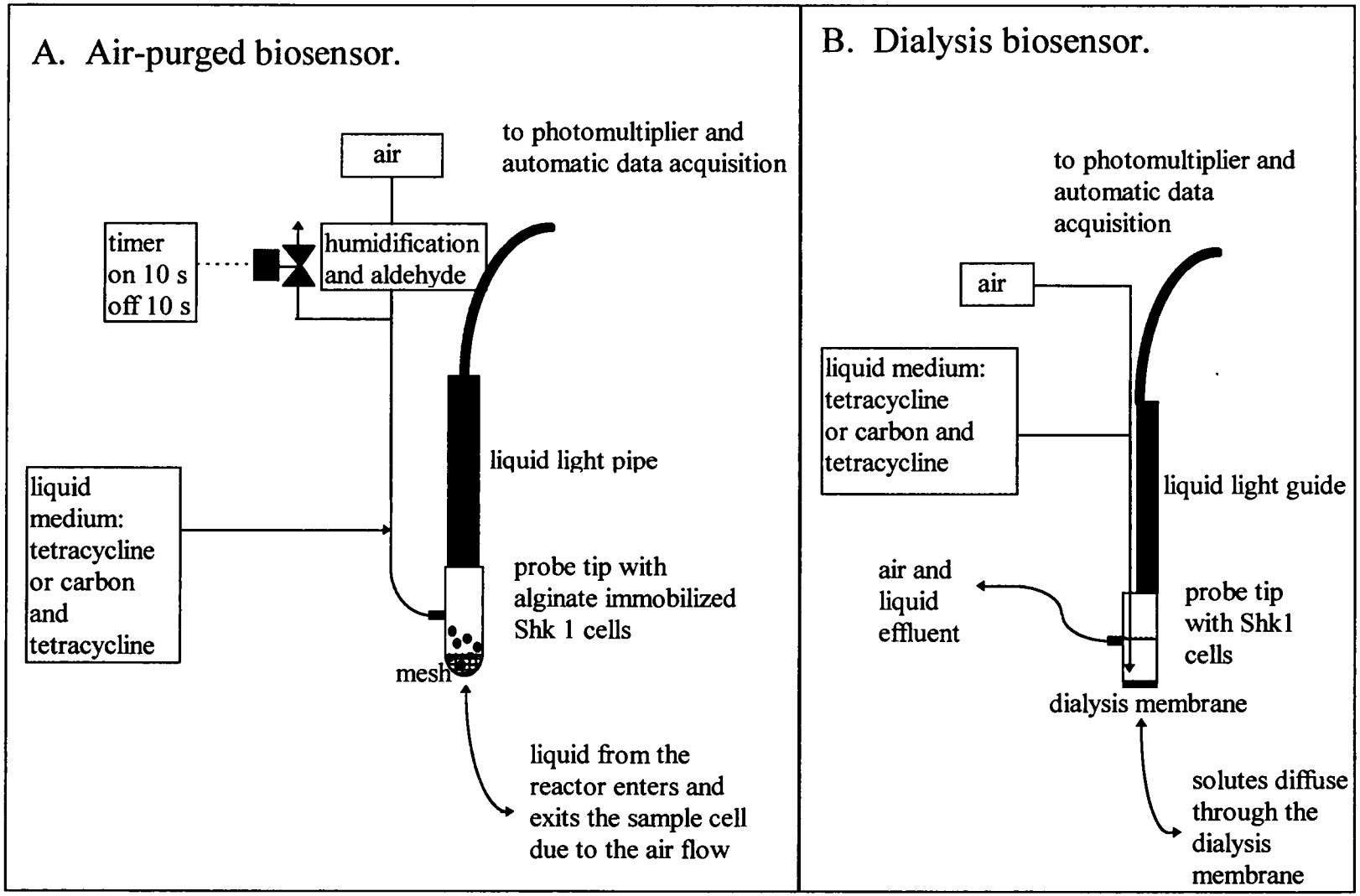

Figure 7-3. Biosensor designs for contacting the Shk 1 reporter strain with a process fluid.

droplets were released into a beaker of cold 0.1 M strontium chloride. The strontium ions cross linked and polymerized the alginate to form solid jelled beads of alginate and cells.

Dialysis Biosensor

The dialysis biosensor consisted of the same unit as the air-purged sensor, except the mesh was replaced with dialysis membrane (Figure 7-3B). Cells were maintained in suspension in the sensor tip, and air and nutrients entered the tip, then exited though an overflow line, maintaining a head-space in the sensor tip. Nutrients and other solutes diffused through the dialysis membrane to contact the bioreporter cells in the sensor tip.

Bioluminescent Response of Biosensors in Test Applications

The sensor response was examined in several configurations including (1) air-purged sensor in beakers, (2) air-purged sensor in activated sludge reactors (Figure 7-4), and (3) dialysis type in reactors and beakers.

Air-purged Sensor in Beakers

Two air-purged biosensors were constructed and each placed in beakers of clear activated sludge reactor effluent. Initially, sensor A was fed a solution of 100 mg/L calcium acetate, 25 mg/L tetracycline, and vapor aldehyde; while sensor B was fed only basal liquid medium containing 25 mg/L tetracycline, without a carbon

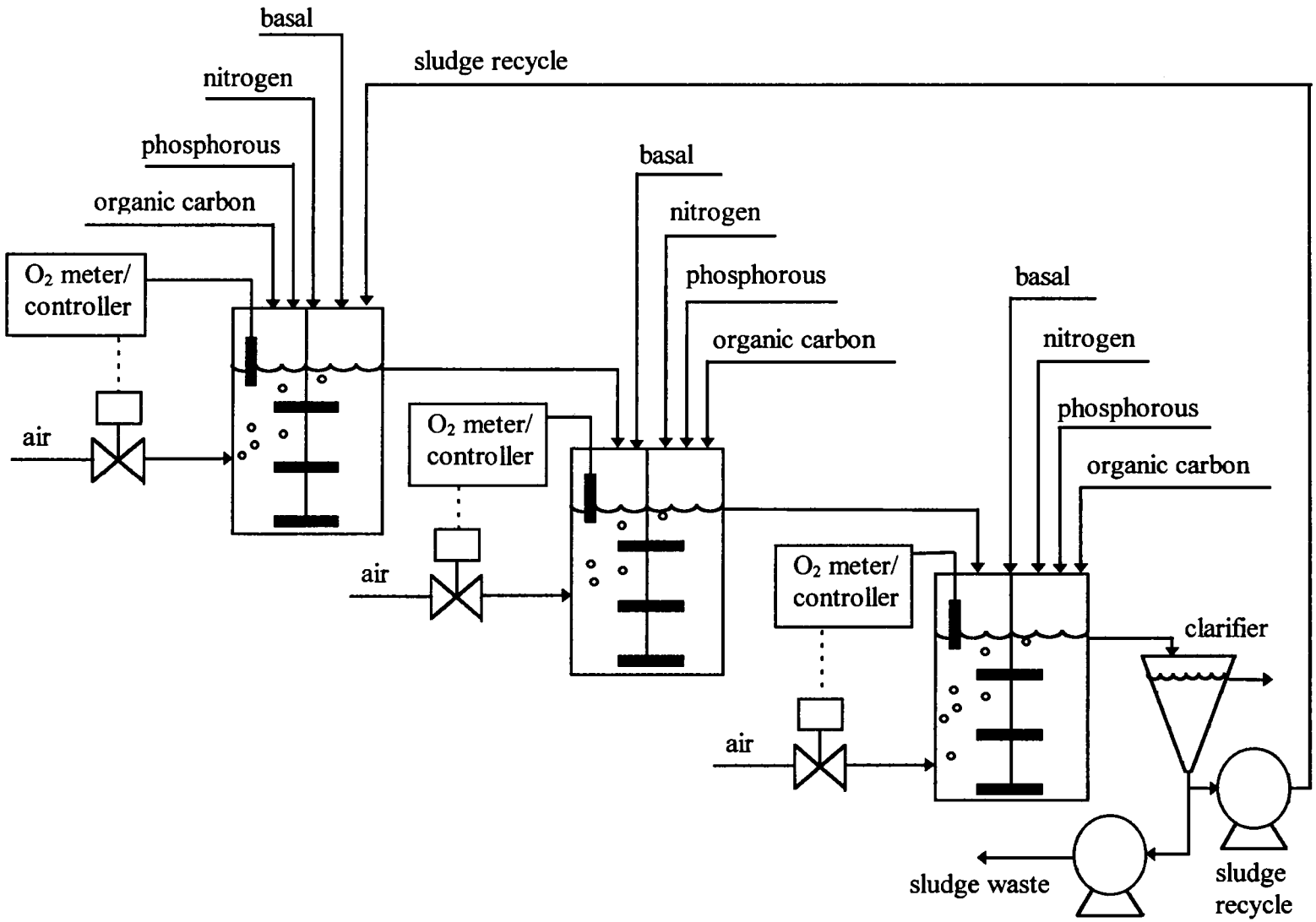

Figure 7-4. Bench-scale activated sludge waste treatment reactor schematic utilized in testing biosensor designs.

source, and received no aldehyde. Periodically, the effluent in the beakers was exchanged with fresh effluent from the bench scale activated sludge reactors. Bioluminescence was monitored over seven days.

The biosensor without carbon and aldehyde feed never produced significant light (above 10 namp) (Figure 7-5). This is important in biosensor design because activated sludge basins are typical of many process applications with respect to carbon starvation. Especially in contaminant and waste treatment systems where the goal is to degrade wastes or the contaminant to very low levels. By design, the bacteria are starved for the waste. A supplementary carbon source should be provided to the reporter cells to achieve a useable bioluminescent signal.

In the carbon fed biosensor, bioluminescence increased at each effluent change and returned to low levels with about one day cycle times. The beakers were in a light tight cardboard box and fed vapor aldehyde. After three cycles, an air line was introduced to the beaker to purge the box of aldehyde vapor (the cells were getting pulses of air so they should not have been experiencing oxygen limitation). After this, a one day cycle of light was observed, but bioluminescence did not decline to as low a level. Although continuous light was achieved for 6 days, the signal was not constant and not high. Much improvement is needed to utilize this signal for process control.

Air-purged Sensor in Activated Sludge Reactors

The air-purged sensors (A and B) were each placed in a basin of the activated sludge reactor system (Figure 7-4). At 0.6 days, sensor B was transferred from the

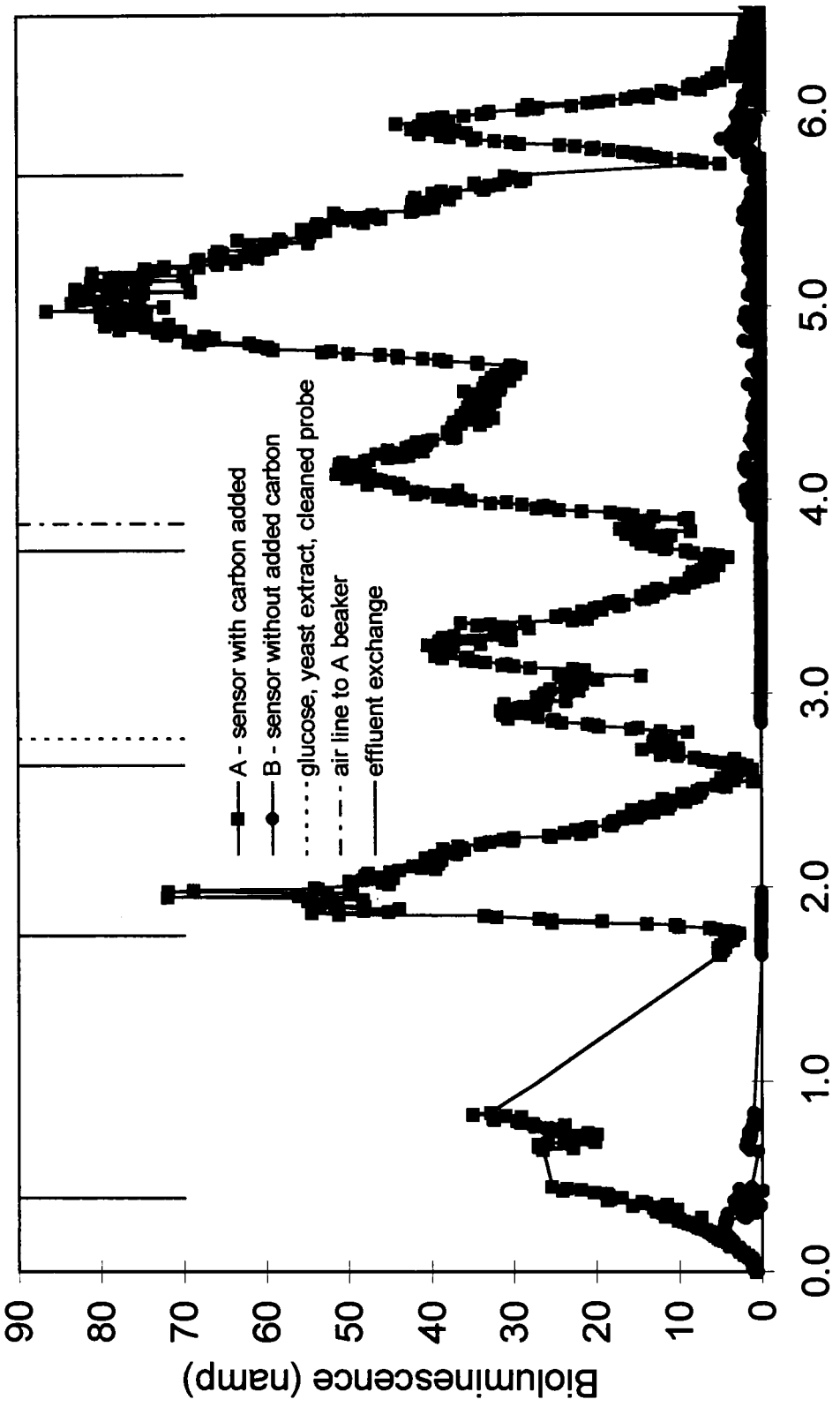

Figure 7-5. Bioluminescent response of the air purged biosensors in beakers.

activated sludge basin to a beaker with sludge effluent. At about 1.2 days, settled sludge was added to the beaker of effluent and sensor B. Sensor A was removed from the reactor and placed in a beaker of effluent. Bioluminescence was monitored from each biosensor for two days.

Both biosensors were fed carbon in this test, but neither biosensor produced significant light while in the activated sludge reactors (Figure 7-6). The sludge was being convected in and out of the biosensor by the pulsing air stream. The activated sludge microorganisms could have consumed all available carbon before diffusion to the immobilized cells could occur, essentially leaving the reporter cells as starved as they were in the beaker and not fed carbon. One of the sensors was placed in a beaker of effluent to see if bioluminescent activity could be revived. Soon after placing in the beaker bioluminescence increased. When bioluminescence was at a significant level above background, sludge was added to the beaker. Bioluminescence immediately decreased in response to sludge addition.

Dialysis in Beaker and Reactor

Two dialysis type biosensors were constructed and sensor A was placed in a basin of the activated sludge reactor system, while sensor B was placed in a beaker of sludge effluent. Bioluminescence was monitored from each biosensor for 3.7 days. As in the air-purged biosensor design, the sensor placed in the activated sludge reactor produced no light above baseline, while the biosensor in the beaker of effluent

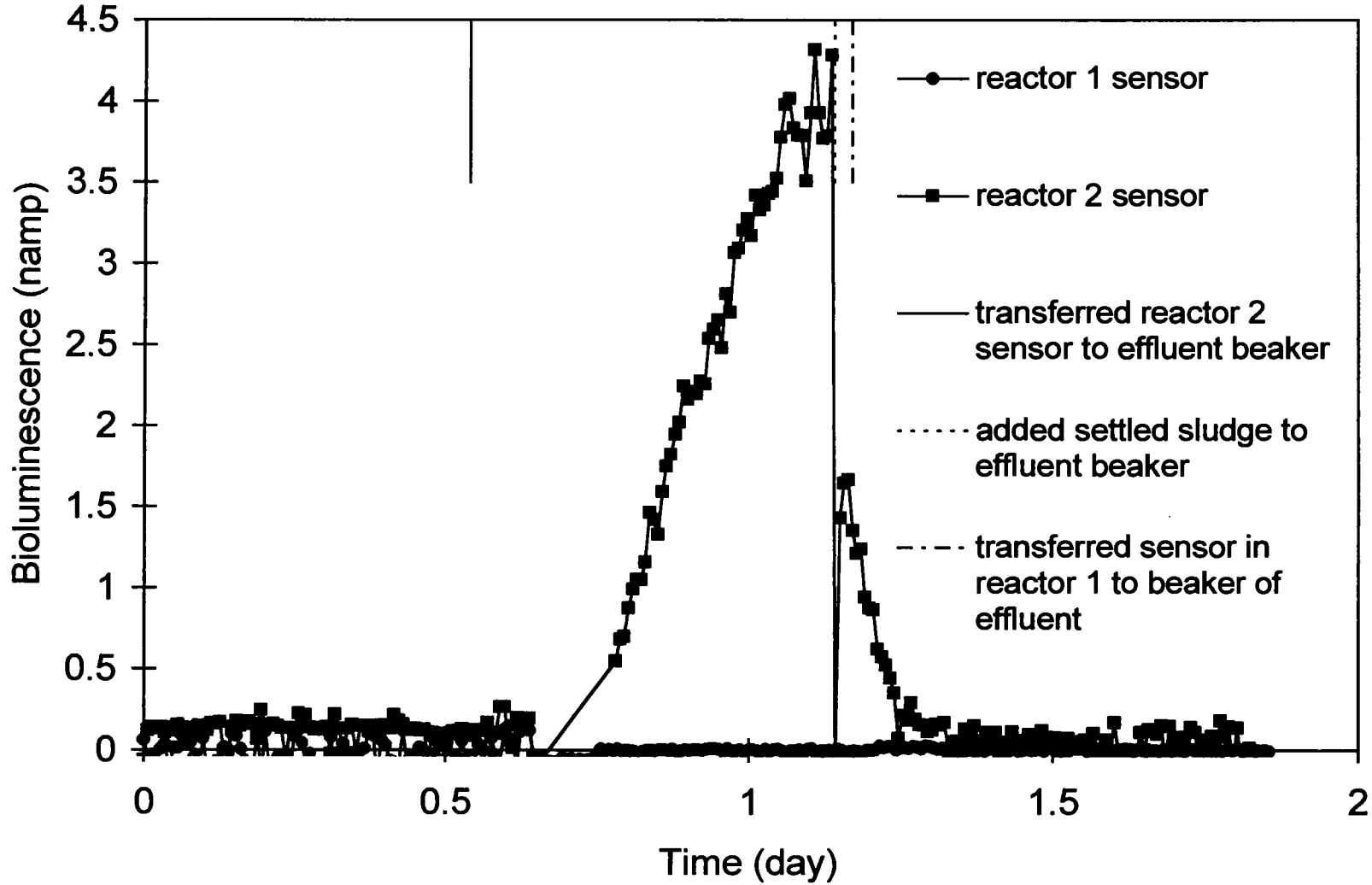

Figure 7-6. Air purged sensor in reactors.

produced the characteristic approximately one day pulse of light before returning to baseline levels (Figure 7-7).

Shk 1 Bioluminescent Response to Activated Sludge Components

The bioluminescent response of the Shk1 bioreporter to variations of waste activated sludge was measured to aid in determining why the sensor designs did not produce bioluminescence when exposed to activated sludge. The variations of activated sludge were (1) clear effluent, (2) activated sludge, (3) supernatant of activated sludge, and (4) media exposed to activated sludge via dialysis membrane. Bioluminescent response of five dilutions of each of these four variations were examined over 4 hours.

Methodology

Shk 1 cells (50uL) and 200 uL of the above listed sludge solutions and reactor media were placed in each Microbeta plate well. Dilutions were 100%, 50%, 25%, 12.5% and 0% of the various sludge solutions. The resulting pH (after combining)of the medium was 7.2, effluent pH was 8.0, sludge 7.6, supernatant 8.1, dialysis solution 8.2. The dialized sludge solution was produced by placing five mL of medium in a dialysis tube, then the tube was placed in a beaker containing activated sludge for eight hours.

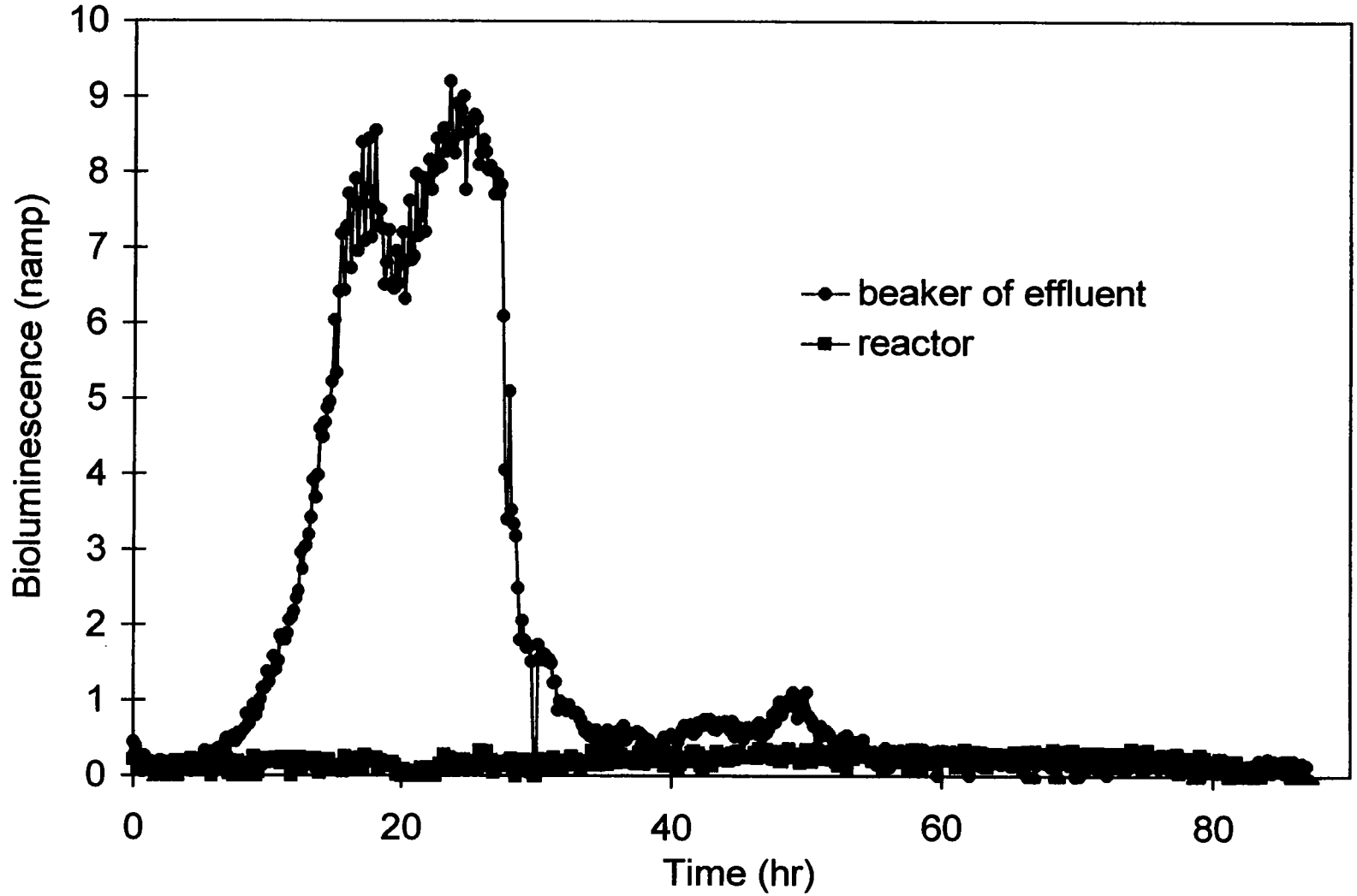

Figure 7-7. Dialysis type biosensor in a reactor and in an effluent beaker.

Results

The activate sludge treatment yielded about half of the initial magnitude of bioluminescence as the other treatments (Figure 7-8). Bioluminescence of all treatments increased with time. The dilutions of activated sludge indicated 100% activated sludge yielded about half the bioluminescence as 50% activated sludge (Figure 7-9). These results indicated that the physical presence of the sludge interfered with light production, rather than a toxic by-product produced by sludge microorganisms or a nutrient limitation. Two hypotheses are proposed (1) The sludge microorganisms consume all available carbon, leaving starved bioreporter cells, and (2) the opacity of the sludge blocks some light from the photomultiplier.

Discussion

Neither of the biosensor designs produced a useable bioluminescent signal for automated control - even in the more controlled beaker setting. The continuous sampling system seems to produce a more useable scheme for incorporating bioluminescent reporters in control applications. However, a hybrid of the two systems, combining continuous bioreporter production with a probe type biosensor would be more familiar and convenient to process control measurement.

Contacting the cells with the process fluid is a major part of bioreporter technology development. The types of contacting examined were (1) batch preparation of cells, mixing with process sample (toxicity assessment of wastewater, batch degradation TCE and toluene), (2) continuous production of cells; mixing

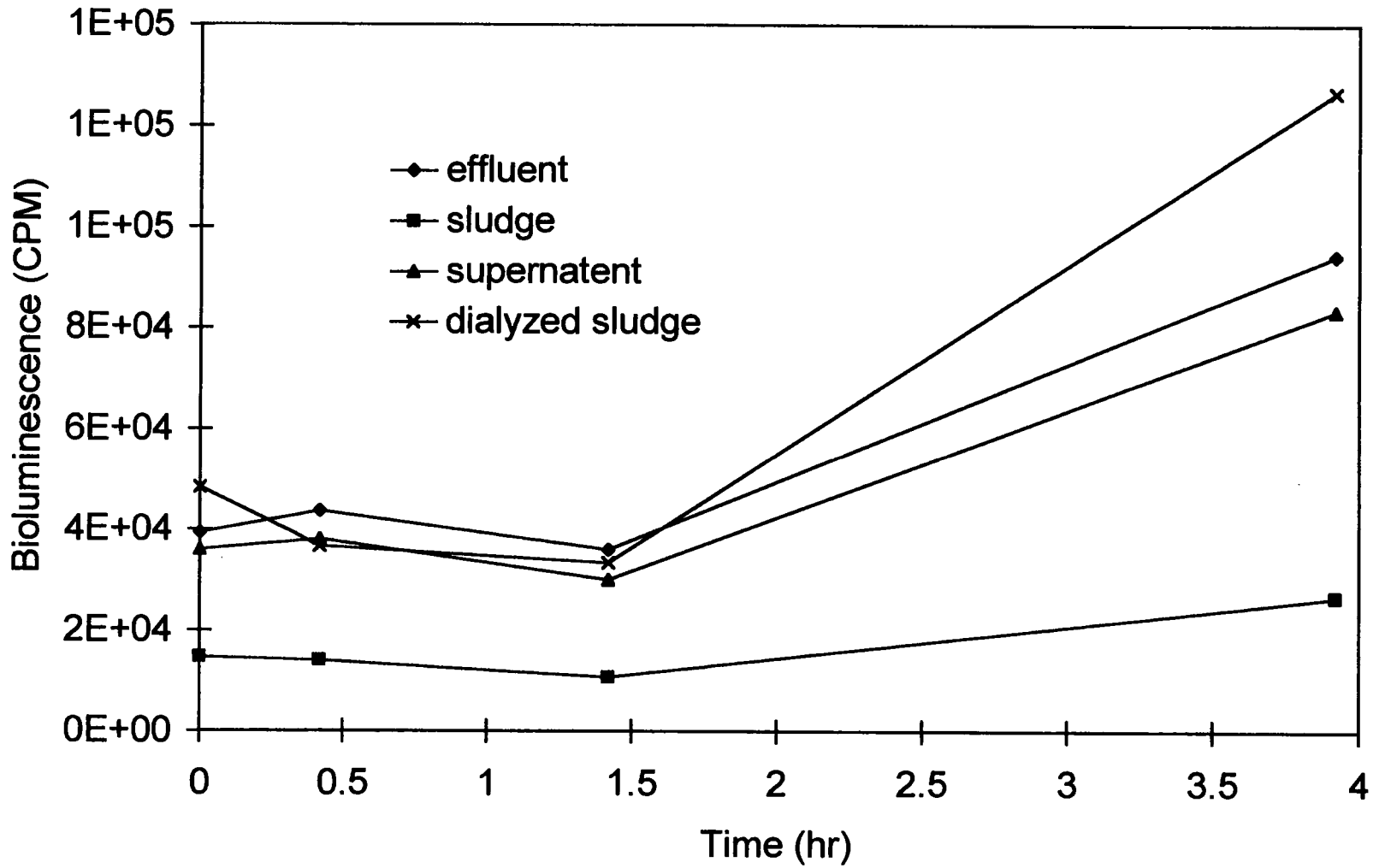

Figure 7-8. Shk 1 bioluminescent response to components of sludge.

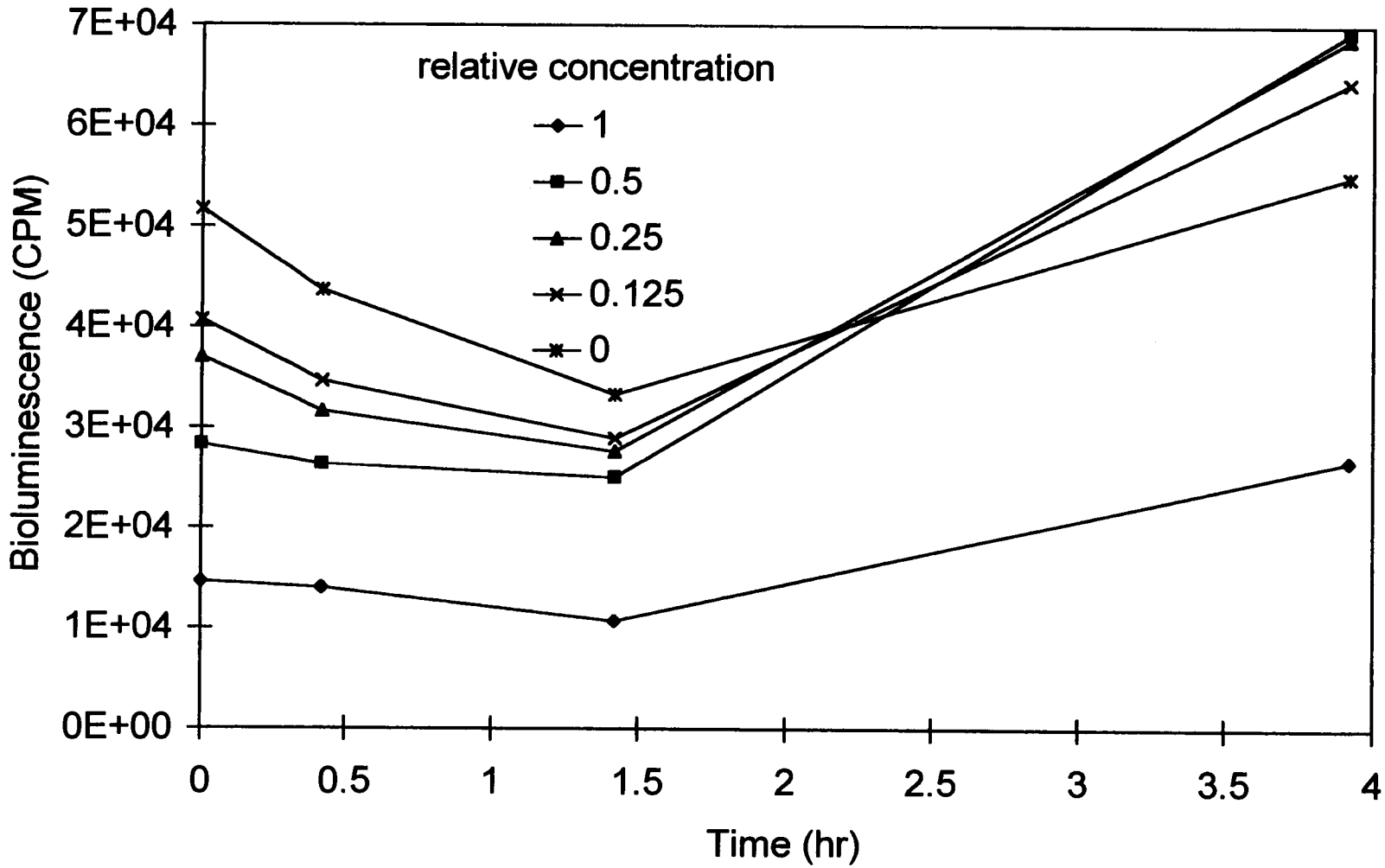

Figure 7-9. Shk 1 bioluminescent response to dilutions of sludge.

process fluid and reporters in a separate environment, (3) immobilized cells contacting in the actual process fluid, and (4) continuous production of cell within the process fluid. The most successful of these were batch, and removing fluid from process and contacting with continuously produced cells in separate chamber. However, these are the least likely to be used industrially. They are labor intensive, it is more difficult to attain quantitative reproducibility, and they have the longest delay time. One of the strongest advantages of the *lux* system is its on-line capabilities. Engineering a sensor to contact the process fluid without removing the process fluid from the process is an essential and significant part of bioreporter technology development.

CHAPTER 8

DISCUSSION AND CONCLUSIONS

In experiments with an inducible and a constitutive bioluminescent reporter physiological as well as genetic properties were found to affect the bioluminescent response to environmental conditions. This chapter presents (1) interpretations of significant experimental results, (2) an example bioreporter application of monitoring and control of a co-metabolic process, and (3) recommendations for future work.

Originally, experiments were performed to determine the effect of toluene on degradation and bioluminescence. During the course of these experiments, other parameters were found to be of significant potential importance for light output. These parameters included oxygen concentration, type and concentration of growth substrate, batch versus continuous cultivation, and toxicant exposure. In addition, several physical systems were designed to contact the reporter cells with the process fluid for process monitoring. Table 8-1 summarizes the major significant experimental results observed from these experiments.

A simple mechanistic mathematical model was developed that described bioluminescence and the degradation of toluene and TCE under batch and continuous cultivation conditions. The model incorporated (1) degradation dependence on inducer and growth substrate, co-metabolic substrate, and biomass concentrations and (2) bioluminescence dependence on inducer and growth substrate, biomass and luciferase concentrations.

Table 8-1. Summary of major significant experimental results.

Effector	Results	Figure
Toluene concentration	TCE degradation rates and the rate of increase in bioluminescence were the same for initial toluene concentrations between 10 mg/L and 50 mg/L (*tod-lux*).	3-12 3-13
Multiple contaminant exposure (toluene and TCE)	TCE degradation was not observed until the toluene was degraded to very low levels (*tod-lux*).	3-11
Exposure to toxicants	Bioluminescence decreased with exposure to bacterial toxicants cadmium, hydroquinone and 2,4-dinitrophenol. The reduction in bioluminescence was more severe with increasing toxicant concentration.	3-17 3-18
Cultivation conditions		
Batch	Bioluminescence increased at a rate faster than cell division, followed by a rapid decline of bioluminescence that began in mid-log phase cell growth. (*tod-lux* and Shk 1).	3-2 3-5
Chemostat	Bioluminescence increased in response to increased feed substrate concentration (toluene for TVA8 and acetate for Shk 1). The increased feed substrate concentration resulted in increased steady-state cell density. Bioluminescence decreased as cell density approached steady-state values. (*tod-lux* and Shk 1).	4-2 4-15
Turbidostat	Increased light output was observed with unlimited substrate availability when compared with a chemostat of the same dilution rate.	4-1 4-15
Reporter/fluid contacting system design	Batch and continuous contacting of the bioreporter culture with process fluid in a vessel separate from the process allowed on-line toxicity assessment. Designs to measure light from the bioreporter within the process fluid (biosensor) required carbon addition for bioluminescence, but even with carbon addition sustained bioluminescence was not observed	3-18 5-2 5-5

Interpretations of Major Significant Experimental Results

Interpretations of major experimental results include determination of kinetic parameters, bioluminescence dependence on transcription rate, accumulation of luciferase, growth substrate and toxicant concentration, and bioluminescent reporters as an aid to process design and control

Determination of Kinetic Parameters

Kinetic parameters determined from experimental results included maximum degradation rates of toluene and TCE, Michaelis-Menten constants for TCE and toluene, parameters in bioluminescent modeling. Two different methods for determining the toluene maximum degradation rates yielded values within 25 % of each other (14 and 18 mg tol/mg cell day). The maximum toluene degradation parameter for TVA8 was obtained by (1) a fit to the steady-state chemostat cell density data and (2) converting the maximum cell growth of the TVA8 batch growth experiments by assuming a yield coefficient of 1.0 mg cell/mg toluene. Obtaining this parameter from two different methods illustrates the consistency of experimental techniques.

Transcription Rate Dependence on Toluene Concentration

Both the batch (B2) and continuous (TVA8) experiments suggested the range at which transcription of the *lux* and *tod* enzymes was proportional to toluene concentration was below 5 mg/L. The constant rate of increase in bioluminescence

with initial toluene concentrations between 10 and 50 mg/L (Figure 3-13) coupled with the constant TCE degradation rates for initial toluene concentrations between 10 and 100 mg/L (Figure 3-12) indicates that toluene concentrations less than 10 mg/L result in maximum (saturated) transcription rates of *tod* and *lux* system enzymes.

Accumulation of Luciferase to Explain Transient Bioluminescent Behavior

An intracellular accumulation of luciferase was proposed to explain transient bioluminescence behavior. In batch growth of both TVA8 and Shk 1 reporters bioluminescence increased at a rate greater than cell growth. In addition, in continuous cultivation, when steady-state cells (both Shk 1 and TVA8) were exposed to an increase in feed growth substrate, bioluminescence increased at a rate greater than cell density. These observations indicated that some factor responsible for bioluminescence was accumulating in the cell. An accumulation of active luciferase molecules was proposed to explain the mechanism for this behavior. In modeling the relatively short time period (less than 10 hr) batch degradation experiments, this mechanism seemed to fit the bioluminescent data; however, this alone did not describe the long time period (several days) continuous experiments. A term representing *in vivo* enzyme decay was included in the continuous system model which represented the continuous bioluminescent behavior.

Bioluminescence Dependence on Oxygen Concentration

Although oxygen is a substrate of the bioluminescence reaction and bioluminescence was shown to cease at very low oxygen concentrations, dependence on oxygen concentration was not incorporated into the bioluminescence and degradation model. Experiments were designed to maintain adequate oxygen concentration and oxygen mass transfer rates to eliminate this variable from influencing bioluminescence. Both the batch and continuous systems contained a large head-space compared to the liquid volume, and both provided vigorous mixing. In addition, oxygen was sparged to the chemostat liquid volumes. In the batch growth experiments bioluminescence declined at approximately maximum bulk cell growth point. It was proposed that this was due to oxygen limitation. The cell density for TVA8 at this point was 1.0 OD_{600}, so at cell densities below this the rate of oxygen consumption by the biomass was most likely less than the rate of mass transfer from the head-space to the liquid phase. The batch continuous culture experiments utilized cell densities of 0.4 OD_{600} and less; therefore, oxygen concentrations were probably not influencing bioluminescence. Although under other experimental conditions, oxygen concentration and mass transfer rate can affect bioluminescence.

Bioluminescence Dependence on Growth Substrate

Bioluminescence exhibited a dependence on growth substrate concentration. In batch degradation experiments with 10 mg/L initial toluene, bioluminescence

increased dramatically upon exposure to toluene and then declined when toluene was degraded. The degradation of the toluene took only 70 minutes. There was enough *lux* enzymes produced to allow significant light output, and it seems unlikely that upon cessation of transcription, the *lux* enzymes would degrade so quickly to decrease light. The same phenomena was observed with the TVA8 chemostat. As toluene feed was increased, specific bioluminescence increased in response to the increased toluene availability in the reactor. However, as cell densities increased, and reactor toluene concentrations decreased, bioluminescence decreased. This behavior was observed over longer time periods in the chemostat, so lack of transcription coupled with enzyme degradation could not be ruled out as causation of the decline in bioluminescence. This ambiguity was resolved with the Shk 1 chemostat. Transcription with the Shk 1 reporter was constitutive, so the decline in bioluminescence as cell densities increased and the reactor approached growth substrate limiting conditions was not due to lack of induction/transcription. Each of these experiments indicates that the growth substrate concentrations must have limited light production. The bioluminescence substrates ATP, $FMNH_2$ and $NADH_2$ are a result of metabolism of the growth substrate. Therefore, it was proposed that bioluminescence was dependent on growth substrate availability. The Shk 1 turbidostat versus chemostat experiments clearly demonstrate that increased substrate availability results in increased bioluminescence as the chemostat and turbidostat were operated at the same dilution rate and cell density.

Bioluminescence Dependence on Toxicants

In batch and continuous sampling scenarios bioluminescence declined more severely with increasing toxicant concentration. In addition, the decrease in bioluminescence mimicked the decrease in oxygen consumption rate in response to hydroquinone. Bioluminescence in this case was an easily measurable signal of disruption of metabolic activity, which would be important in degradative processes. Although the effect of toxicants were not included in toluene and TCE degradation system modeling, these results are important in the bioreporter application. The effect of specific conditions (inducer and growth substrate concentration) on bioluminescence can be examined, predicted and used for process monitoring and control. Unexpected process disturbances (toxic components in the feed) can affect bioluminescence. Fortunately, many of the factors that affect bioluminescence also affect the degradative process and it is advantageous that bioluminescence will respond to these process disturbances as well.

Bioluminescent Reporters as an Aid to Process Design and Control

Cellular processes (transcription, translation, maintenance of the proton motive force for ATP generation) proceed at maximum rates at high growth substrate, nitrogen, phosphorous, oxygen and micronutrient concentrations. Bacterial populations will increase until one of these requirements limits bacterial growth, as in the continuous and batch growth experiments (Figures 3-2 and 3-5). Unless physical removal of cells is achieved, the bacteria will grow until they are limited. Growth

source limitations not only inhibit bioluminescence, but can also limit degradative processes as bioluminescence and degradation depend on many of the same factors (oxygen, growth substrate). The bioluminescent reporter can be used as measurement for control of specific well characterized process conditions(addition of inducer), warning of unexpected process disturbances (toxicity), and aid reactor design.

Co-metabolic Processes

In activated sludge waste treatment, bacteria consume easily degradable material that is utilized for cellular growth and energy. This waste treatment process selects for bacterial communities that optimize the process. On the contrary, co-metabolic processes require the bacteria to perform a function of no benefit to them. This is an important and fundamental difference that must be taken into account when designing co-metabolic processes and process control scenarios. For example, due to competition for the *tod* enzyme and enzyme toxicity, (1) high levels of *tod* enzyme should be available, (2) the cells should be in optimum condition (not nutrient limited), and (3) the amount of inducer that competes with TCE should be minimized.

This conceptual model of degradation and bioluminescence has implications in design strategy for TCE degradation and using the bioreporter to improve monitoring and control of the degradative processes. A simple design is proposed for TCE degradation that applies the mechanisms elucidated in this research.

A Proposed TCE Degradation System

A simple TCE bioremediation system is proposed to degrade TCE from a contaminated aquifer in an above ground treatment reactor utilizing conclusions from this work. The following principles are applied.

1. Induction of the *tod* operon by toluene must be separated in time or space from the degradation of TCE due to competition for the *tod* enzyme.
2. Cells must be provided in an optimum condition to ensure the best co-metabolic activity towards TCE.
3. Reporter cell bioluminescence is used as the measurement for control loops controlling toluene pulsing and cell wasting.

The system consists of a primary and secondary removal reactor (Figure 8-1). The primary removal reactor is a continuously-stirred-tank reactor with automated liquid phase removal in addition to the traditional overflow for level control. The secondary removal reactor is for removing remaining substrate and is designed to operate under carbon limitation.

The control algorithm is as follows (Figure 8-2), toluene is fed to the first reactor until light reaches a pre-determined magnitude (toluene off set-point) and then toluene feed is stopped. Then, TCE and supplemental carbon are supplied. The cells will be induced, but toluene will not be present, so TCE will be degraded. Bioluminescence will decrease due to lack of induction and enzyme degradation but not energy limitation. When light reaches a pre-determined lower set-point (toluene on set-point) the supplemental carbon source and TCE feed is stopped, and the cycle

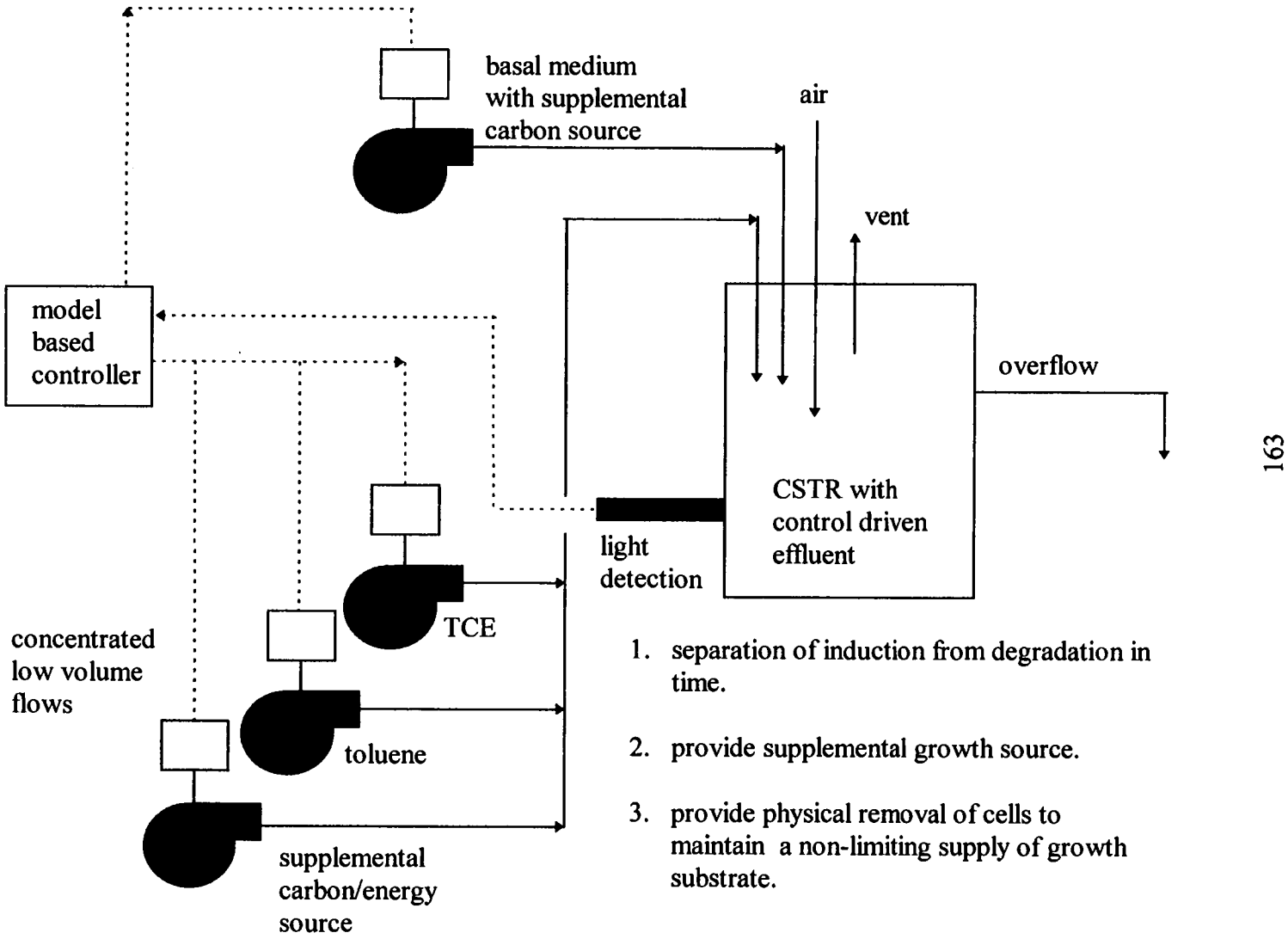

Figure 8-1. Proposed TCE remediation design using bioluminescence for monitoring and control of the bacterial process.

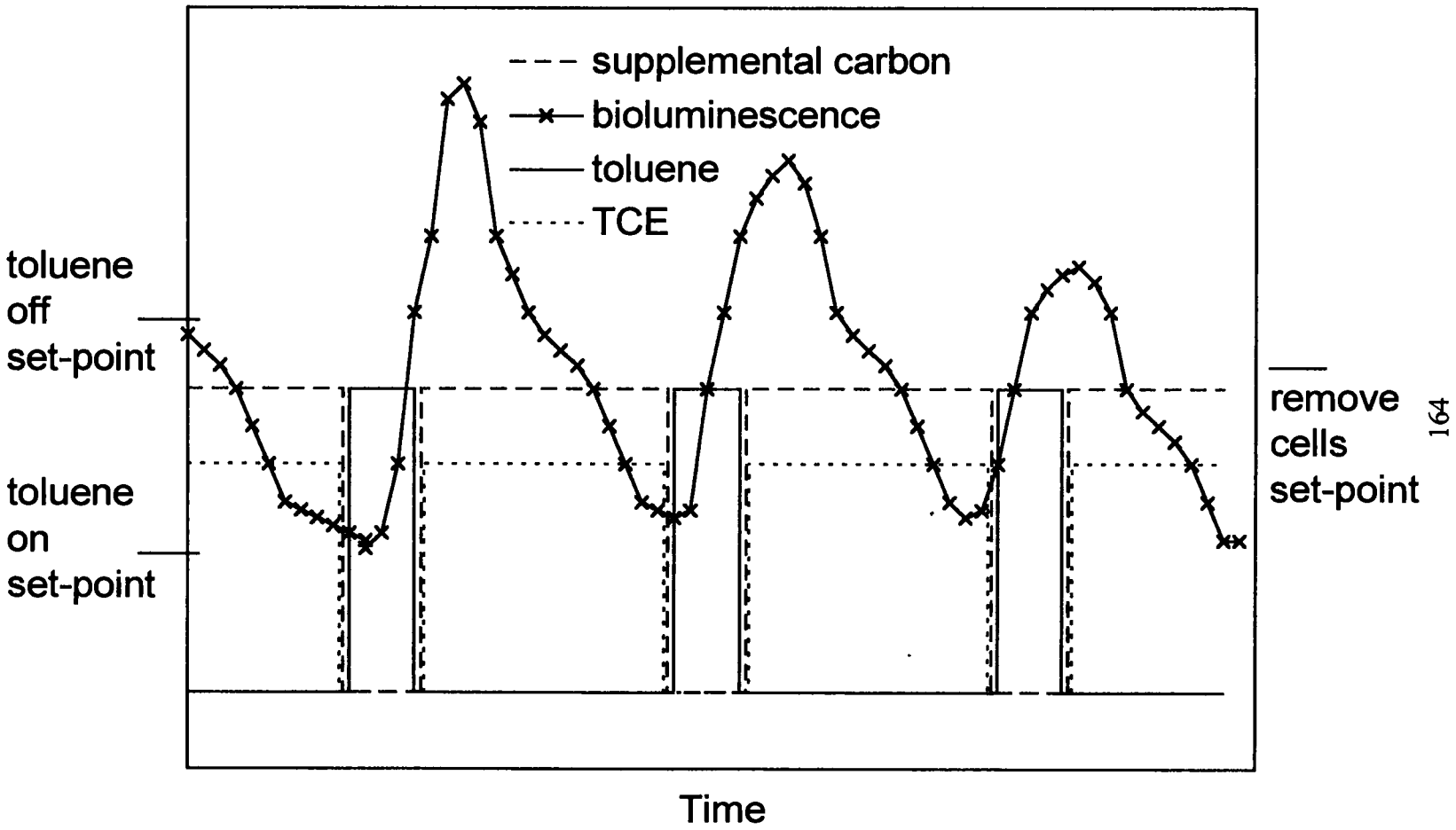

Figure 8-2. Simple control algorithm for toluene, TCE and supplemental carbon source additions, as well as cell removal from primary reactor.

begins again. In addition to using bioluminescence to determine when to begin and end toluene feed pulses, bioluminescence will determine when cells should be removed from the primary reactor. As cell density increases to carbon limited conditions in the primary reactor, bioluminescence peaks will decrease (Figure 6-2). When toluene is pulsed to the reactor and bioluminescence does not reach a pre-determined set-point (remove cells set-point) cells are removed from the reactor.

The increase in bioluminescence to the toluene off set point indicates the cells are induced and the *tod* operon is being transcribed. The decrease in bioluminescence indicates the production rate of *lux* enzymes is less than the degradation rate of *lux* enzymes. This can be correlated to *tod* enzyme production and degradation rates as well as TCE removal rates. A predictive model will determine the toluene on set-point. The model will be based on enzyme production and degradation rates of the *lux* and *tod* system as well as TCE whole cell and enzyme toxicity mechanisms.

Recommendations for Future Work

Carbon Starvation versus Induction Limitation

Chemostat experiments utilizing the Shk 1 and the *tod-lux* reporter indicated that the decline in bioluminescence as conditions approached steady-state was perhaps due to growth substrate limitation and possibly lack of induction. Although there is a net flux of toluene being degraded in the chemostat, is the amount contacting each cell enough for induction of the *tod* operon? Is the toluene being degraded by enzymes

produced from a basal level of transcription? Simple experiments with a *lac-lux* reporter can answer these questions. The *lac* promoter is a common genetic engineering tool because it is well characterized. Lactose is an inducer of β-galactosidase protein synthesis from the *lac* operon. However, IPTG is also an inducer, but is not metabolized by most bacteria. Therefore, IPTG can be used for induction independent of energy production in the cell. Fundamental characterization of carbon limitation versus lack of induction in a chemostat can be examined using a *lac-lux* fusion.

Estimation of *in vivo* Enzyme Degradation Rates

A turbidostat allows cells to grow under continuous yet ample carbon conditions. Toluene pulsing in combination with an alternative non-inducing carbon source will enable a definitive determination of effective *in vivo* stability of *lux* and *tod* enzymes. For example, toluene could be fed to the chemostat until the cells were well induced, then replaced with a non-inducing carbon and energy source. TCE and bioluminescence could be measured. The decline in bioluminescence can be attributed to the reduction in the enzyme pool rather than carbon starvation. These mechanisms cannot be separated in chemostat experiments. Similarly, TCE degradation should begin when the toluene is cleared from the reactor but the cells are still induced. When TCE degradation ceases it will be due to loss of *tod* enzymes, not carbon starvation. A turbidostat providing mechanical wasting of cells is the ideal reactor to elucidate these *in vivo* effective enzyme decay rates.

Biosensor Engineering

Further development of a means of contacting bioreporter with process fluids is warranted. A turbidostat can provide cells to the dialysis type biosensor design, maintaining a constant supply of bioreporter with high and steady light output. The advantages over an immobilized or batch incorporation of reporter cells is that if severe toxic loads completely destroy the cells, the turbidostat automatically supplies new cells that will respond when the severe toxicity is diminished. Obviously, in the sensor designs examined in this research, factors important in bioreporter functioning were not well elucidated.

REFERENCES

REFERENCES

1. Applegate, B., C. Kelly, L. Lackey, J. McPherson, S. Kehrmeyer, F. Menn, P. Bienkowski and G. Sayler. 1996. *Pseudomonas putida* B2: A *tod-lux* bioluminescent reporter for toluene and trichloroethylene cometabolism. Journal of Industrial Microbiology. 18:4-9.

2. Applegate, B.M., S.R. Kehrmeyer and G.S. Sayler. 1997. Generation of a chromosomally-based *tod-lux* reporter fro detection and quantification of BTEX compounds in aqueous solutions. In preparation.

3. Battistoni, P. G. Fava and M.L. Ruello. 1993. Heavy metal shock load in activated sludge uptake and toxic effects. Water Resources. 27(5):821-827.

4. Bailey, J.E. and D.F. Ollis. 1986. Biochemical Engineering Fundamentals. McGraw-Hill. New York, NY.

5. Belkin, S., D.R. Smulski, A.C. Vollmer, T.K. Van Dyk and R.A LaRossa. 1996. Oxidative stress detection with *Escherichia coli* harboring a *katG'::lux* fusion. Applied and Environmental Microbiology. 62:2252-2256.

6. Brock, T.D., D.W. Smith, M.T. Madigan. 1984. Biology of Microorgansims. Prentice-Hall, Inc. Englewood Cliffs, N.J.

7. Bronstein, I., J. Fortin, P.E. Sanley, G.S.A.B. Stewart and L.J. Kricka. 1994. Chemiluminescent and bioluminescent reporter gene assays. Analytical Biochemistry. 219:169-181.

8. Brown, R.A., W. Mahaffey, R.D. Norris, 1992. *In situ* bioremediation: The state of the practice. *In situ* bioremediation. National Research Council, Water Science and Technologies Board.

9. Chang, H. and L. Alvarez-Cohen. 1995. Transformation capacities of chlorinated organics by mixed cultures enriched on methane, propane, toluene, or phenol. Biotechnology and Bioengineering. 45:440-449.

10. Chang, H., and L.Alvarez-Cohen. 1995. Model for the cometabolic biodegradation of chlorinated organics. Environmental Science and Technology. 29:2357-2367.

11. Chang, M., T. C. Voice and C.S. Criddle. 1992. Kinetics of competitive inhibition and cometabolism in the biodegradation of benzene, toluene and p-xylene by two *Pseudomonas* Isolates. Biotechnology and Bioengineering. 41:1057-1065.

12. Chase, A.M. 1950. Studies on cell enzymes systems. IV. The kinetics of heat inactivation of *Cypridina* luciferase. Journal of General Physiology. 33:535.

13. Cheney, W. and D. Kincaid. 1985. Numerical Mathematics and Computing. Brooks/Cole Publishing Company, Monterey, California.

14. Davis, B. D. and E. S. Mingioli. 1950. Mutants of *Escherichia coli* requiring methionine or vitamin B12. Journal of Bacteriology. 60:17-28.

15. DeWeger, L.A., P. Dunbar, W.F. Mahafee, B.J.J. Lugtenberg, and G.S. Sayler. 1991. Use of bioluminescent markers to detect *Pseudomonas spp.* in the rhizosphere. Applied and Environmental Microbiology. 57:3641-3644.

16. DuBow, M.S. and A. Guzzo. (1992) Luminescent bacterial biosensors to detect toxic agents and elucidate molecular mechanisms of toxicity. Environ Can/ et al Proc 15th Int Symp on Wastewater Treatment/4th Workshop on Drinking Water, Montreal, PQ.

17. Dutka, B. J., N. Nyholm, J. Petersen. (1983) Comparison of several microbiological toxicity screening tests. Water Research, 17(10), 1363-1368.

18. Fetter,C.W. 1992. Contaminant Hydrogeology. Macmillan Publishing Company, New York, NY.

19. Furukawa, K.J. Hirose, S. Hayashida and K. Nakamura. 1994. Efficient degradation of trichloroethylene by a hybrid aromatic ring dioxygenase. Journal of Bacteriology. 176:2121-2123.

20. Gibson, D.T., G.J. Zylstra and S. Chauhan. 1990. Biotransformations catalyzed by toluene dioxygenase from *Pseudomonas putida* F1. in *Pseudomonas*: Biotransformations, Pathogenesis, and Evolving Biotechnology (eds S. Silver et al.).

21. Gibson, D.T., J.R. Koch and R.E. Kallio, July 1968, Oxidative degradation of aromatic hydrocarbons by microorganisms I. enzymatic formation of catechol from benzene. Biochemistry, 7(7):2653-2662.

22. Gibson, D.T., W. Yeh, T. Liu and V. Subramanian. 1982. Toluene dioxygenase: A multicomponent enzyme system from *Pseudomonas putida*. Oxygenases and Oxygen Metabolism. 51-61.

23. Hao. O.J. and C.H. Chang. 1988. Metal toxicity on phosphate removal in pure culture and in activated sludge. Journal of Environmental Engineering. 114(1):38-53.

24. Hastings, J.W. and K.H. Nealson. 1977. Bacterial Bioluminescence. Annual Reviews in Microbiology. 31:549-95.

25. Hastings, J.W., C.J. Potrikus, S.C. Gupta, M. Kurfurst and J.C. Makemson. 1985. Biochemistry and physiolgy of bioluminescent bacteria. Advances in Microbial Physiology. 26:235-291.

26. Hazen, T.C. 1991. Test plan for in situ bioremediation demonstration of the Savannah River integrated demonstration project. Publication WSRC-RD-91-23, DOE/OTD TTP no. SR0566-01 (U). Westinghouse Savannah River Complany, Aiken, S.C.

27. Heitzer, A., O.F. Webb, J.E. Thonnard, and G.S.Sayler. 1992. Specific and quantitative assessment of naphthalene and salicylate bioavailability by using a

bioluminescent catabolic bacterium. Applied and Environmental Microbiology. 58:1839-1846.

28. Heitzer, A., K. Malachowsky, J.E. Thonnard, P.R. Bienkowski, D.C. White and G.S.Sayler. 1994. Optical biosensor for environmental on-line monitoring of naphthalene and salicylate bioavailability with an immobilized bioluminescent catabolic reporter bacterium. Applied and Environmental Microbiology. 60:1487-1494.

29. Humphrey, A.E., December 1984, Commercializing biotechnology: challenge to the chemical engineer, Chemical Engineering Progress.

30. Kelly, C., C. Lajoie, A. Layton, and G. Sayler. 1997. A bioluminescent reporter bacterium for toxicity monitoring in biological wastewaster treatment systems. In preparation.

31. Kilroy, A.C. and N.F. Gray. 1992. The toxicity of four organic solvents commonly used in the pharmaceutical industry to activated sludge. Water Research. 26(7):887-892.

32. King, J.M.H., P.M. DiGrazia, B. Applegate, R. Burlage, J. Sanseverino, F. Larimer, and G.S. Sayler. 1990. Rapid, sensitive bioluminescenct reporter technology for napthalene exposure and biodegradation. Science. 249:778-781.

33. Kong, Z., P Vanrolleghem, P. Willems, and W. Verstraete. 1996. Simultaneous determination of inhibition kinetics of carbon oxidation and nitrification with a respirometer. Water Resources. 30(4):825-836.

34. Lau, P.C.K., H. Bergeron, D. Labbe, Y. Wang, R. Brouseau and D.T. Gibson. 1994. Sequence and expression of the *todGIH* genes involved in the last three steps of toluene degradation by *Pseudomonas putida* F1. Gene. 146:7-13.

35. Li, S. and L.P. Wackett. 1992. Trichloroethylene oxidation by toluene dioxygenase. Biochemical and Biophysical Research Communications. 185:443-451.

36. Lu, Chih-Jen, Chu-Yin Chang and ChiMei Lee. 1995. Aerobic biodegradation of trichloroethylene by microorganisms that degrade aromatic compounds. In Bioremediation of Chlorinated Solvents. Ed. R. E. Hinchee, A. Leeson and L. Semprini. Battelle Press, Columbus OH.

37. Maniatis, T., E.F. Fritsch, and J. Sambrock. 1982. Molecular Cloning. A Laboratory Manual. Cold Spring Harbor Laboratory. Cold Spring Harbor, New York.

38. Meighen, E.A. 1991. Molecular biology of bacterial bioluminescence. Microbiological Reviews. 55:123-142.

39. Menn, F., G.J. Zylstra and D.T. Gibson. 1991. Location and sequence of the todF gene encoding 2-hydroxy-6-oxohepta-2,4-dienoate hydrolase in *Pseudomonas putida* F1. Gene. 104:91-94.

40. Meyers, A. 1996. Personnal communitcation.

41. Meynell, G. G. and E. Meynell. 1965. Theory and Practice in Experimental Bacteriology, p. 33. Cambridge University Press, New York, NY.

42. Nealson, K.H. and J.W. Hastings. 1979. Bacterial bioluminescence: Its control and ecological significance. Microbiological Reviews. 43:496-518.

43. Norberg, A.B. and N. Molin. 1983. Toxicity of cadmium, cobalt, uranium and zinc to *Zoogloea ramigera*. Water Resources. 17(10):1333-1336.

44. Paton, G.I., G. Palmer, A. Kindness, C. Campbell, LA. Glover and K. Killham. 1995. Use of luminescence-marked bacteria to assess copper bioavailability in malt whisky distillery effluent. Chemosphere. 31(5):3217-3224.

45. Pinkart, H.C. 1996. Cell envelope dynamics and solvent tolerance in *Pseudomonas putida*. Dissertion, University of TN.

46. Riley, R.G., J.M. Zachara, F.J. Wobber, April 1992, Chemical contaminants on DOE lands and selection of contaminant mixtures for subsurface research, U.S. Department of Energy, Office of Energy Research, Subsurface Science Program.

47. Rittmann, B.E., A.J. Valocchi, E. Seagren, C. Ray, B. Wrenn, J.R. Gallagher, August 1992, A Critical review of in situ bioremediation, Topical Report, Gas Research Institute and U.S. Department of Energy.

48. Robertson, B.R. and D.K Button. 1987. Toluene induction and uptake kinetics and their inclusion in the specific-affinity relationship for describing rates of hydrocarbon metabolism. Applied and Environmental Microbiology. 53:2193-2205.

49. Rogers, K.R. and C.L. Gerlach. 1996. Environmental biosensors a status report. Environmental Science and Technology. 30:486-491.

50. Sayler, G.S., U. Matrubutham, R. Palmer and C. Kelly. 1995. Application of Molecular Biology to Real Time Monitoring in Bioremediation. Proceedings for the OECD Workshop Amsterdam 1995 on Wider Applications and Diffusion of Bioremediation Technologies.

51. Shuler, M. L. and F. Kargi. 1992. Bioprocess Engineering Basic Concepts. Prentice Hall, New Jersey.

52. Skinner, J.H., 1991, Bioremediation Research Issues, Environmental Biotechnology for waste treatment, Environmental Science Research, Ed. G.S. Sayler et al. 41:61-70.

53. Stanier , 1957. Journal of Cellular and Comparative Physiology. 49:25.

54. Steinberg, S.M., E.J. Poziomek, W.H. Engelmann, and K.R. Rogers. 1995. A review of environmental applications of bioluminescence measurements. Chemosphere. 30(11):2155-2197.

55. Stewart, G.S.A.B and P. Williams. 1992. *lux* genes and the applications of bacterial bioluminescence. Journal of General Microbiology. 138:1289-1300.

56. Stom, D. I., T.A. Geel, A.E. Balayan, G.I. Shachova, A. M. Kuznetsov, and S. E. Medvedeva. 1992. Bioluminescent method in studying the complex effect of sewage components. Archives of Environmental Toxicology. 22:203-208.

57. Strotmann, U. J. and H. Eglsaer. 1995. The toxicity of substituted phenols in the nitrification inhibition test and luminescent bacteria test. Ecotoxicology and Environmental Safety. 30:269-273.

58. Subramanian, V.T. Liu, W. Yeh, M. Narro and D.T. Gibson. 1981. Purification and properties of NADH-ferredoxinTOL reductase: A component of toluene dioxygenase from *Pseudomonas putida*. Journal of Biological Chemistry. 256:2723-2730.

59. Svenson, A., Z. Linlin, and L. Kaj. 1992. Primary chemical and physical characterization of acute toxic components in wastewaters. Ecotoxicology and Enivronmental Safety. 24:234-242.

60. Tyagi, R. D., and D. Couillard. 1988. Toxic effects of inhibitors in biological wastewater treatments processes. The Canadian Journal of Chemical Engineering. 66:97-106.

61. Van Kyk, T.K., D.R. Smulski, T.R. Reed, S. Belkin, A.C. Vollmer and R. LaRossa. 1995. Responses to toxicants of an *Escherichia coli* strain carrying a *uspA;::lux* genetic fusion and an *E. coli* strain carrying a *grpE'::lux* fusion are similar. Applied and Environmental Microbiology. 61:4124-4127.

62. Van Duren, B.L. and S. Banerfee. 1976. Covalent interaction of metabolites of the carcinogen trichloroethylene in rat heatic microsomes. Cancer Research. 36:2419-22.

63. Volskay, V.T. Jr. and C.P.L. Grady Jr. 1988. Toxicity of slected RCRA compounds to activated sludge microorgansisms. Journal of the Water Pollution Control Federation. 60(10):1850-1856.

64. Wackett, L.P. 1991. The mechanism of trichloroethylene oxidation by toluene dioxygenase: Implications for bioremediation. Final Technical Report for Year 1 & 2. Airforce Grant.

65. Wang, Y.M. Rawlings, D.T. Gibson, D. Labbe, H. Bergon, R. Brousseau and P.C.K. Lau. 1995. Identification of a membrane protein and a truncated LysR-type regulator associated with the toluene degradation pathway in *Pseudomonas putida* F1. Molecular and General Genetics. 246:570-579.

66. Wackett, L.P., and D.T. Gibson. 1988. Degradation of trichloroethylene by toluene dioxygenase in whole-cell studies with *Pseudomonas putida* F1. Applied and Environmental Microbiology. 54:1703-1708.

67. Yeh, W.K., D.T. Gibson and T. Liu. 1977. Toluene dioxygenase: a multicomponenst enzyme system. Biochemical and Biophysical Research Communications. 78:401-410.

68. Zylstra, G.J., L.P. Wackett and D.T. Gibson. 1989. Trichloroethylene degradation by *Escherichia coli* containing the cloned *Pseudomonas putida* F1 toluene dioxygenase genes. Applied and Environmental Microbiology. 55:3162-3166.

69. Zylstra, G.J., W.R. McCombie, D.T.Gibson, and B.A. Finette. 1988. Toluene degradation by *Pseudomonas putida* F1: Genetic organization of the *tod* operon. Applied and Environmental Microbiology. 54:1498-1503.

70. Zylstra, G.J. 1989. Toluene degradation by *Pseudomonas putida* F1: Nucleotide sequence on the *todC1C2BADE* genes and their expression in *Eschericha coli*. Journal of Biological Chemistry. 264:14940-14946.

APPENDICES

FORTRAN Code for Model Solution

```
C     X = LIQUID PHASE SUBSTRATE CONCENTRATION
C     V = VAPOR PHASE SUBSTRATE CONCENTRATION
C     S = TOTAL SUBSTRATE CONCENTRATION AS IF ALL IN LIQUID
PHASE
C          1 = TOLUENE, mg/L
C          2 = TCE, mg/L
C      X( ) 3 = LUCIFERASE,  mg/cell
C          4 = BIOMASS, mg/L

      PROGRAM CHEMOSTAT

      INTEGER I,J, NSTEP
      REAL   TIME, H
      REAL   KLITE, KMLITE, KMLUC
      REAL   X(10), V(10), S(10)
      REAL   KMAT(3,3)

      OPEN(UNIT=80,FILE='COMP.OUT',STATUS='OLD')
      N=4
      H=0.0002
      NSTEP = 80000

CCCCCCCCCCCCCCCCCCCCC VARY LIGHT EQ PARAMETERS
CCCCCCCCCCCCCCCCCCCCCC
      KMAT(1,1) = 1750.0
      KMAT(1,2) = 50.0
      KMAT(1,3) = 100.0

      KMAT(2,1) = 5.0
      KMAT(2,2) = 5.0
      KMAT(2,3) = 10.0

      KMAT(3,1) = 5.0
      KMAT(3,2) = 5.0
      KMAT(3,3) = 10.0
CCCCCCCCCCCCCCCCCCCCCCCCCCCCCCCCCCCCCCCCCCCCCCCCCCCCCCCCCCCC
CCCCCCCCCCCCCCCCC

      DO 20 I=1,1
       DO 19 J=1,1
```

```
      DO 18 K=1,1
      KLITE  = KMAT(1,I)
      KMLITE = KMAT(2,J)
      KMLUC  = KMAT(3,K)

      WRITE(80,*)' KLITE     KMLITE   KMLUC'
      WRITE(80,*)KLITE,KMLITE,KMLUC
      TIME=0.0
      S(1) = 0.0
      S(2) = 0.0
      X(3)=0.0
      X(4)=29.5
      CALL RK4SYS(N,TIME,X,V,S,H,NSTEP,KLITE,KMLITE,KMLUC)
 18    CONTINUE
 19   CONTINUE
 20  CONTINUE
     CLOSE(UNIT=80)
     STOP
     END

CCCCCCCCCCCCCCCCCCCCCCC  BEGIN RUNGE ROUTINE
CCCCCCCCCCCCCCCCCCCCCCCCCCCCCCC
    SUBROUTINE RK4SYS(N,TIME,X,V,S,H,NSTEP,KLITE,KMLITE,KMLUC)
     INTEGER N, K, NSTEP, PRINT
     REAL   H2,H,TIME,START
     REAL   KLITE,KMLITE,KMLUC,LIGHT
     REAL   CFTOL,YLDT
     REAL   X(10),V(10),S(10)
     REAL   Y(10),F1(10),F2(10),F3(10),F4(10),DIF(10)

     FIRST=1
     H2=0.5*H
     NUM1 = 1
     NUM2 = 1
     START=TIME
     PRINT=25000

     WRITE(80,*)' TIME  TOLUENE TCE   LUCIF  CELL  LIGHT'
     CALL HENRYS(X,V,S)
     DO 7 K=1,NSTEP
     CFTCE=5.6
```

```
CCCCCCCCCCCCCCCCCCCCC  STEP TOLUENE FEED
CCCCCCCCCCCCCCCCCCCCCCCCCCCCCC
      IF (TIME.LT.2.95) THEN
           CFTOL=9.6
           ELSEIF ((TIME.GE.2.95).AND.(TIME.LT.5.27)) THEN
            CFTOL=9.6
           ELSEIF ((TIME.GE.5.27).AND.(TIME.LT.7.292)) THEN
            CFTOL=28.0
           ELSEIF ((TIME.GE.7.292).AND.(TIME.LT.8.445)) THEN
            CFTOL=69.0
           ELSEIF ((TIME.GE.8.445).AND.(TIME.LT.10.375)) THEN
            CFTOL=125.0
           ELSEIF ((TIME.GE.10.375).AND.(TIME.LT.11.492)) THEN
            CFTOL=187.5
           ELSEIF ((TIME.GE.11.492).AND.(TIME.LT.12.103)) THEN
            CFTOL=0.0
           ELSEIF ((TIME.GE.12.103).AND.(TIME.LT.14.32)) THEN
            CFTOL=125.0
           ELSEIF ((TIME.GE.14.32).AND.(TIME.LT.15.521)) THEN
            CFTOL=69.0
            ELSE
              CFTOL=28.0
      ENDIF
CCCCCCCCCCCCCCCCCCCCC  END STEP TOLUENE FEED
CCCCCCCCCCCCCCCCCCCCCCCCCCCCCC

        CALL XPSYS(X,V,F1,KMLUC,CFTOL,CFTCE,YLDT)
        DO 2 I=1,N
           Y(I)=X(I)+H2*F1(I)
 2      CONTINUE
        CALL XPSYS(Y,V,F2,KMLUC,CFTOL,CFTCE,YLDT)
        DO 3 I=1,N
           Y(I)=X(I)+H2*F2(I)
 3      CONTINUE
        CALL XPSYS(Y,V,F3,KMLUC,CFTOL,CFTCE,YLDT)
        DO 4 I=1,N
           Y(I)=X(I)+H*F3(I)
 4      CONTINUE
        CALL XPSYS(Y,V,F4,KMLUC,CFTOL,CFTCE,YLDT)
        DO 5 I=1,2
           DIF(I) = H*(F1(I)+2.0*(F2(I)+F3(I))+F4(I))/6.0
           S(I)=S(I)+DIF(I)
 5      CONTINUE
```

```
      DO 6 I=3,4
        X(I)=X(I)+ H*(F1(I)+2.0*(F2(I)+F3(I))+F4(I))/6.0
 6     CONTINUE

      CALL HENRYS(X,V,S)
      TIME=START+REAL(K)*H

      LIGHT=X(4)*KLITE*X(3)*X(1)/(KMLITE+X(1))

      IF (K.EQ.PRINT)THEN
       WRITE(80,100) TIME+10.0,V(1),V(2),X(3),X(4),LIGHT
       PRINT=PRINT+300
      ENDIF
 7     CONTINUE

 100  FORMAT (1X,F7.2,F7.2,F7.2,F7.2,F7.2,F9.2,F9.2)
    RETURN
    END


CCCCCCCCCCCCCCCCCCCCCCC BEGIN XPSYS ROUTING
CCCCCCCCCCCCCCCCCCCCCCCCCCCCCCCC
    SUBROUTINE XPSYS(X,V,F,KMLUC,CFTOL,CFTCE,YLDT)
    REAL     RATE1,RATE2,LVOL,VVOL,AIR,FEED
    REAL     CFTOL,CFTCE,KTOL,KTCE,KMTOL,KMTCE,YLDT
    REAL     KMLUC,KD
    REAL     V(10),X(10),F(10)

    KTOL  = 14.0
    KMTOL = 2.7
    KTCE  = 1.3
    KMTCE = 6.4
    KD    = 2.0
    LVOL  = 0.3
    VVOL  = 0.7
    AIR   = 4.6
    FEED  = 0.979
    YLDT = 1.0

    RATE1=-KTOL*X(4)*X(1)/(KMTOL*(1.0+X(2)/KMTCE)+X(1))
    RATE2=-KTCE*X(4)*X(2)/(KMTCE*(1.0+X(1)/KMTOL)+X(2))

    F(1)=(FEED/LVOL)*(CFTOL-X(1))-AIR*V(1)/LVOL+RATE1
```

```
      F(2)=(FEED/LVOL)*(CFTCE-X(2))-AIR*V(2)/LVOL+RATE2
      F(3)= X(1)/(KMLUC+X(1))-KD*X(3)
      F(4) = -(FEED/LVOL)*X(4)- YLDT*RATE1
      RETURN
      END

CCCCCCCCCCCCCCCCCCCCCC  BEGIN HENRYS ROUTINE
CCCCCCCCCCCCCCCCCCCCCCCCC
      SUBROUTINE HENRYS(X,V,S)
      INTEGER  I
      REAL     VOLG, VOLL
      REAL     H(10)
      REAL     X(10), V(10), S(10)

      VOLG = 0.7
      VOLL = 0.3
      H(1) = 0.27
      H(2) = 0.36

      DO 5 I=1,2
         V(I)= S(I)/( (1/H(I)) + (VOLG/VOLL) )
         X(I) = V(I)/H(I)
 5     CONTINUE

      RETURN
                                        END
```

VITA

Christine Kelly was born in Longmont, Colorado on November 17, 1966. She attended primary school in Longmont, and secondary school in Tucson, Arizona, graduating from Sahuaro High School in 1985. In December 1989 she earned her Bachelor of Science degree in Chemical Engineering from the University of Arizona. After working as a process engineer for A.E. Staley in Loudon, Tennessee, she entered the doctoral program at the University of Tennessee, Knoxville. She earned her Doctor of Philosophy in Chemical Engineering in May 1997.